Ganapathi Anantharaman

Synthesis and Structural Studies of Group 12 Metallasiloxane and Phosphonate aggregates: Precursors for Metal Silicate and Phosphate Assemblies

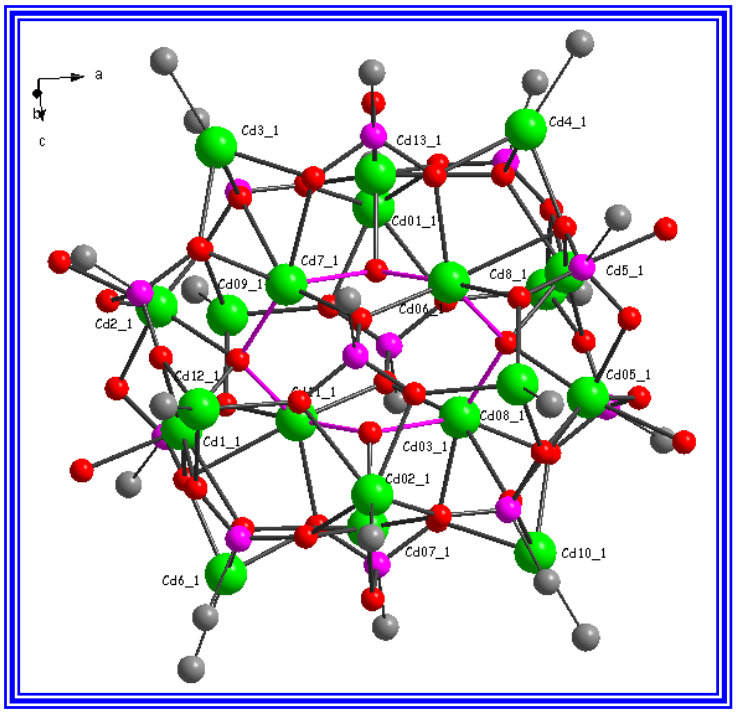

Synthesis and Structural Studies of Group 12 Metallasiloxane and Phosphonate aggregates: Precursors for Metal Silicate and Phosphate Assemblies

Dissertation

zur Erlangung des Doktorgrades

der Mathematisch-Naturwissenschaftlichen Fakultäten

der Georg-August-Universität zu Göttingen

vorgelegt von

Ganapathi Anantharaman

aus Madras

(Indien)

Göttingen 2003

D 7

Referent: Prof. Dr. Dr. h.c. mult. H. W. Roesky
Korreferent: Prof. Dr. K. Samwer

Tag der mündlichen Prüfung: 02.07.2003

Dedicated to my parents for
their love and affection

Acknowledgement

The work described in this doctoral thesis has been carried out under the guidance and supervision of Professor Dr. Dr. h. c. mult. H. W. Roesky at the Institut für Anorganische Chemie der Georg-August-Universität in Göttingen between March 2000 and May 2003.

My sincere thanks and gratitude are due to

Professor Dr. Dr. h. c. mult. H. W. Roesky

for his constant guidance, motivation, suggestions, and discussions throughout this work. I also thank him for the freedom I enjoyed during my stay at Göttingen.

I would like to express my special thanks to Professor Dr. R. Murugavel and Dr. Mrinalini G. Walawalkar for their kind help and motivation during this work. I also thank them for their help while writing this thesis. I thank Professor Dr. Martin Suhm and Corrina for their collaboration in gas phase high-resolution IR studies. I thank Professor J. Magull, Denis Vidovic, Mr. Hans-Georg Schmidt, Dr. Mathias Noltemeyer, and Mr. Bunkóczi Gábor for their help in the X-ray crystal structure investigations and their friendliness. I thank Mr. W. Zolke, Mr. J. Schöne, Dr. G. Elter, (NMR investigations), Brigitta Angerstein, Dr. Marc Baldus, (Solid-State NMR Measurements), Dr. D. Böhler, Mr. T. Schuchardt (Mass Spectral measurements), Mr. M. Hesse, Mr. H.-J. Feine (IR Spectral measurements), Mr. J. Schimkowiak, Mr. M. Schlote and the staff of the Analytical Laboratories for their timely support during this research work.

I thank all my colleagues in our research group for the good and motivating work atmosphere. I would like to express my special thanks to Dr. Peter Böttcher, Dr. Suzana Kiel, Dr. Saji P. Varkey, Dr. Ajax Mohamed, Dr. Klaus Klimek, and Dr. Mark Schorrmann for their help in the initial stages of my work and Hans-Jürgen Ahn, S. Shravan Kumar, Dr. Dante Neculai, Dr. Mirela Neculai, Y. Peng, Dr. Y. Ding, Dr. G. Bai, Torsten Blunck, Dr. Andreas Stasch, Peter Lobinger, Michael Gorol, Sanjay Singh, Kerstin Most, Dr. N. Mösch–Zanetti, Dr. Jörg Prust, Dr. Carsten Ackerhans, Dr. Holger Hohmeister, Dr. Jörg Janssen, Zhu, Chai, and Umesh Nehete for their friendly atmosphere. I thank specially Vojta Jancik for his help during my work. I also thank all the Graduiertenkolleg (GRK) members for their friendliness. The help rendered by Dr. M. Witt during the writing of this thesis is gratefully acknowledged.

I thank B. Venkatesh and R. Lavanya for their help and friendliness during my stay in Göttingen. My special thanks to Dr. N. D. Reddy and his family for their encouragement during this work. I also thank my parents, brothers and sisters, and relatives for their moral support during this work.

All the Indians who have been living in Göttingen during this period made me feel at home, though I was far away from home. My special thanks to former batchmates and labmates in IIT Bombay for their encouragement to continue my studies.

Abbreviations

*t*Bu	*tert*-butyl
br	broad
av	average
d	doublet
δ	chemical shift
C	Celsius
EI	electron impact ionization
Et	ethyl
IR	infrared
J	coupling constant
K	Kelvin
λ	wavelength
M	metal
m	multiplet
M^+	molecular ion
m/z	mass / charge
Me	methyl
MS	mass spectrometry, mass spectra
μ	bridging
NMR	nuclear magnetic resonance
CP-MAS	Cross Polarisation Magic Spinning Angle
ν	wave number
Ph	phenyl
ppm	parts per million
*i*Pr	*iso*-propyl
q	quartet
R	organic substituent
s	singlet
S	solvent
sept	septet
SBU	Secondary Building Unit

t	triplet
tert	tertiary
THF	tetrahydrofuran
L	ligand
TMS	tetramethylsilane
Z	number of molecules in the unit cell
ZSM	Zeolite Socony Mobil
APO	aluminumophosphate
MeAPO	metal aluminumphosphate
SAPO	silicoaluminumphosphate
tbp	trigonal bipyramidal

1. Introduction

Several natural resources have become an essential part of modern day life. Considering the limitation of the availability of such systems in nature, many researchers have contributed to various aspects of this area of science, namely, identification of resources, understanding their roles in particular functions, their classification / categorisation, and possible synthetic alternatives. To mimic nature, the first step would be to consider larger natural systems as a collection of smaller ensembles and understand them. This can be achieved by two different pathways: a) to break the natural systems by force into smaller fractions and b) to develop smaller building blocks containing functionalities which can be used for assembling them to produce the natural systems. Material scientists, biochemists, polymer chemists, and solid-state chemists make efforts to design materials that have properties close to natural systems. Owing to the importance of zeolites in various facets of modern day-to-day life (*e.g.* from detergents to catalyst supports in various transformations), a large portion of the scientific community has been induced to indulge in the area of research on naturally occurring minerals (metaloxides, silicates and phosphates *etc.*). As the work in this presentation deals with the synthesis and characterisation of model compounds / secondary building units of both silicate and phosphate molecular sieves and minerals, the next few sections will introduce these two topics briefly.

1.1. Silicates

Silicate minerals and silica constitute the major portion of earth's crust in the form of rocks, soil, clay, and sand.[1-3] The report based on geochemical studies on the earth's mass indicates the major mass (68.1 %) is mantled by oxides and silicates. Most of these silicate rocks arose from the igneous rocks during magma (*e.g.* lava). The formation of a particular type of rock depends on factors such as the composition, lattice energy, melting points, rate of

cooling, and the crystalline nature of individual minerals *etc*. As magma cools down several products are formed which include: olivine [$(Mg^{2+},Fe^{2+})_2SiO_4$], pyroxene ($M_2^{2+}Si_2O_7$), amphibole [$M_7^{2+}\{(Al,Si)_4O_{11}\}(OH)_2$], biotite mica [$(K,H)_2(Mg,Fe)_2(Al,Fe)_4(SiO_4)_3$], orthoclase feldspar ($KAlSi_3O_8$), muscovite mica [$KAl_2\{AlSi_3O_{10}(OH)_2\}$], quartz ($SiO_2$), zeolites, and hydrothermal minerals.[1,3-6] The basic structural unit in all silicates is the SiO_4 tetrahedron. The presence of metal ions in the silicates is responsible for their structural diversity and thermal stability. Silicates were classified based on the mode of oxygen binding to silicon atoms, either monomeric SiO_4 unit or sharing of oxygen atoms in the corner with other silicon atoms, thereby forming chains, rings, sheets, and three-dimensional networks.[1-3]

1.2. Historical Development of Zeolites from the Perspective of Silicate Chemistry

The history of zeolites dates back to 1756 when they were discovered by the swedish mineralogist Cronstedt.[7] He observed that certain stones when heated using a blowtorch started to hiss and bubble, as though they were boiling. He called these stones zeolites, a greek word that denotes “boiling stone”. Later Weigel and Steinhoff found that *chabazite*, a naturally occurring mineral, adsorbs selectively methanol, ethanol, or formic acid but not acetone, benzene, and ether.[8] McBain interpreted this phenomenon in terms of molecular size differentiation between the molecules trapped in the empty spaces of dehydrated zeolites and hence he called it “*molecular sieve effect*”.[9] Further studies on zeolites were extended to applications of these materials as ion exchangers, gas sorption matrices and stereo selective catalysts.[10-13]

Zeolites, according to the original definition, are aluminosilicates with the general composition $M_{x/n}[(AlO_2)_x(SiO_2)_y]\cdot mH_2O$ where cations M of valance *n* neutralise the negative charges in the aluminosilicate framework. The primary building units of zeolites are SiO_4 and AlO_4 tetrahedra linked together *via* either corner or edge sharing. This leads to the formation

of four-, and six-membered rings (SBU). Furthermore, these rings could be combined to form three–dimensional structures with regular arrays of channels.[14-17]

Although a large number of naturally occurring zeolites were known, only *chabazite* was found to withstand repetitive hydration / dehydration cycles without destroying the lattice. Unfortunately, *chabazite* is precious and has a very low abundance. This led scientists to find alternative routes to replicate zeolites. In 1949 Milton synthesised the first man-made zeolites, Linde A and X, *via* hydrothermal routes and Linde X was found isostructural with the naturally occurring mineral *faujasite*.[18] Following this strategy a variety of zeolites was prepared by varying either the starting material compositions (such as silica and alumina) or the reaction conditions.[19] The extensive utility of zeolites is also due to their structural diversity within the frameworks. Zeolites are microporous materials containing regular pores and channels of molecular dimensions within the crystalline lattice.[20,21] The presence of cations within the framework contains coordinated water molecules that can be removed by heating and the resulting empty space is highly useful for the adsorption of small molecules. Moreover, these cations (it may be even H^+) can be exchanged with other metal ions having higher positive charges, thereby creating an imbalance of charge density within the framework that can be utilized for catalysis. The catalytic properties can be further modified by the aluminum content of the zeolites.[14]

The first type of synthetic zeolites, ZSM-5, with high variation of Si/Al ratio (from 20 to infinity) was synthesised in 1972, by a hydrothermal route in the presence of tetraalkylammonium cations.[22] In a later report, it was shown that the Al-free ZSM-5 can also be synthesised.[23,24] The presence of the tetraalkylammonium ions within the surface of the framework can be removed by calcination and hence the resulting Si-(OH)-Al could be used as an acidic catalyst for cracking of crude oil and conversion of methanol to gasoline mixture.[25-27] Moreover, the hydroxyl groups present in these sieves can be used for the

incorporation of other metal ions. Metal-doped zeolites have been extensively used as catalysts in many petroleum manufacturing processes for the separation and cracking of alkanes.[28-31] Nowadays a variety of zeolites is in use for regioselective and shape selective catalysts for the synthesis of fine organic chemicals.[14, 32] Recently, there have been reports on the synthesis of open framework zeolites with large pore sizes using appropriate structure directing agents.[33]

1.3. Need for Model Compounds

The synthesis and catalytic studies of zeolites have been dominated in the last century leaving behind some questions: (a) factors controlling the mechanism of the crystallisation of zeolites has not yet been fully understood [19,34,35] (b) in case of hetero-metal incorporated zeolites, the exact location of the metal ion is difficult to determine [36,37] (c) even though the catalytic activity of zeolites has been studied for a variety of reactions, the understanding of the catalytic centers, *e.g.* the intermediates, the coordination geometry of the catalytic active site *etc.*, is still in elementary stages or rather speculative. This makes it necessary to synthesise suitable model compounds that can either mimic the geometry of the building blocks in zeolites or have the presence of catalytic centers essential for a particular transformation.

This has given necessity for studying other naturally occurring silicate / phosphate minerals. In some cases, the utility of these minerals has been studied well for a long time, *e.g.* asbestos, feldspar, willemite, *etc*.[1,38-40] The studies on soluble-silica are particularly important in the industry[41] as it helps to understand the nature of the intermediate formation of orthosilicic acid and polysilicic acid. The existence of orthosilicic acid has been claimed and proven in the solution, but there are no reports on its isolation in the solid state due to the self-condensation and cross-linking tendencies leading to the precipitation of “polysilicic

acid" with variable compositions $[SiO_x(OH)_{4-2x}]_n$. Moreover, it was postulated that orthosilicic acid is formed as an intermediate during the hydrothermal synthesis of zeolites / silicate minerals. Under alkaline conditions these reactive intermediates condense with added metal precursors to yield zeolites. So a vital step in silicate chemistry is to understand the condensation behaviour of Si-OH groups and the tailoring of the reactions to obtain specific products. The following section describes the reports on the chemistry of stable silanols and metallasiloxanes.

1.4. Metallasiloxanes as Model Compounds and Precursors

In recent years considerable attention has been focused on the synthesis of advanced materials from their single source molecular precursors.[42-47] This method has been used for synthesising the metal oxide precursors through the respective metal alkoxides using sol–gel method.[48-53] The primary task would be then to rationalise the formation of these materials with respect to the molecular level control and to syntheses of new materials with tailored properties. Moreover, the preparation of compounds containing three-dimensional structures has given an insight into the atomic level control of the final materials by this method.[42-47,54-58] This leads to the homogeneity and the desired composition of the resulting materials. Recently, this idea has been extended toward the preparation of metal silicate and phosphate systems due to their wide range of applications in material science and catalysis.

The Si–OH group containing compounds, which can be regarded as derivatives of orthosilicic acid $[Si(OH)_4]$ by subsequently substituting the hydroxyl groups, have been termed as monosilanols (R_3SiOH), silanediols $[R_2Si(OH)_2]$, disilanols $[\{R_2Si(OH)\}_2O]$, silanetriols $[RSi(OH)_3]$ and trisilanols $[\{RSi(OH)\}O]_3$ (R can be any alkyl, aryl or alkoxy substituent) (Chart 1).[59]

The organic moiety "R" attached to the silicon atom plays a vital role in the stability of the silanols.[59-62] Some of these silanols have been used as starting materials to prepare a variety of metallasiloxanes.[63-66,71] As pointed out earlier, the Si–O–M linkages are the

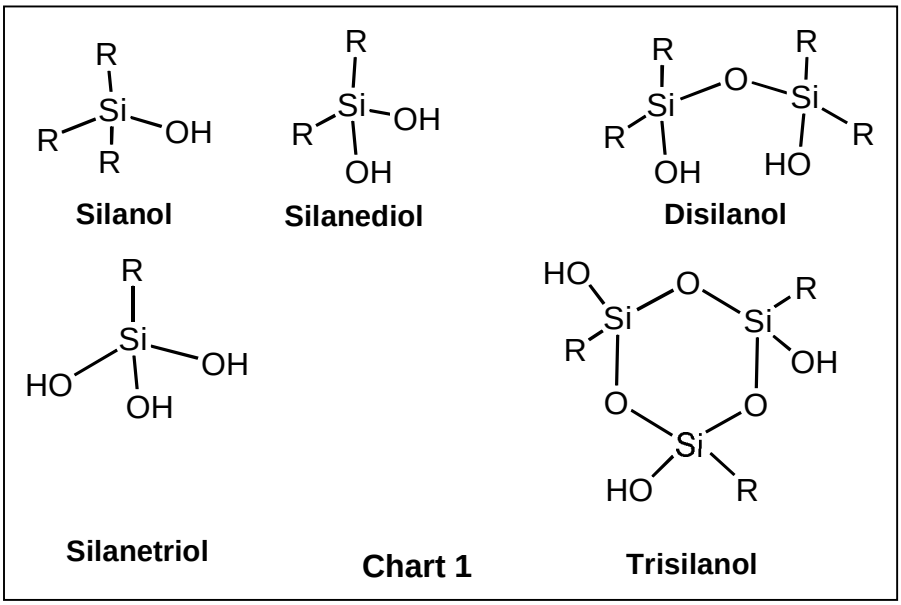

Chart 1

prominent structural moieties in most of the silicate minerals as the presence of a metal atom within the siloxane framework changes the properties of the metallasiloxane compounds. The utility of soluble metallasiloxanes as model compounds for open-framework silicates and heterogeneous catalytic systems, and also potential precursors for mixed metal oxide system has been well documented recently.[64-74]

Metallasiloxane synthesis is known since end of the 19th century.[75] The metallasiloxanes derived from monosilanols have been extensively studied over the past several decades. The structures obtained from these reactions vary from dimeric, trimeric, tetranuclear and to polymeric units of $[M(OSiR_3)_x]_n$.[63,76-78] However, for the metallasiloxane framework with two- and three-dimensional cores, one has to use silanols bearing more than one hydroxyl group on silicon. In the last two decades also, silanediols and disilanols have been widely used to prepare metallasiloxane compounds. The reactions of silanediols and disilanols with metal precursors yielded acyclic, cyclic and polymeric units of the resulting

metallasiloxanes with different rings sizes and chain lengths.[65,66,78-80] It has been also realized the metallasiloxane obtained from silanetriols or incompletely condensed silanols, *e.g.*, trisilanols with transition metal complexes could be used as realistic models for the metal-modified silica surfaces.[67]

A significant aspect in the synthesis of silanetriols that needs attention is its facile self-condensation with elimination of water in the presence of acidic impurities or at higher temperatures. The stability of these compounds depends on the organic group attached to the silicon atom in the silanetriols. A variety of silanetriols in which silicon is bonded to carbon, nitrogen, oxygen or a transition metal have been reported.[59] Initial reaction with the *tert*-butyl silanetriol with rhenium oxide resulted in self-condensation forming a four-membered siloxane ring.[81] Later, Roesky *et al*. have prepared a series of stable aminosilanetriols by incorporating bulky organic groups on the aromatic ring. These silanetriols contain an additional trimethylsilyl moiety bound to nitrogen to prevent self-condensation reaction. Silanetriols have been extensively used for the further preparation of a variety of three-dimensional cage structures.[71-74] Among them, the core structures of neutral and anionic aluminumsiloxanes, either from aminosilanetriols or a cobalt cluster substituted silanetriol resembling the SBU's of zeolites (Scheme 1).[82,83] The studies on hydroformylation reaction of 1-hexene have been carried out using the cobalt cluster substituted group 13 metallasiloxanes as catalysts. The results indicate that the catalytic properties of these compounds decreases down the series of aluminum to indium siloxanes due to the decrease in acidic nature of these metal atoms.[83]

Extension of these studies has been focused on the preparation of compounds with group 4, 5, and group 14 metallasiloxane cage structures,[71,84-86] among them the important being the isolation of the first stable cubic titanasiloxane containing peroxo groups attached to titanium, which is a key intermediate peroxo species involved in epoxidation reactions of

olefins. It was prepared by substitution of the alkoxy group on titanium (Scheme 2) in cubic titanosilaxane with the *tert*-butyl peroxo moiety using *tert*-butyl hydrogen peroxide. [87]

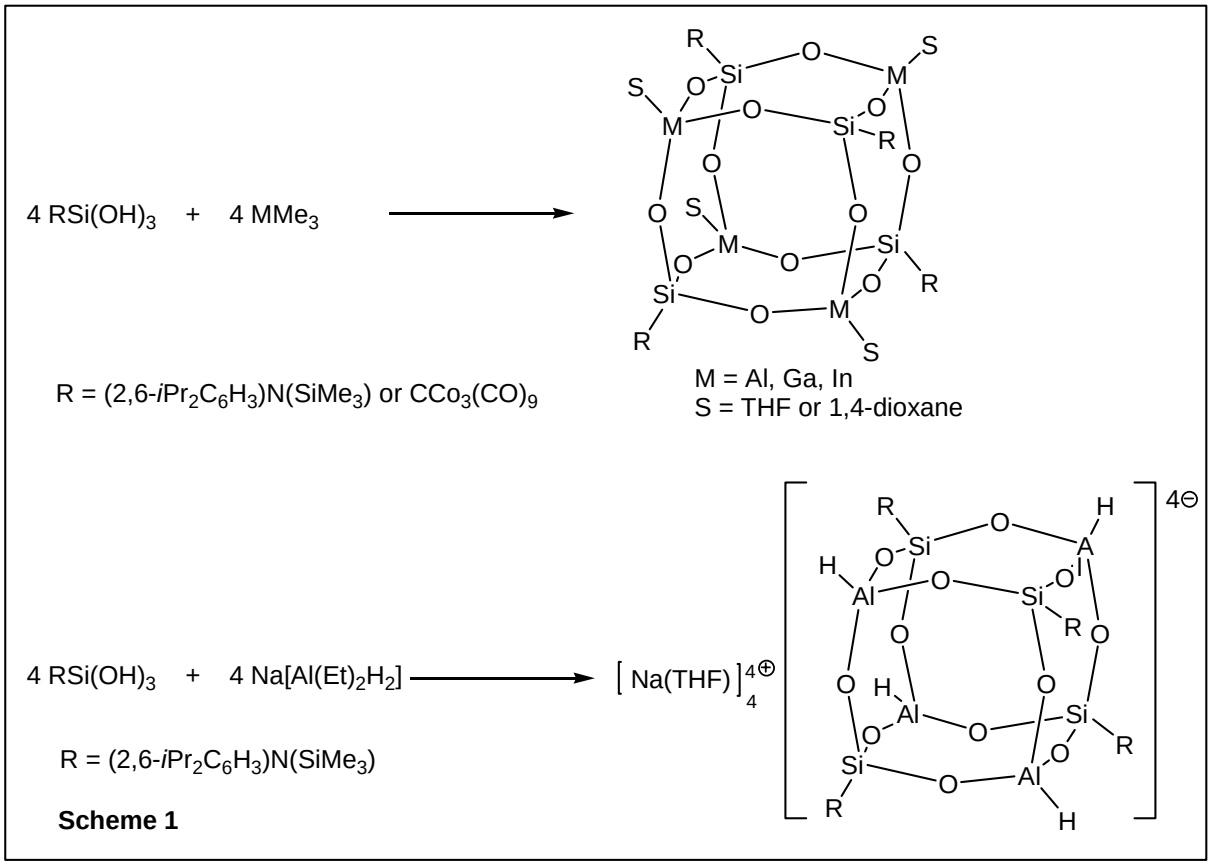

Scheme 1

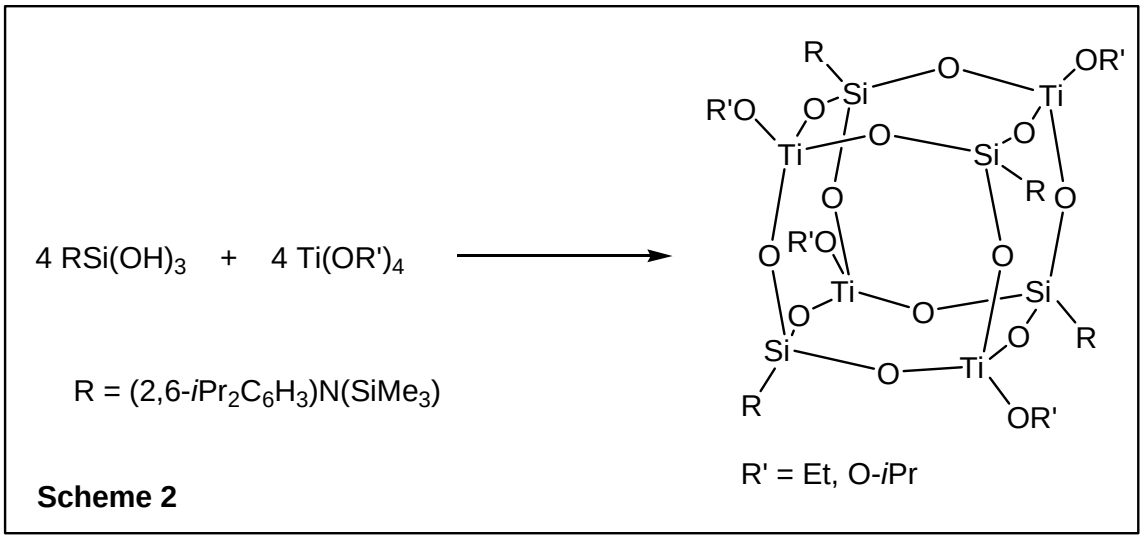

Scheme 2

In 1967, it was thought that since $AlPO_4$ is isoelectronic to SiO_2, it might be possible to prepare zeolites containing tetrahedral PO_4 groups in the framework by a synthesis in acidic medium rather than in alkaline medium used for the synthesis of zeolites.[19] Since then

the chemistry of metallaphosphates has been extensively studied in view of preparing new varieties of molecular sieves.

1.5. Phosphates

The solid-phase inorganic phosphates constitute a variety of materials of considerable technological importance. They are widely occurring in nature in the form of minerals and also in the bones of living animals.[88] They are the important source for the preparation of phosphoric acid and other phosphorus compounds. Apart from the scientific interest, phosphate materials reflect their practical applications as fertilisers, catalysts, phosphors, ion conductors, piezoelectric materials, biotechnological materials, and sorbents.[89] Moreover, the presence of organophosphates in the backbone of DNA and RNA regulates the reproductive cell processes, and they are also involved in many metabolic and energy transfer reactions.[1]

The metallaphosphate chemistry has shot into prominence since the first synthesis of aluminumphosphate based zeolites by Flanigen *et al.* in 1982.[90] This strategy was extended to the synthesis of MAPO, SAPO, MeAPSO, EIAPO, and EIAPSO by modifying either by incorporation of metal atoms or isomorphic substitution by silicon, in the aluminumphosphate framework.[91] The synthesis of aluminumphosphate has demonstrated that the molecular sieves are not only the traditional aluminumsilicates / high silica zeolites, but also all other microporous materials which have a three-dimensional and appreciably covalent framework. In 1991, Gier and Stucky have published the first berryllo- and zinco-phosphate and -arsonate molecular sieves.[92] These studies have been further extended to the synthesis of mixed metal phosphates containing multidimensional rings and channels.[93-95] Another important development in this area is preparation of open framework structures of metallaphosphates with large pore sizes using structure directing agents. The open framework

phosphates thus synthesised will have a greater utility in terms of adsorption of larger organic groups or incorporation of catalytically active metal complexes.[33]

1.6. Metal Phosphonates

Similar to silanols, P–OH containing compounds stabilised by organic groups are extensively used for the preparation of metallaphosphate or metallaphosphonate systems. The metallaphosphonates are used as potential molecular precursors for metallaphosphates. The ligands derived from phosphoric acid groups are widely used for this purpose (Chart 2).[96-104]

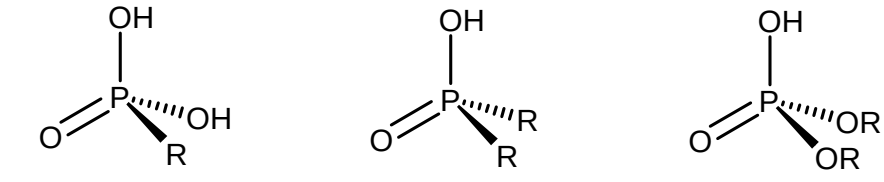

Chart 2

In recent years, metallaphosphonate systems have been widely studied due to their applications in the area of ion exchange, catalysis, sorption, sensors, non-linear optics,[105-107] and also their ability to act as model compounds for SBUs of zeolites.[96-100] The metal phosphonates can be divided into two categories depending on their three-dimensional structures:

(a) layered metal phosphonates

In layered metal phosphonates, the binding mode within the system can be considered as inorganic phosphates which consists of layers of organic moieties between two adjacent inorganic metal phsophates, *e.g.* the layered structures of the α–zirconium phosphate $Zr(HOPO_3)_2$ is comparable to $Zr(RPO_3)_2$ and $Ca(RPO_3H)_2$. The common features in the above cases are the planar network of the Zr and Ca metal centers that are connected together with

the phosphonate oxygen atoms above and below the planes leading to the option to bind these layers by using suitable bifunctional ligands such as $H_2O_3P–R–PO_3H_2$. Clearfield and others have used this synthetic strategy and prepared a variety of one-, two-, and three-dimensional structures by interconnecting the layers using different bis(phosphonic acids).[105] The layered metal phosphonates were prepared generally by hydrothermal routes by heating the aqueous mixture of appropriate metal salts, phosphonic acid and an amine. The resulting compounds have porous lamellar structures and the space between these layers can be utilized for absorbing small organic molecules. Furthermore, the presence of unreacted OH groups can be utilised to introduce hetero-metal centers.

Recently, Zubieta and coworkers have synthesized a variety of vanadyl phosphates and organophosphonates with two- and three-dimensional layered structures which are proven as catalysts for the conversion of butane to maleic anhydride.[107]

(b) metal phosphonate cages

The molecular structures of metal phosphonate cages have been studied extensively since the metal phosphonate cages can be considered as SBUs of zeolites / molecular sieves. Furthermore, these building blocks have been perceived as potential precursors for the preparation of metal phosphate molecular sieves. There have been a few successful synthetic routes to prepare tetrameric, cubic, hexagonal, and other related structures of SBUs of zeolites.[97-100] One of the routes involves the condensation of metal alkyls with different alkyl phosphonic acids with the elimination of alkanes as side products (Scheme 3). The other method is the reaction of metal chlorides with trimethylsilyl phosphate with the elimination of trimethylsilyl chloride.[96] There also have been reports on the synthesis of novel three-dimensional aggregates of mixed metal phosphonates containing Lewis acidic metals, *e.g.* group 13 metals and alkali metal ions. These studies have been extended to other transition

metal containing metallaphosphonates.[97,108-111] The results of these studies were remarkable especially with the aggregate formation of copper and zinc phosphonates containing multinuclear metal centers.[108-110]

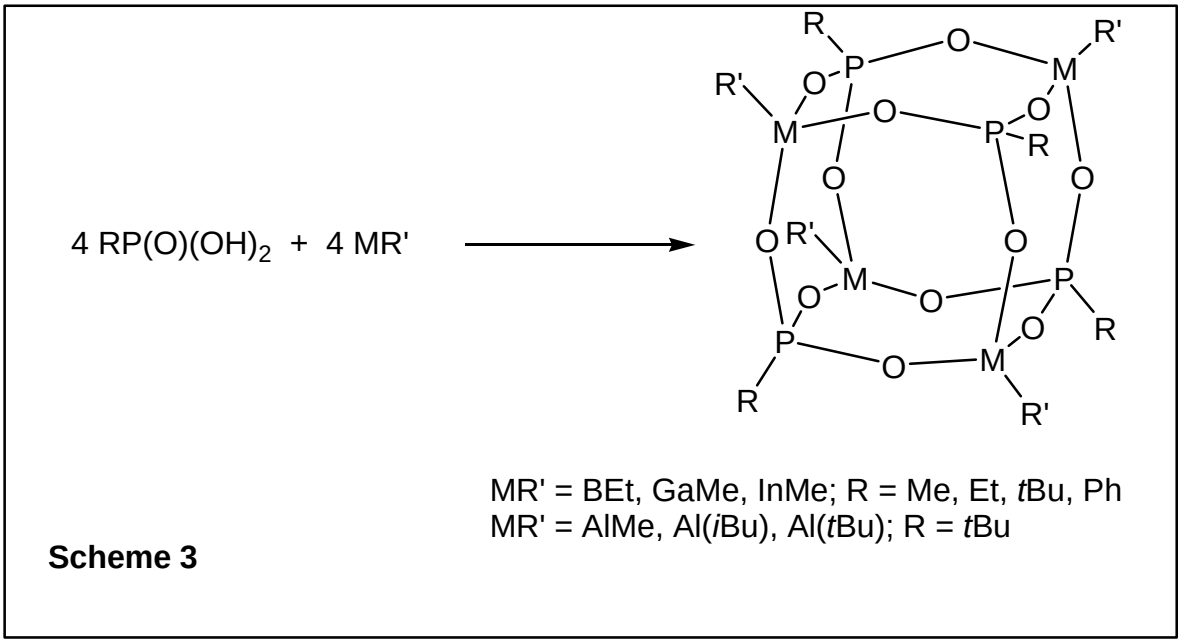

Scheme 3

1.7. Scope and Aim of the Present Work

The Sections 1.1–1.6 describe the importance of studies on metallasiloxanes and -phosphonates in terms of scientific and industrial applications. Further it is also clear that the studies on incorporation of transition metal atoms in the siloxane and phosphonate framework is of importance because these compounds can be considered as models for heterogeneous catalytic systems. There have also been attempts to demonstrate the use of metallasiloxanes / -phosphonates as molecular precursors for metallasilicate and phosphate materials.[68-70]

The molecular structures of metallasiloxanes / -phosphonates would also give an understanding of the molecular level propagation in the formation of three-dimensional extended structures *via* aggregation of molecules.[72,112] Initial attempts of the synthesis and characterisation have been reported in recent years.

This presentation describes the studies on group 12 metal systems (especially zinc and cadmium derivatives) since zinc is a transition metal having resemblance to the main group metals.

The objectives of the present work are

1. to synthesise bulky silanols / phosphonic acids to study the effect of the steric control on the cluster synthesis,
2. to synthesise and characterise the soluble zinc siloxanes which could be used as precursors for zinc silicate phosphor and zinc silicate three-dimensional assemblies,
3. to synthesise mixed metal zinc siloxanes which could serve as suitable synthons for the preparation of mixed metal silicate materials,
4. to synthesise suitable zinc phosphonate compounds that can be utilized for precursors for the corresponding zinc phosphates,
5. to extend the above methodology to cadmium siloxanes / phosphonates which can be used as precursors for the preparation of cadmium containing materials,
6. to control the stoichiometry of the resulting zinc siloxanes and phosphonates,
7. to synthesise iron siloxanes which could serve as suitable models for naturally occurring iron silicates and for the preparation of iron containing silicates.

2. Results and Discussion

In recent years, significant progress has been made toward the development of mechanisms for the formation of zeolites, metallasilicates, aluminum and zinc phosphate molecular sieves.[19,33,113] In this regard there have been several reports on thermochemical calculations of the dense and the microporous phases. There have also been studies on the role of template in the formation of a particular structure.[19,33] Some models account for the final framework structures by postulating various building blocks, where the primary building units are starting monomeric metal oxide polyhedra and small four-ring, six-ring and other secondary building units (SBUs) as in zeolites. Some of these polyhedra have been synthesized recently using different methods.[71-74,96,97]

On the other hand, there is an increasing effort to synthesize suitable molecular metal precursors for the preparation of new varieties of metallasilicates and phosphate materials. One of the main aim of this investigation is to try and synthesize smaller soluble siloxanes and phosphonate molecules containing group 12 metals and whose core structure would resemble one or more of these SBUs and also a suitable synthon for the corresponding metal silicate or phosphate containing compounds.

Over the last few years, our research group has demonstrated that alkane elimination reactions involving metal alkyls and organosilanetriols were the most facile route for high yield syntheses of polyhedral metallasiloxanes and -phosphonates (Schemes 1 - 3).[71-74,97] This synthetic strategy seems to be more suitable than routes involving metal halides. In the present study several reactions of group 12 metal alkyls and iron amide with an aminosilanetriol or phosphonic acids have been carried out.

2.1 Zinc Containing Silicates

The synthesis of tailored materials using molecular precursors has been widely used in recent years as an alternative to the standard solid-state procedures that involve crushing,

grinding, ball milling, and high-temperature calcination reactions. Moreover, in the latter case, the resulting mixture may not be homogeneous and it is very difficult to remove the impurities. As an example, manganese-doped zinc orthosilicate (*willemite*, Zn2SiO4, a naturally occurring mineral), due to its high luminescence, has been widely used as a green-phosphor in the display industry and for the construction of electroluminescent devices.[38] Emission from this material is attributed to a d-level spin-forbidden transition for the Mn2+ ions.[39] Tilley et al. have prepared the zinc orthosilicate by thermal decomposition of molecular zinc siloxane and polymeric zinc siloxane compounds however, the resulting zinc orthosilicate is contaminated with silica.[114] This implies the necessity of the "atomic level control" on compounds with three-dimensional structures.

On the other hand, zinc incorporated H-ZSM-5 is utilised in the petroleum industry for the aromatisation of alkanes with increased conversion rates and high selectivities.[28] Also the Lewis acidic nature of the zinc atoms in Zn/H-ZSM-5 makes it useful as a catalyst for the conversion of methyl halides to hydrocarbons and for the dehydrofluorination of freons.[115] Although the catalytic properties of the Zn/H-ZSM-5 system are reported, the mechanism at the catalytic centers of the above reactions have not yet been understood.[28] It has been realised over the past decade that metallasiloxanes derived from silanetriols could be used as model compounds for metal doped zeolites and they serve as potential precursors for metal containing silicate assemblies.[71-74]

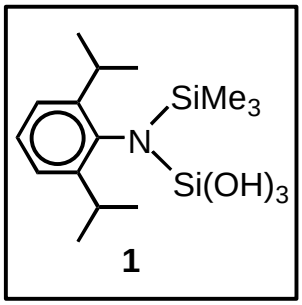

Figure 1. Aminosilanetriol Used in the Metallasiloxane Synthesis

Recently, it has been shown that the condensation of aminosilanetriol **1** (Figure 1) with metal alkyls resulted in polyhedral metallasiloxanes in high yield under elimination of alkanes as side products. Moreover, the characteristic feature of these compounds is that the "atomic level control" of reactants to products is maintained. In the present study we have synthesised zinc siloxanes using dialkyl zinc compounds as metal source.

2.1.1 Synthesis of an Anionic Zinc Siloxane

Due to their ability to act as model compounds for the molecular sieves, the study of alkali metal substituted metallasiloxane systems is important, *e.g.* the structure of an anionic aluminumsiloxane containing square pyramidal Na^+ ions having similar coordination geometry around Na^+ as in the sodium zeolite-A.[82a] There have been no efforts made on the synthesis of anionic zinc siloxanes from other well-studied silanols. This led us to examine the synthesis of anionic zinc siloxanes through a reaction of aminosilanetriol **1** with a mixture of $ZnMe_2$ and MeLi.

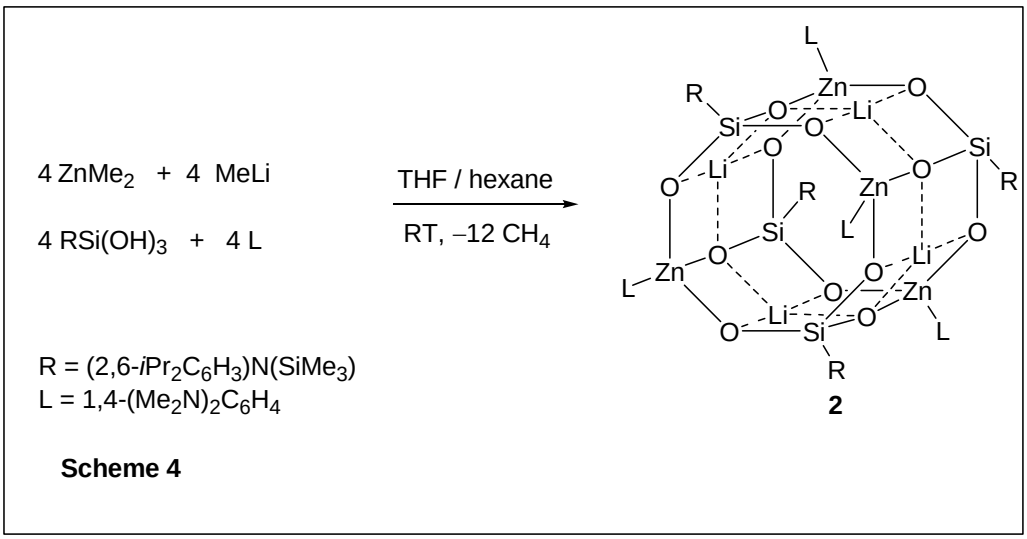

Scheme 4

The reaction of **1** with a mixture of $ZnMe_2$ and MeLi, (1:1), in the presence of an added base (L) in THF/hexane at room temperature afforded $[(L)ZnLi(O_3SiR)]_4$ (L = 1,4-$(NMe_2)_2C_6H_4$, R = (2,6-*i*$Pr_2C_6H_3$)N($SiMe_3$)) (**2**) in moderate yield (Scheme 4).[116] Our initial attempts to crystallise the resulting compound from the reaction mixture without addition of

an amine were not successful. The addition of *N*,*N*,*N*',*N*'-tetramethyl-l,4-phenylenediamine (L) was essential to obtain single crystals of **2** suitable for a X-ray structural analysis. Compound **2** is soluble in common organic solvents.

Compound **2** has been fully characterized by means of analytical, spectroscopic, and single crystal X-ray diffraction studies. The absence of bands in the range 3000 - 4000 cm^{-1} in the IR spectrum indicates that all three –OH groups of **1** have reacted with zinc dimethyl. The ^1H NMR spectrum of compound **2** (in C_6D_6 or THF-d_8) shows broad resonances for the protons on the silanetriol. An intense singlet at δ 2.81 ppm in the ^1H NMR for the methyl protons on the nitrogen atoms of L, both for coordinated and non-coordinated nitrogen containing methyl groups was obtained. This indicates that the amine is not coordinated in solution to zinc atoms as in the case of the solid-state structure. The variable temperature of the ^1H NMR spectrum also gave no indication for the coordination of the amine. So we assume that the broadening of the resonances in the ^1H NMR spectrum is due to dynamic processes and skeletal rearrangements of **1** in solution. It is probable that the structure of **2** in solution is different from that found in the solid-state.

2.1.2. Molecular Structure of $[(L)ZnLi(O_3SiR)]_4$ (L = 1,4-$(NMe_2)_2C_6H_4$, R = (2,6-*i*$Pr_2C_6H_3$)N($SiMe_3$)) (2)

Compound **2** crystallises in the monoclinic space group $P2_1/n$ with one molecule of hexane in the asymmetric unit. The molecular structure of compound **2** has a planar central eight-membered Li_4O_4 ring sandwiched between two puckered eight-membered $Zn_2Si_2O_4$ rings. Each lithium atom is coordinated to four oxygen atoms of the zinc siloxane framework. No additional solvent molecules are coordinated to lithium, thus making them four-coordinated. The coordination geometry is quite contrast to the lithium or sodium ions of the previously reported anionic aluminumsiloxanes where the cations possess square pyramidal

geometry.[82a] The oxygen atoms in the two eight-membered $Zn_2Si_2O_4$ rings are bridging to zinc, silicon, and lithium atoms in a μ_3-O fashion, whereas the oxygen atoms in the eight-membered Li_4O_4 cycles are bridging in a μ_4-O fashion. Each zinc atom is coordinated to one of the N-atoms of the added base (Figure 2). Hydrophobic groups, surrounding the central $Li_4Zn_4Si_4O_{12}$ polyhedron, render the compound **2** highly soluble in common organic solvents.

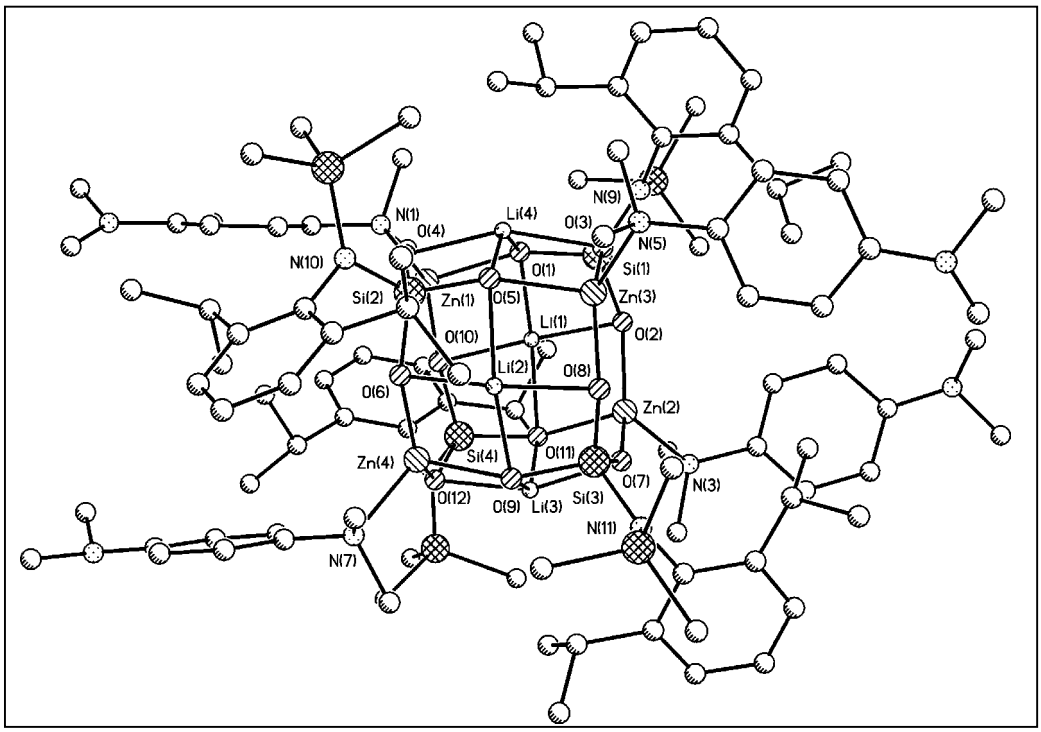

Figure 2. Molecular Structure of 2

The average Si–O bond length in compound **2** (1.624 Å) is slightly longer than those observed for other group 13 metallasiloxanes.[82] The average Zn–N bond length (2.120 Å) is comparable to that in similar compounds reported in the literature.[117] The shortest Zn–O bond distance is observed for Zn–μ_3–O bond (~1.899 Å) and the longest is observed for Zn–μ_4–O (~2.023 Å). Similarly, two different short and long bond distances for Li–O were also noticed (Li–μ_3–O 1.998(3), and 2.016(3) Å, Li–μ_4–O 2.029(3), and 2.089(3) Å). A similar Li–O bond length for anionic group 13 metallasiloxanes has also been reported.[82]

2.1.3. Synthesis of Zinc Siloxanes (3-8)

Earlier studies on zinc siloxanes show that the degree of aggregation of monosilanols is influenced by the steric and electronic properties of the substituents on oxygen. Thus the reactions with different substituted organo monosilanols with zinc dialkyls or -amides yielded dimeric, trimeric and tetranuclear zinc siloxanes.[76,114,118] In the present study, we have maintained the concentration of aminosilanetriol constant and varied only the zinc dialkyl concentration. This synthetic strategy would enable us to understand the degree of aggregation and the condensation process in these reactions.

2.1.4. Synthesis of $[Zn(THF)(O_2(OH)SiR)]_4$ (R = (2,6-*i*$Pr_2C_6H_3$)N($SiMe_3$)) (3)

The reaction of **1** with $ZnEt_2$ in a 1:1 molar ratio produced predominantly **3** by sequential formation of Si–O–Zn linkages (Scheme 5).[119] Whereas in case of the reaction between **1** and zinc dimethyl not only **3** but also another product was formed for which an additional resonance was found in the silicon NMR spectrum at δ 71.8 ppm. Compound **3** is highly soluble in common organic solvents such as benzene, toluene, diethyl ether and THF. Compound **3** was characterised by means of analytical and spectroscopic techniques. Furthermore, the structure of **3** was confirmed unambiguously by single crystal X-ray diffraction studies.

The IR spectrum of **3** shows a broad band around 3300 cm^{-1} for the OH stretching frequencies of the silanol groups. The ^1H NMR spectrum of **3** displays sharp resonances due to aryl, isopropyl and methyl protons and a slightly broad resonance is assigned to the protons of coordinated THF molecules. The appearance of two sets of different NMR signals for methyl protons in isopropyl groups is consistent with the crystal structure of **3** if the rotation of the aromatic groups about the C–N bond is restricted. The absence of any resonances assignable to zinc ethyl protons suggests that both ethyl groups have reacted with silanetriol

under the formation of **3**. By comparing the analytical and spectroscopic data we were able to predict partially the structure of **3**. However, single crystal X-ray diffraction studies, finally confirmed the formation of a drum-shaped core.

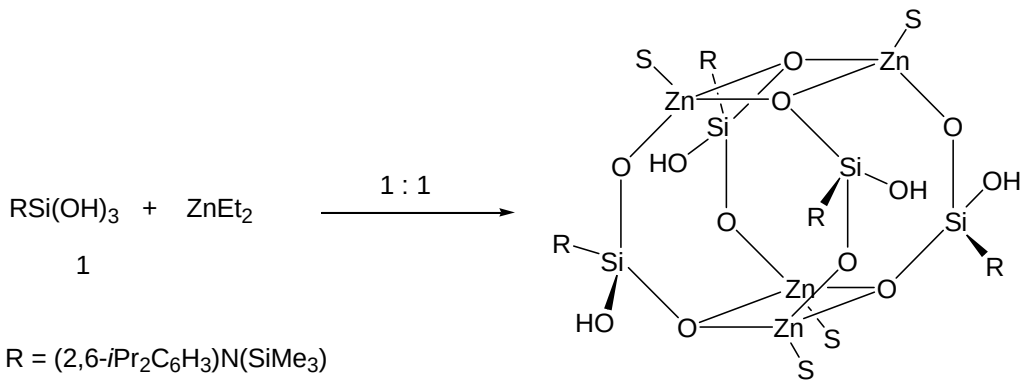

Scheme 5

2.1.5. X-ray Crystal Structure of $[Zn(THF)(O_2(OH)SiR)]_4$ (R = (2,6-*i*$Pr_2C_6H_3$)N($SiMe_3$)) (3)

The molecular structure of **3** is shown in Figure 3. Compound **3** crystallises in the monoclinic space group $P2_1$ with one molecule of solvent toluene in the asymmetric unit. The molecule of **3** possesses a pseudo four-fold (S_4) symmetry and consists of two eight-membered $Zn_2Si_2O_4$ units connected by four Zn–O bonds forming a drum-shaped core. These two $Zn_2Si_2O_4$ rings are puckered and adopt a boat conformation. The four-membered Zn_2O_2 rings are almost planar and the zinc atoms of each ring are very close to the oxygens of the adjacent staggered ring.

The average Si–O bond length in **3** (1.61 Å) is slightly shorter than the values found in silanetriols, whereas the Si–OH bond lengths (av 1.64 Å) are comparable with those of silanetriols.[120,121] There are two types of Zn–μ_3–O bond distances observed in the Zn_2O_2

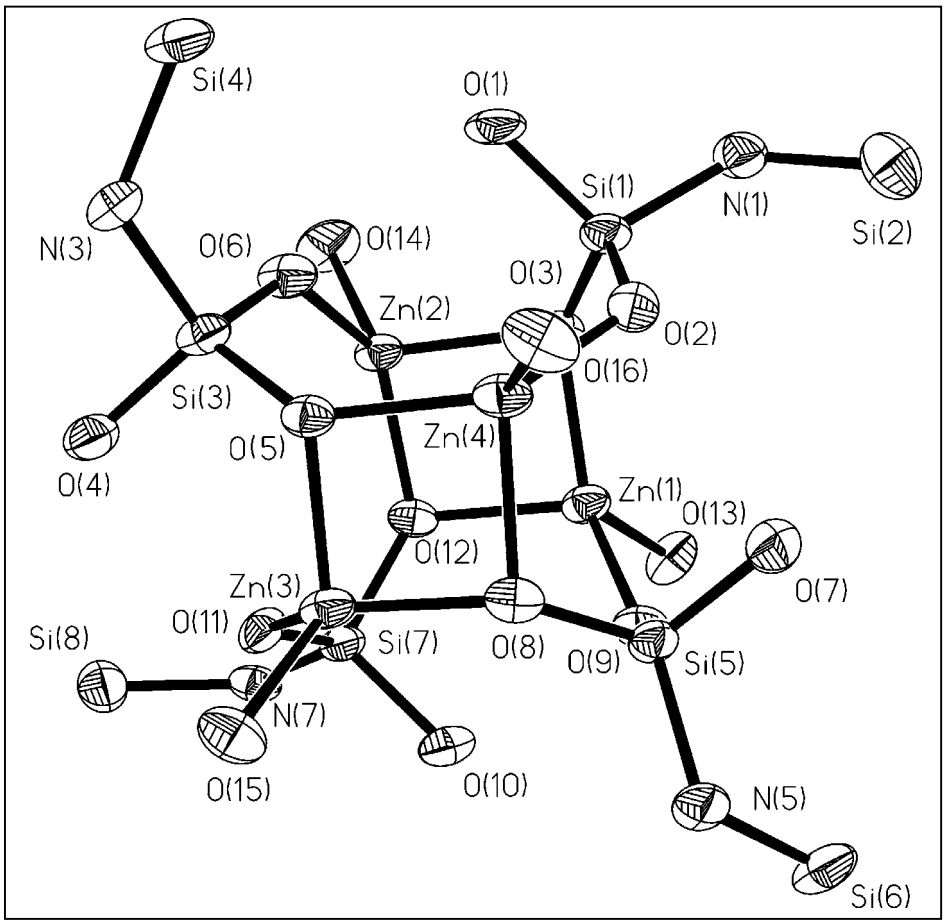

Figure 3. ORTEP plot of 3 showing the core structure (50 % probability level)

rings that are also responsible for the eclipsed conformation. The bond lengths of the σ–bonded Zn–μ_3–O (Zn(1)–O(3) 1.950(7), Zn(2)–O(12) 1.938(7), Zn(3)–O(8) 1.939(8) and Zn(4)–O(5) 1.943(8) Å) are similar to reported values for zinc siloxanes,[118] however, these values are shorter than the coordinated ones (av 2.016(7) Å). The distances of coordinated Zn–μ_3–O bonds and the coordinated THF oxygens are almost equal. The average Zn–μ_2–O (*e.g.* Zn(1)–O(9), Zn(2)–O(6), Zn(3)–O(11) and Zn(4)–O(2)) bond distance is 1.867(9) Å which is shorter than the σ–bonded Zn–μ_3–O distance in the ring. The diagonal distances between the zinc atoms in Zn_2O_2 (Zn(1)–Zn(2) 2.8396(19) Å and Zn(3)–Zn(4) 2.850(3) Å) suggest that there is a weak Zn•••Zn interaction.[122] The O–Zn–O bond angles within the Zn_2O_2 ring are close to 90^o showing that the four–membered rings are almost perfect rectangles.

2.1.6. Synthesis of $[Zn_4(THF)_4(ZnMe)_4(O_3SiR)_4]$ (R = (2,6-*i*$Pr_2C_6H_3$)N($SiMe_3$)) (4)

To find out the effect of the reagent stoichiometry on the product formed in the reaction, a reaction similar to that involving synthesis of **3** was carried out using $ZnMe_2$ and $RSi(OH)_3$ (2:1) in THF / hexane at room temperature. The onset of vigorous exothermic reaction was accompanied by methane gas evolution affording $[Zn_4(THF)_4(ZnMe)_4(O_3SiR)_4]$ (R = (2,6-*i*$Pr_2C_6H_3$)N($SiMe_3$)) (**4**) in good yield (Scheme 6).[123] Normally, as the aggregation of the molecule increases, the resulting compound solubility decreases.

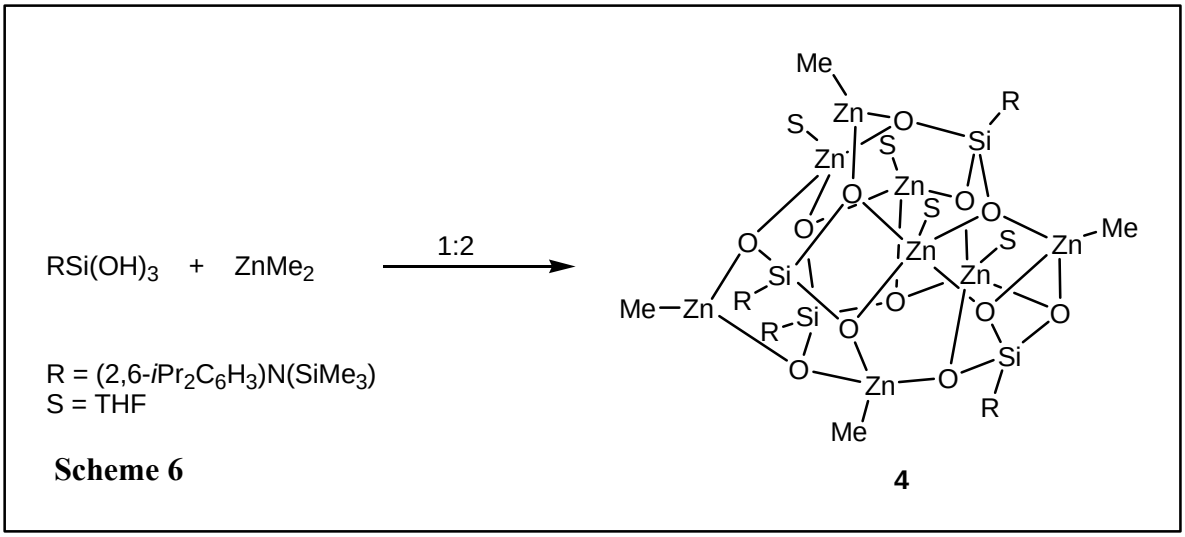

Scheme 6

However, in **4**, the presence of more methyl groups on the surface increases the solubility that helps to study the compound's nature in solution. Compound **4** has been characterised by analytical, spectroscopic and single crystal X-ray diffraction studies. The ^1H NMR spectrum (in C_6D_6) shows several multiple resonances for the methyl ($SiMe_3$, Zn–Me and *i*Pr), isopropyl–CH, and aryl protons, thus making the spectral assignment difficult. Furthermore, changing the deuterated solvent gave similar NMR resonances for the substituents. Two resonance values were obtained for the silicon in the SiO_3 moiety at –61.34, and –60.87. Based on the NMR results it was impossible to compare the solution structure of **4** to the solid-state. Therefore it can be assumed that compound **4** undergoes a dynamic process involving skeletal rearrangement, indicating the absence of a similar structure in solution.

2.1.7. Solid-State structure of $[Zn_4(THF)_4(ZnMe)_4(O_3SiR)_4]$ (R = (2,6-*i*$Pr_2C_6H_3$)N($SiMe_3$)) (4)

The solid-state structure of **4**·$(toluene)_3$ reveals that its molecular structure is made up of a $Zn_8Si_4O_{12}$ core as shown in Figure 4. The arrangements of zinc and silicon atoms within the molecule **4** are shown in Figure 5. The imaginary lines drawn between zinc and silicon atoms show that four of the eight zinc atoms and silicon atoms alternatively occupy the corners of a distorted cube. These zinc atoms have lost both methyl groups and each contains

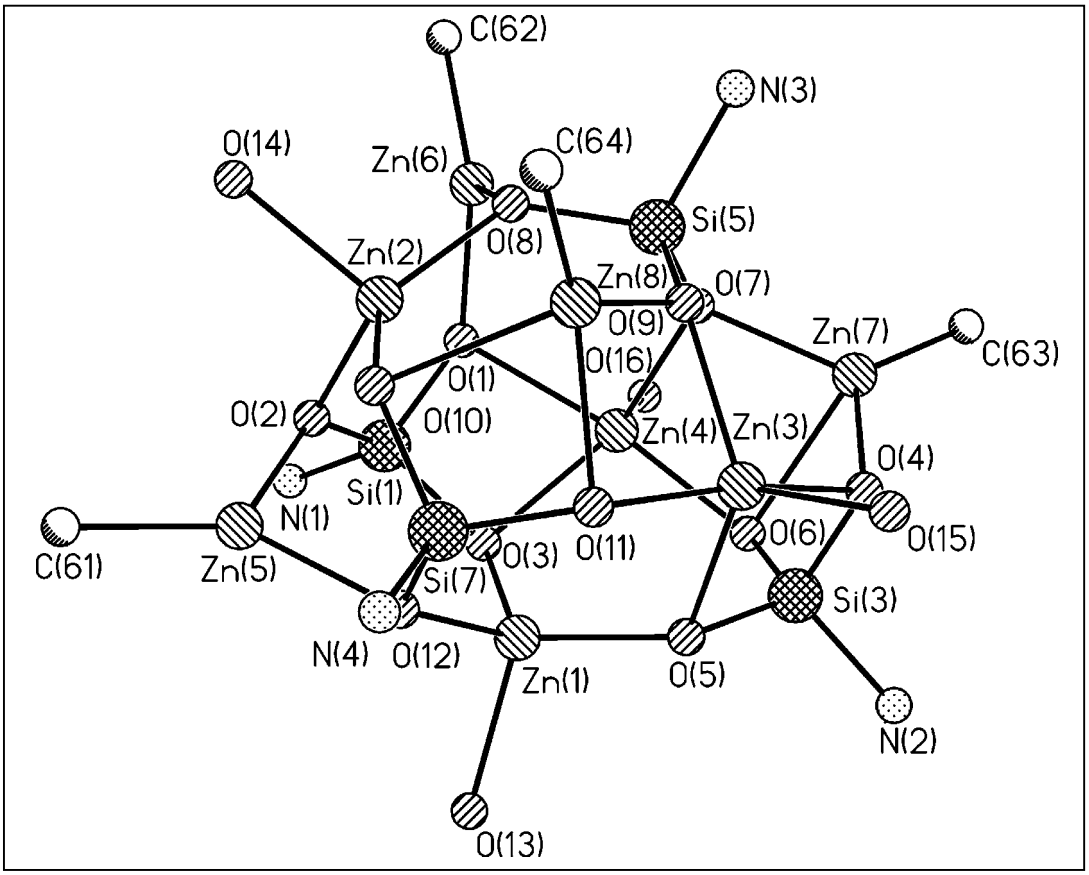

Figure 4. Core Structure of larger zinc siloxane aggregate 4

a coordinated THF molecule. The remaining four zinc atoms occupy adjacent faces of the cube and contain one methyl group on it. Interestingly, in **4,** the zinc atoms have three different coordination spheres around them.[118] Moreover in **4**, two have a trigonal planar geometry (Zn(5) and Zn(6)), two are in trigonal bipyramidal (Zn(3) and Zn(4)) environments

and the remaining four exhibit tetrahedral geometry (Zn(1), Zn(2), Zn(7) and Zn(8)). Thus four-, eight-, and ten-membered Zn_2O_2, Zn_4O_4, and Zn_5O_5 rings are formed.

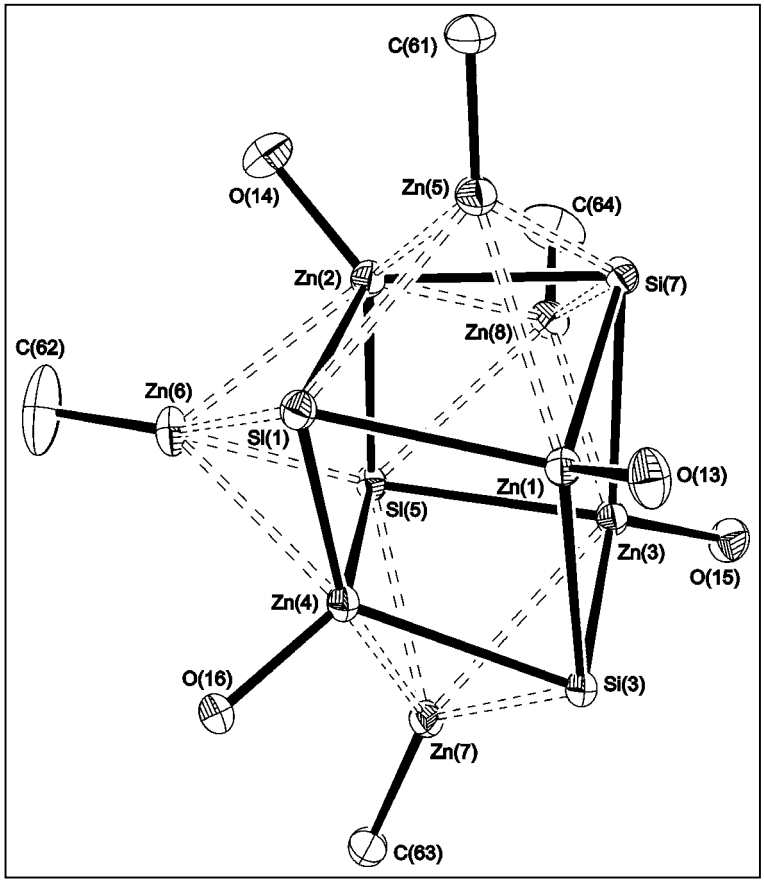

Figure 5. Arrangement of the Zinc and Silicon Atoms in 4

The Zn•••Zn distances (Zn(2)–Zn(5) 2.881(1), Zn(3)–Zn(8) 2.977(1), Zn(4)–Zn(7) 2.950(1) Å) indicate weak M–M interactions.[122] Similarly, the average bond distance between Zn•••Si is 2.748(1) Å and suggests that there may be interactions between them (the single bond distance between Zn and Si in $Zn[Si(SiMe_3)_3]_2$ is 2.342 Å[124]). The average bond lengths of Zn–C and Si–O (1.948(4) and 1.635(3) Å) are in agreement with the reported values.[118] Moreover, two unusually long Zn–O bond lengths are observed for the two tetrahedral zinc atoms (Zn(7)–O(6) 2.317(3) Å, Zn(8)–O(10) 2.352(3) Å) and the remaining fall in the range of 1.911(3) to 2.203(3) Å.

2.1.8. Conversion of 3 to 2 and 4

The formation of eight-membered ($Zn_2Si_2O_4$) and four-membered (Zn_2O_2) rings and the orientation of the OH groups around silicon atoms in **3** suggests that it could be reacted further to yield **2** and **4,** which have been previously made from **1** (Scheme 7).[119] Thus, four equivalents of zinc dimethyl react with **3** at room temperature to produce **4**. The fact that all of the spectroscopic and analytical data of this product were identical to those of **4**[123] strongly suggests that **4** could be an intermediate species in this reaction. Similarly, **2** was made from **3** with the addition of methyl lithium in the presence of *N*,*N*,*N*,*N*'-tetramethyl-l,4-phenylenediamine (L).[116]

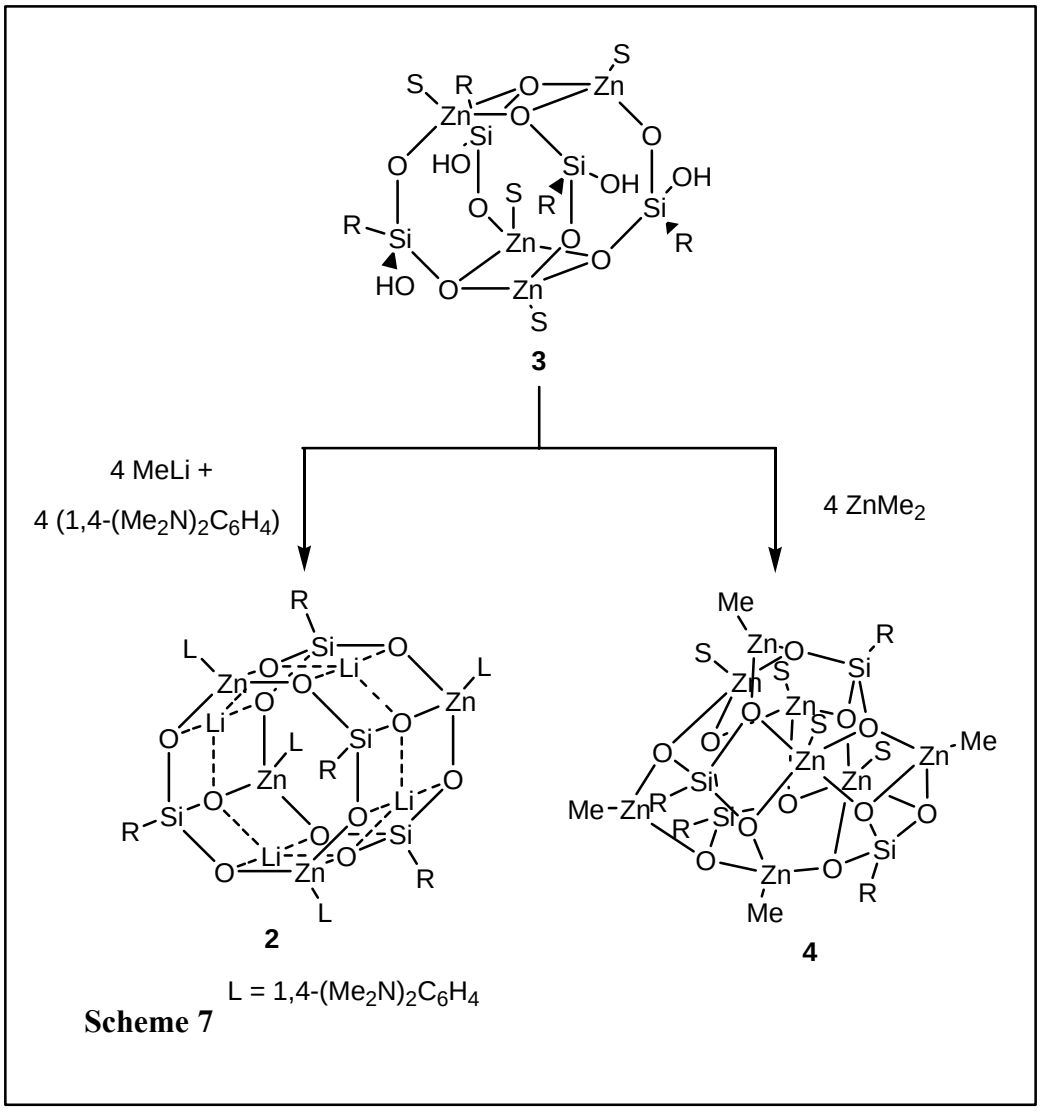

Scheme 7

2.1.9. Synthesis of $Zn_8Me_7(dioxane)_2(O_3SiR)_3$ (R = (2,6-*i*$Pr_2C_6H_3$)N($SiMe_3$)) (5)

The reactions of **1** with varying ratios of zinc alkyls and silanetriol (1:1 and 1:2) resulted in the formation of **3** and **4**. Furthermore, since **1** contains three acidic OH groups, there might be another product that can be possibly isolated from the reaction of $ZnMe_2$ and **1** (from 3:1 molar ratio). Addition of three equivalents of zinc dimethyl to **1** in a mixture of dioxane / hexane or THF / hexane led to the formation of **5** in 80 % yield. Compared to the other cases **3** - **5**, the Zn / Si ratio in this case (8:3) was less than in the initial reaction mixture (3 : 1).

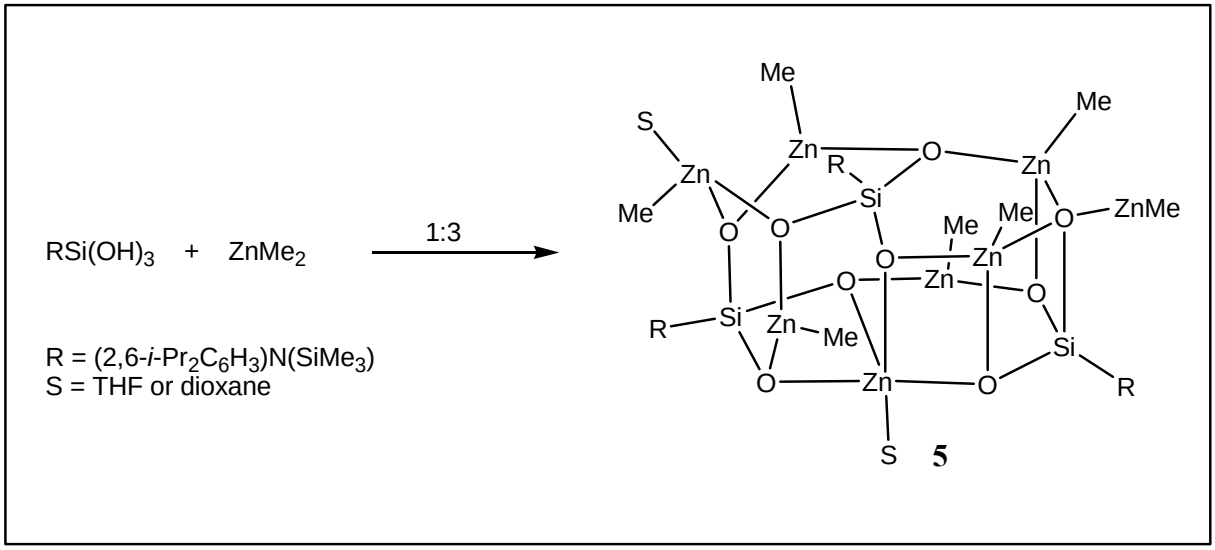

Zinc siloxane **5** also shows good solubility in organic solvents in benzene, toluene, THF etc. The integrated ^1H NMR intensities reveal that there are nearly seven methyl groups remaining on the zinc atoms. Other resonances due to the $SiMe_3$- and aromatic protons in the organic substituents were also obtained, however, a broad resonance was noticed for the *i*Pr and dioxane protons. Moreover two different resonances were also observed for the SiO_3 and $SiMe_3$ in the region of –62.2 and 6.18 ppm indicating the unique environments of the silicon atoms in the solution.

2.1.10. X-ray Crystal Structural Analysis of $Zn_8Me_7(dioxane)_2(O_3SiR)_3$ (R = (2,6-*i*$Pr_2C_6H_3$)N($SiMe_3$)) (5)

Single crystals for the X-ray structure determination were obtained from a dioxane/hexane mixture. The molecular structure of **5** consists of a $Zn_8O_{12}Si_3$ core and it can be viewed like the merging of two improper hexagonal drum-shaped units (Figure 6). Out of eight zinc atoms only seven of them participate in the formation of the zinc siloxane cage structure leaving the other zinc atom outside of the core. The $Zn_8O_{12}Si_3$ core is made up of a single eight-membered Zn_3O_4Si ring, five puckered six-membered Zn_2O_4Si rings, and pairs of four-membered Zn_2O_2 and $ZnSiO_2$ rings linked by Si–O–Zn and Zn–O–Zn units. Among eight zinc atoms only one zinc atom has lost both methyl groups whereas the rest of seven retained a methyl group. Similar to the molecular structure of **4**, in this case also zinc adopts different coordination geometries where two of them are in trigonal planar while the five other atoms are in tetrahedral environment. The eighth zinc atom is two-coordinated.

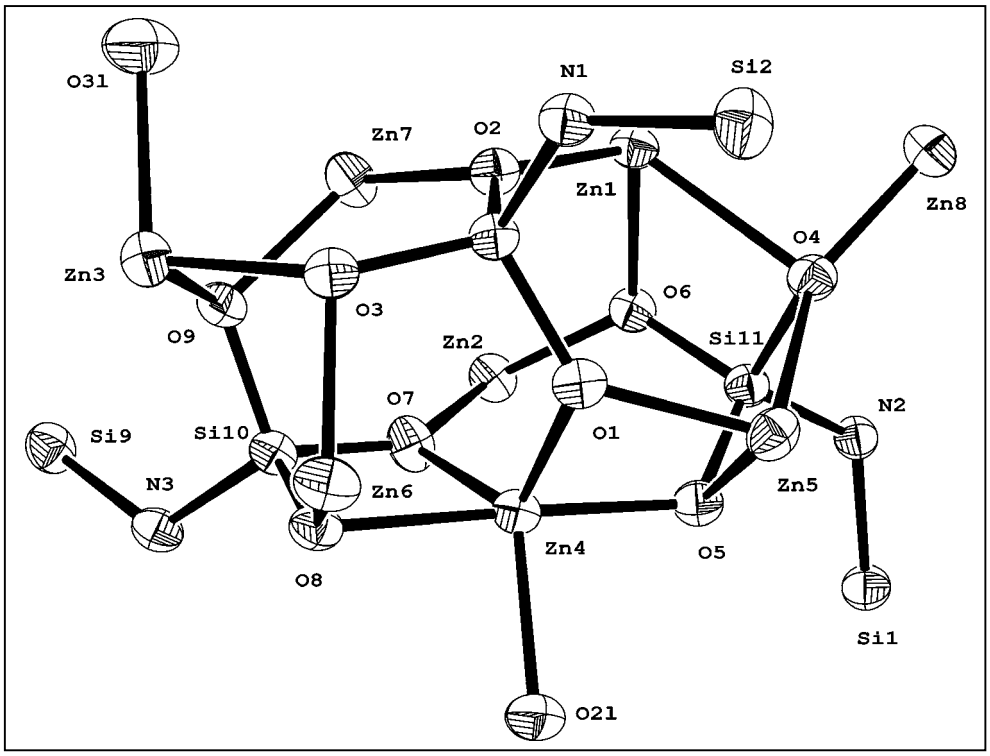

Figure 6. Core Structure of 5

The presence of more zinc atoms with respect to silicon is also indicative of the presence of additional Zn–O–Zn units. Compared to the structures of zinc siloxanes **2** – **4**, in this case most of the bridging oxygen atoms were triply bridging both zinc and silicon atoms, except O4, which is quadruply bridging. Thus, there is a diversity in the Si–O bond distances of Si11 ranging from 1.619 (4) - 1.663(4) Å, whereas, the remaining Si–O bond distances of the other two silicon atoms averaging 1.635(3) Å. The shortest Zn–O bond distance is found for Zn8–O4 (1.856(4) Å), the remaining fall in the range of 1.938 (4) to 2.365 (4) Å.

2.1.11. Synthesis of Intermediate Zinc Siloxane Compounds (6 - 8)

After the syntheses of compounds **2 - 5** have been accomplished, the interest was focused on the isolation of other possible intermediates during the conversion of **3** into **4**. The reaction between zinc dimethyl and **1**, in a 1.75:1 ratio, affords a white precipitate containing a mixture of compounds **6 - 8**, which was separated from the rest of the solution mixture and its ^{1}H NMR and ^{29}Si NMR recorded in toluene-d_8 (Scheme 9). From the remaining mother liquor single crystals of **7** were obtained within a week. The IR of the crude mixture is devoid of absorptions in the region 3500 - 3000 cm^{-1} indicating that all the Si–OH groups have reacted. The ^{29}Si NMR spectrum (in toluene-d_8) shows four singlets each in the region for $SiMe_3$ and SiO_3 at δ 3.9, 4.05, 4.90, 5.67, and –55.26, –60.93, –62.04, –65.99 ppm respectively. Single crystals of **6** [$Zn_7Me_2(THF)_5(O_3SiR)_4$] obtained from a toluene-d_8 solution was used for NMR measurements. Based on the silicon NMR, it was obvious that more than one product was present in the mixture. But it was difficult to understand the presence of compounds **6 - 8** in solution, which was later confirmed by the single crystal X-ray diffraction studies of **6** and **7,** whereas the core structure of compound **8** (^{29}Si NMR δ – 65.98 ppm) was tentatively assigned from the comparison of its ^{29}Si NMR spectra with the literature value for the similar environment of a silicon atom surrounded by four zinc atoms

(through oxygen atoms, solid state CP-MAS ^{29}Si NMR δ –66.4 ppm[125]), determined during the study on zincosilicate synthesis, where traces of the formation of a similar arrangement of silicon as in **8** have been found. However, one cannot rule out other possibilities for the structure of compound **8**. Moreover, the isolation of this product could be possible by using the appropriate reaction conditions like in other cases. The silicon atoms in the SiO_3 moieties of **6** resonate at δ –61.1 and –53.6 ppm, respectively, due to the presence of silicon atoms in different environment.

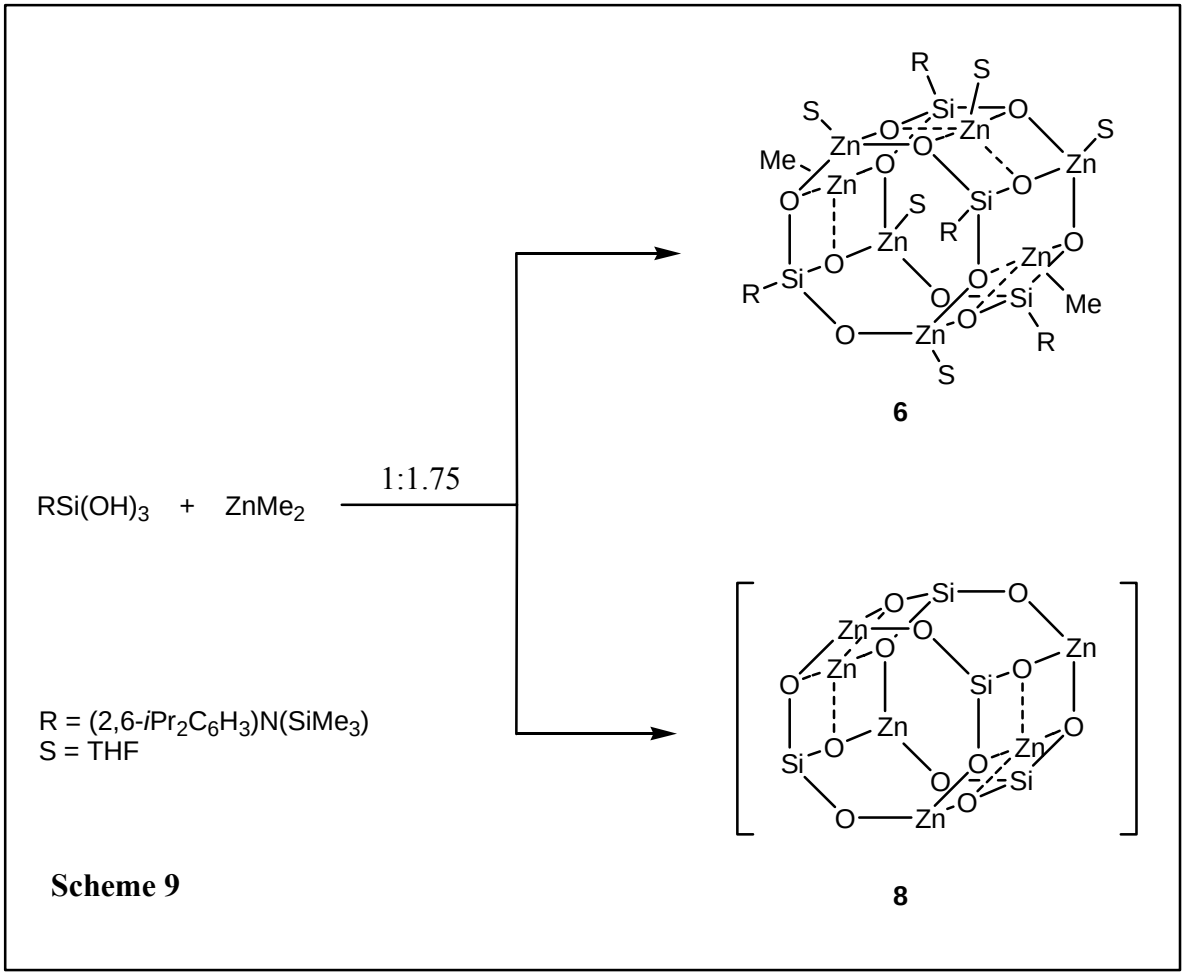

Scheme 9

The lowest value can be assigned to the silicon present in the eight-membered $Zn_2O_4Si_2$ ring due to the presence of central square pyramidal zinc atoms that shield the electron density from these silicon atoms. The other value can be assigned to the silicon present in the eight-membered $Zn_2O_4Si_2$ ring containing tetrahedral zinc atoms present in the middle of this ring. On the other hand, it was necessary to carry out the singe crystal X-ray diffraction studies to

understand the composition of zinc siloxane present in **6** as well as in **7**. It was found that the core of **7** is the same as in compound **4.**

2.1.12. Solid-State Structure of $[Zn_7Me_2(THF)_5(O_3SiR)_4]$ (R = (2,6-*i*$Pr_2C_6H_3$)N($SiMe_3$)) (6)

The X-ray crystal structure of **6** reveals that the compound crystallises in the centrosymmetric triclinic space group with half of the molecule in the asymmetric unit. The final refined core structure in **6** is shown in Figure 7. The molecular structure consists of a $Zn_7Si_4O_{12}$ core in which $Zn_4Si_4O_{12}$ units form a cubic polyhedron. The remaining three zinc atoms (Zn(1), Zn(4), and Zn(7)) occupy the three different faces of the cube. The cubic core contains six puckered eight-membered $Zn_2Si_2O_4$ rings, and four Zn_2O_2 and $ZnSiO_2$ rings

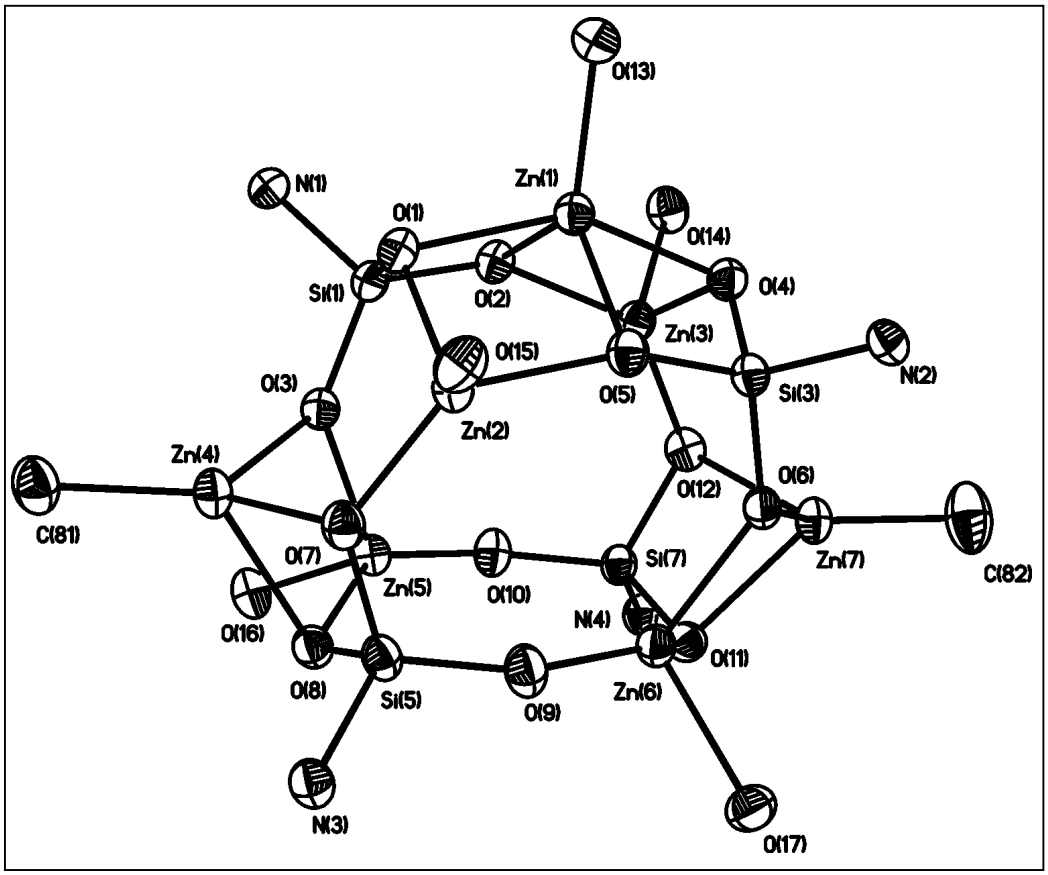

Figure 7. Core Structure of 6

respectively. An interesting aspect of the molecule **6** is the presence of a square pyramidal zinc atom in the face of an eight-membered ring that shares all four oxygen atoms of $Zn_2Si_2O_4$

unit. The remaining two zinc atoms share only three out of four oxygen atoms in $Zn_2Si_2O_4$ unit and also contain a methyl group thereby adopting a tetrahedral geometry around the zinc atoms. The zinc atoms within cubic $Zn_4Si_4O_{12}$ are also in tetrahedral geometry with a molecule of THF to complete the fourth coordination around zinc centers.

Similar to the zinc siloxanes **2 - 5**, described *vide supra*, there are different types of oxygen atoms of silanetriol binding the zinc atoms in the core structure of **6** (Figure 7). The Si–O and Zn–O bond distances fall in the range of 1.585 (2) – 1.657 (2) Å and 1.838 (2) – 2.170 (2) Å respectively. Such a variable distances have also been observed for other zinc siloxanes, **2 - 5**.

2.1.13. Comparison of Spectral Aspects of Compounds 3 - 7

The solubility of the compounds **2 - 6** in most of common organic solvents, irrespective of the aggregate formation, is high. In particular the solubility of **2** and **3** is good even in pentane. However, the solubility of the other compounds **4 - 6** is increased by the presence of surface methyl groups on the zinc atoms making the characterization of the compounds possible in deuteriated benzene or chloroform solvents. The yields of the products varied from moderate to good except in case of **2** and **6** (Table 1).

All the zinc siloxanes prepared in the present work are thermally stable and do not melt below 250 °C except **2** and **3**. Under electron impact mass spectral conditions (70 eV) no peak attributable to the molecular ion of **2 - 6** can be observed. Only smaller fragmented peaks were detectable. The IR spectra are devoid of any absorption in the region 3000 - 3500 cm^{-1} for compounds **2**, and **4 - 6**, indicating complete reaction of all Si–OH groups with zinc dialkyls, whereas the IR spectrum of **3** shows a broad band around 3300 cm^{-1} for OH stretching frequencies for unreacted silanol groups. Similar to all the other metallasiloxanes, compounds **2-6** show very strong absorptions from 900 to 1000 cm^{-1} assignable to ν(Si–O–

Zn) vibrations (Table 1). Depending on the type of the Si–O–Zn bonds the frequencies of compounds change. It is noteworthy that these vibrations are also observed as prominent bands in other transition metal containing siloxanes.

The comparison of ^{29}Si NMR chemical shift data was made from the spectra obtained from the aminosilanetriol (**1**) and zinc siloxanes (**2 - 6**) that are listed in Table 1. As it can be seen, the ^{29}Si chemical shifts of all zinc siloxanes are shifted to lower field compared to the aminosilanetriol (**1**) (δ –67.3 ppm). The largest shift was observed in the case of compound **6** (δ –53.6 ppm, $\Delta\delta$ = 13.7 ppm), whereas the least low-field shift was observed for compound **3** (δ –62.1 ppm, $\Delta\delta$ = 5.2 ppm).

Table 1. Spectral comparison between the zinc siloxanes (**2 - 6**)

Compound (R = (2,6-*i*Pr$_2$C$_6$H$_3$)N(SiMe$_3$))	Yield (%)	ν (Zn–O–Si) (cm^{-1})[a]	δ ^{29}Si (ppm)
[(L)ZnLi(O$_3$SiR)]$_4$ (**2**)	42	967, 952, 913	–64.8[b]
[Zn(THF)(O$_2$(OH)SiR)]$_4$ (**3**)	62	967, 947, 908	–62.2[c]
[Zn$_4$(THF)$_4$(ZnMe)$_4$(O$_3$SiR)$_4$] (**4**)	64	966, 936, 917	–60.9, –61.3[b]
Zn$_8$Me$_7$(Dioxane)$_2$(O$_3$SiR)$_3$ (**5**)	80	945, 919	–62.2[c]
[Zn$_7$Me$_2$(THF)$_5$(O$_3$SiR)$_4$] (**6**)	75	967, 937, 916	–53.6, –61.1[c]

[a] recorded in Nujol mulls; [b] in C_6D_6; [c] in $CDCl_3$.

2.2. Iron Containing Silicate

2.2.1. Synthesis of Iron(II) Siloxane [{FeL'}$_2${Fe(heterocarbene)}$_2${O_3SiR}$_2$] (R = (2,6-*i*Pr$_2$C$_6$H$_3$)N(SiMe$_3$)) (L' = (N(SiMe$_3$)$_2$) (heterocarbene = 1,3-diisopropyl-4,5-dimethylimidazol-2-ylidene) (9)

The search for better acid catalysts, instead of the homogeneous acid catalysts such as $AlCl_3$, BF_3, H_3PO_4 or H_2SO_4, has become increasingly popular in recent times due to its application in organic reactions such as Friedel-Crafts reaction. The iron doped in H-ZSM-5 is a useful catalyst for the benzylation of benzene and toluene due to the acidic nature of iron similar to aluminium, zinc etc.[126a,b] Moreover the redox property of iron in Fe/ZSM-5 is utilized for the conversion of benzene to phenol with 100 % selectivity in presence of N_2O and has also been used for the oxidative dehydrogenation of propane and *n*-butane.[126c,d] In this catalyst, iron exists in the oxidation state +3.[126] On the other hand, iron plays a vital role in many living systems in which both oxidation states (+2, +3) of iron are known. Among them, Fe^{2+} plays a crucial role in the oxygen transport and storage and also in electron transfer processes.[1,2] Even, in the naturally occurring mineral olivine (Mg^{2+}, Fe^{2+})$_2SiO_4$ and garnets [$M_3^{2+}M_2^{3+}(SiO_4)_3$] (where M^{2+} is Ca, Mg, Fe, and M^{3+} is Al, Cr, Fe) iron exists in oxidation state +2.[1-3]

This Section focuses on the synthesis of heterosiloxanes as model compounds for metal-containing zeolites. In spite of the high significance of iron compounds, very few examples of metallasiloxanes or silsesquioxanes with iron containing both the oxidation state +2 and +3 have been reported.[70,76,127] In previous reactions, we have used metal alkyls as starting materials to investigate the condensation reactions of the aminosilanetriol **1**. However, in this case we used an iron(II) amido compound as the starting material because of the well established instability of iron alkyls.

Addition of $Fe[N(SiMe_3)_2]_2$ to a suspension of **1** at room temperature in the presence of heterocarbene (1,3-diisopropyl-4,5-dimethylimidazol-2-ylidene) affords **9** in low yield. In this case it was necessary to use a stable heterocarbene as the auxiliary coordinating ligand, to obtain crystalline **9**. Single crystals of compound **9** thus obtained were found to be soluble in most common organic solvents.

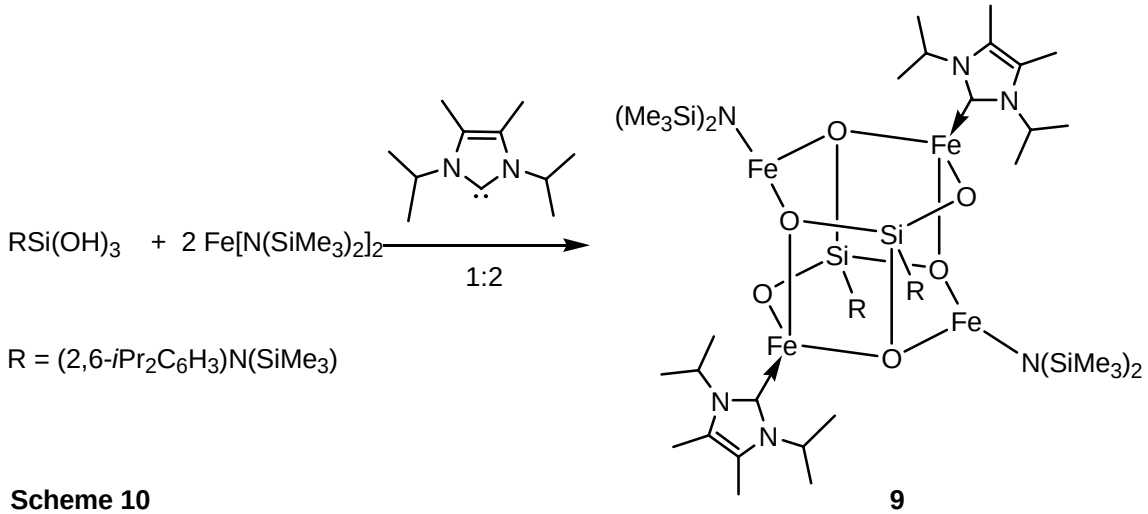

Scheme 10 **9**

2.2.2. X-ray Structure of [{FeL'}$_2${Fe(heterocarbene)}$_2${O_3SiR}$_2$] (R = (2,6-*i*$Pr_2C_6H_3$)N($SiMe_3$)) (L' = ($N(SiMe_3)_2$) (heterocarbene = 1,3-diisopropyl-4,5-dimethylimidazol-2-ylidene) (9)

The molecular structure of **9** has been determined by single crystal X-ray diffraction studies (Figure 8). The molecular structure of **9** consists of a $Fe_4O_6Si_2$ core. This core is made up of two six-membered and two four-membered rings with Fe_2O_3Si and Fe_2O_2 units, respectively. These rings are connected to each other through Si–O bonds to result in the formation of a drum-shaped central unit. The six-membered rings are puckered and exist in a boat conformation. Two of the four iron atoms retain one of the $N(SiMe_3)_2$ groups while the remaining two have lost their amido substituents completely. While the iron atoms containing the amido moiety exist in a trigonal planar configuration, the other two iron centers are

tetrahedrally coordinated. The molecule has a pseudo-inversion center at the middle of the drum. Two of the three oxygen atoms of the silanetriol are involved in both bridging and chelating (μ_3) of ligation, whereas the third oxygen atom acts only as a bridging (μ) ligand and connects two iron atoms.

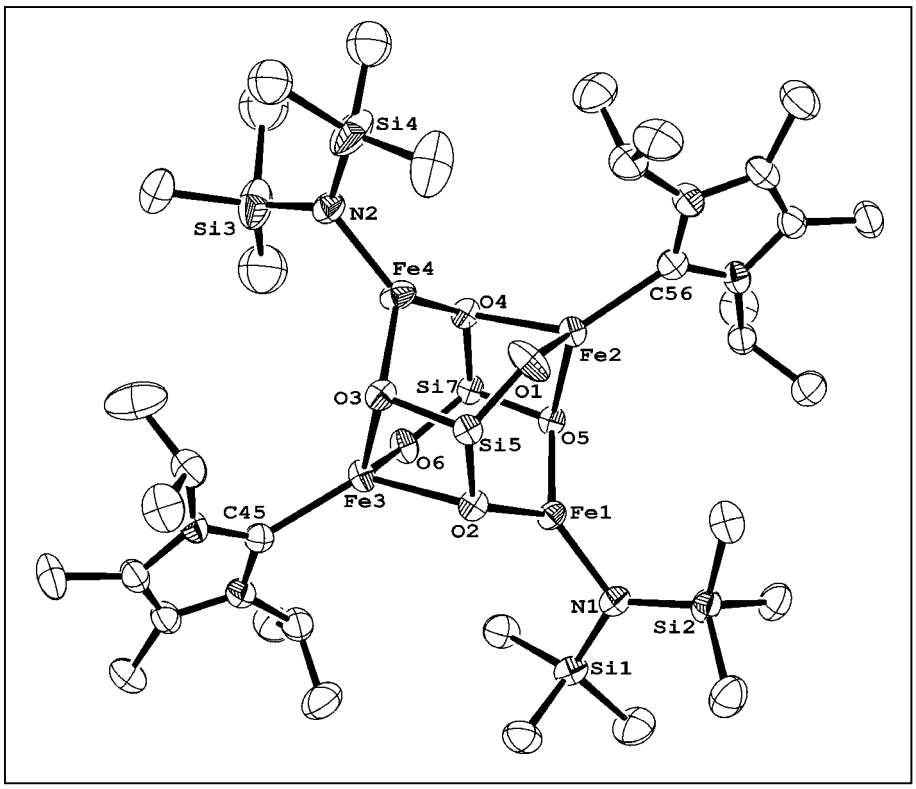

Figure 8. Molecular Structure of 9.

2.3. Group 12 Phosphonates

2.3.1. Zinc Phosphonates

The synthesis of zinc phosphates and phosphonates was mainly aimed at the development of new microporous materials having applications for material science and catalysis. This has led to many varieties of zinc phosphates and phosphonates with novel one-, two-, and three-dimensional structures. These structures highly depend on the reaction conditions such as temperature, nature of the starting materials *e.g.* metal sources, alkyl phosphonic acid or phosphoric acid, other organic reactants or co-ligands, pH, and the stoichiometry of the reactants.[130-133] In a similar synthetic approach, Stucky and coworkers reported the first open framework zinc phosphonate containing 24-ring channels.[134] Among the numerous examples of zinc phosphonate structures known thus far, most of them contain layered structure.[105, 134]

On the other hand, only few examples of multinuclear zinc phosphonates are known. Roesky *et al*. have reported in 1999 the first dodecanuclear zincophosphonate aggregate with a novel $Zn_4(\mu_4–O)$ core starting from *tert*-butylphosphonic acid and zinc diethyl.[108] Recently, Chandrasekhar and coworkers prepared tri- and hexa-nuclear zinc phosphonate cages with alkylphosphonic acids and zinc dichloride in the presence of pyrazoles.[110] Over the last few years our research group has developed a unique route to synthesise the soluble metallaphosphonates starting from alkylphosphonic acids and metal alkyls with the facile elimination of alkane. In the current study *tert*-butylphosphonic acid (**10**) is chosen as the starting material to synthesise zinc phosphonates due to its good solubility properties.

2.3.2. Synthesis of $[\{(ZnEt)_3(Zn(THF))_3\}\{t\text{BuPO}_3\}_2\{\mu_3–OEt\}]$ (11)

The addition of zinc diethyl to $t\text{BuP(O)(OH)}_2$ (**10**) in a mixture of THF/hexane led to the formation of **11** as colorless crystals. The reaction started with the vigorous evolution of

ethane gas. Due to the poor solubility of this compound it was impossible to obtain a solution NMR. This compound was however characterized by IR and mass spectral studies and elemental analysis. The absence of bands in the region 3000 - 3500 cm^{-1} indicates the complete involvement of all P–OH moieties in the reaction. Under EI-mass conditions, no peak attributable to the molecular ion was observed.

2.3.3. X-ray Crystal Structure of [{$(ZnEt)_3(Zn(THF))_3$}{tBuPO_3}$_2${μ_3–OEt}] (11)

Single crystal X-ray diffraction studies were carried out to establish the solid-state structure of **11** which shows that the molecular structure contains a $Zn_6O_{13}P_4$ core with a Zn(μ_3–O) bridge (Figure 9). There are five eight-membered $Zn_2O_4P_2$ rings and three Zn_2O_2 units, respectively. The eight-membered rings are puckered and the four-membered rings are almost coplanar. The overall molecule can be interpreted as an extended improper cubic zinc phosphonate due to the presence of a Zn_3(μ_3–O) unit. Half of the zinc atoms retained the ethyl

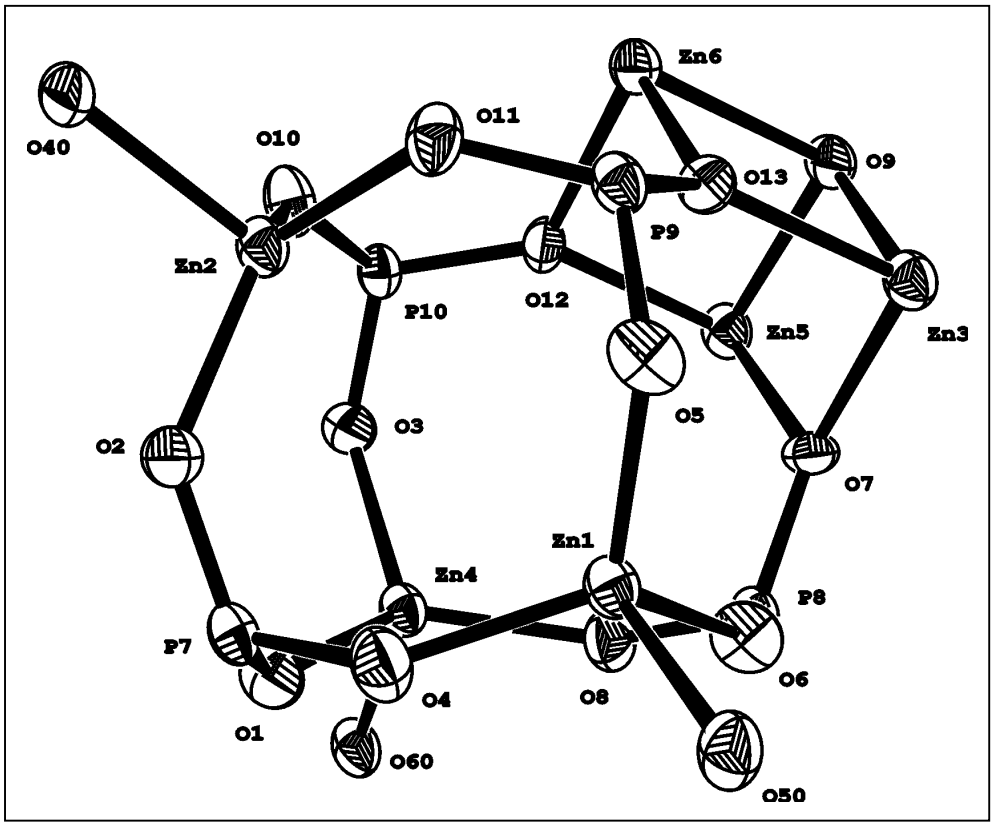

Figure 9. ORTEP Plot of Core Structure of 11 (with 50 % Probability Level)

groups, the others are coordinated by THF molecules. The presence of OEt moiety in the molecule could be attributed to the oxidation of the Zn–C bond in the presence of small quantities of oxygen during the course of the reaction.[128] There are two types of bridging oxygen atoms present in the molecule. The bond distance of Zn–μ–O (av 1.907(7) Å) is shorter than the Zn- μ_3-O (av 2.052(3) Å) bonds and the bond distance of Zn_3–μ_3–O is 2.083 (6) Å. There are two types of phosphorus oxygen bond distances in the range of 1.506 (4) - 1.553 (3) Å, which are comparable to the reported value for similar linkages.[108]

2.3.4. Synthesis of [{$Zn_4Me_4(THF)_2$}{*t*BuPO_3}$_2$] (12)

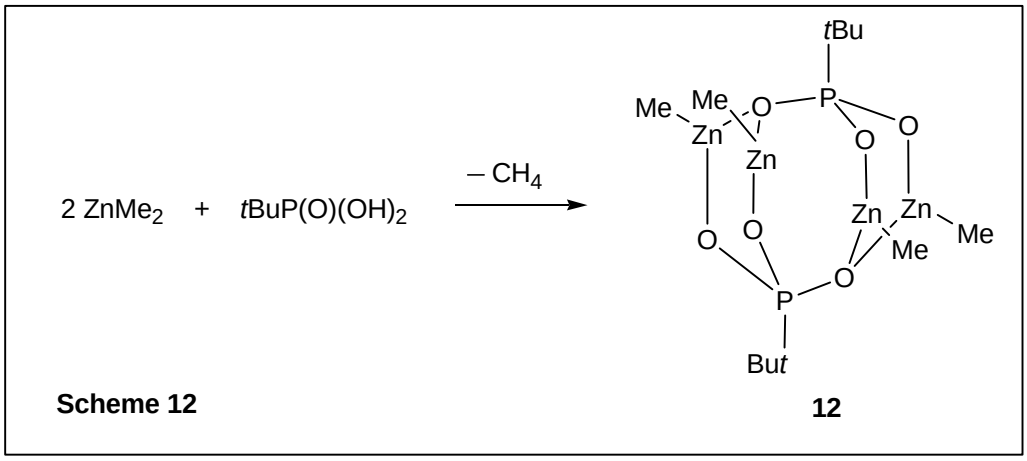

Scheme 12 **12**

The reaction between *tert*-butylphosphonic acid (**10**) with zinc dimethyl in a 1:2 molar ratio in THF/hexane mixture under refluxing conditions afforded compound **12** in good yield (84 %). Compared to **11**, compound **12** is highly soluble in benzene, toluene, and THF solvents. Hence it was easy for us to study the compound **12** in solution by means of ^{1}H and ^{31}P NMR. The ^{31}P NMR spectrum of the crude product shows several resonances, among which the major resonance corresponds to **12** (δ 39.58 ppm). The spectrum also showed the presence of a minor product (^{31}P NMR values δ 31.54, 34.43, 39.27, 40.04 ppm) which could be readily assigned to the dodecanuclear zinc phosphonate that has been reported earlier from our laboratory.[108] It should be noted that the synthetic conditions employed for the synthesis of both the zinc phosphonates are same except that in the present case two equivalents of zinc dimethyl have been used instead of 1.5 equivalents in the previously reported paper.[108] The

^{1}H NMR intensities reveal that compound **12** contains one methyl group on each zinc atom. The methyl protons attached to the zinc atoms resonate at –0.88 ppm, while the methyl protons of the *tert*-butyl group on the phosphorus atoms appear as doublets at δ 1.17 (J_{PH} = 15.43 Hz).

2.3.5. Molecular Structure of [{$Zn_4Me_4(THF)_2$}{tBuPO$_3$}$_2$] (12)

Compound **12** crystallises in the monoclinic space group $P2_1/n$ with two molecules in the asymmetric unit cell. The central core in **12** consists of two six-membered, and two eight-membered rings, respectively as shown in Figure 10. The six-membered ring consist of a Zn_2O_3P unit and the eight-membered ring contains a $Zn_2O_4P_2$ unit. The novelty of this structure is the arrangement of four zinc atoms lying in the same plane forming a rectangle. Moreover, these zinc atoms are further connected by the phosphonate oxygen atoms above and below the plane. Such a type of arrangement has been reported for the layered α-zirconium phosphate [α-$Zr(O_3POH)_2 \cdot 2H_2O$].[136] This is the first molecular zinc phosphonate structure reported so far which resembles inorganic phosphates. Each zinc atom retains a methyl group and the methyl groups attached to zinc are pairwise in trans position. The hydrophobic *tert*-butyl and methyl groups, thus explaining the high solubility of **12** in common organic solvents, surround the periphery of the central $Zn_4O_{12}P_2$ core.

Two of the three oxygen atoms from the phosphonate groups are in a μ coordination to zinc and the third is binding to two zinc atoms in a μ_3 fashion. There are no formal P–O and P=O bonds present. The average P–O bond distance 1.526 (6) Å is slightly shorter than the reported P–O and is longer than the P=O bonds. The two types of Zn–O bonds fall within the narrow range from 1.940 (5) to 2.029 (3) Å. There are two types non-bonded Zn•••Zn contacts present in the tetranuclear zinc units (av. 3.240 to 3.733 Å). The average body-

diagonal of the cube is 4.944 Å while the face diagonal P•••P distance is 3.92 Å. The average Zn–O–P bond angle in the molecule is 123.45°.

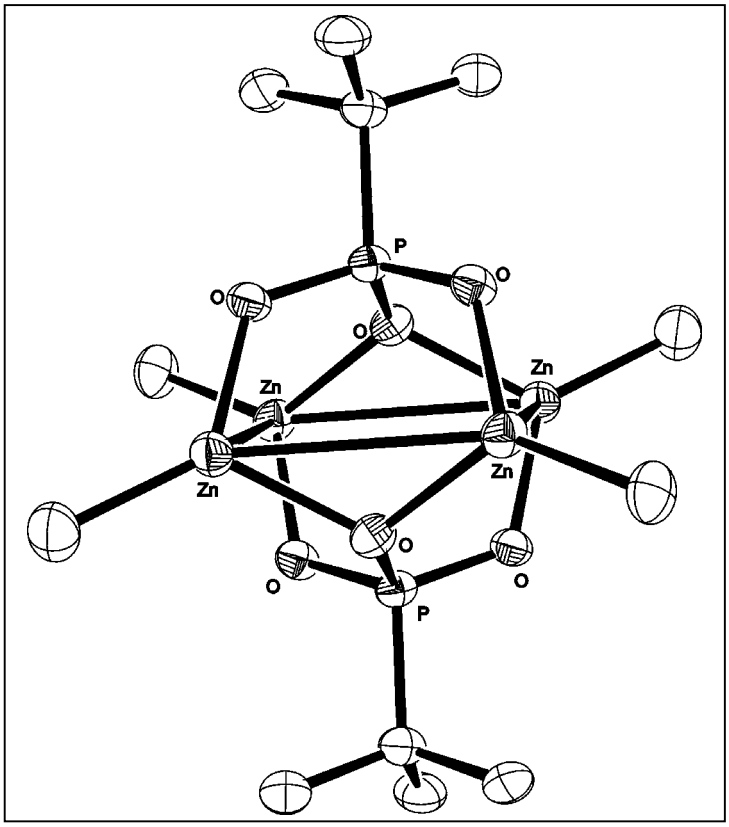

Figure 10. ORTEP Plot of Molecular Structure of 12 (with 50 % Probability Level). Imaginary lines are drawn between zinc atoms to show its planarity

2.3.6. Synthesis of $[(CdMe)_{10}(Cd(THF))_4Cd_6(\mu_4\text{–}O)_2(\mu_3\text{–}OH)_2(t\text{BuPO}_3)_{12}]$ (13)

Compared to zinc phosphonates, the chemistry of cadmium phosphonates has received less attention. Only recently a few examples of layered cadmium phosphonates have been reported.[137] On the other hand, only a handful of examples of molecular transition metal phosphonates possessing multinuclear metal atoms were known in the literature.[108-110,138] Prior to this study, no example of molecular cadmium phosphonate was known.

Addition of cadmium dimethyl to a THF solution of *tert*-butylphosphonic acid afforded **13** as colorless crystals. These crystals could be obtained in better yields by addition of stoichiometric amounts of water to the above reaction mixture. Compound **13** is insoluble

in any of the common organic solvents and hence the attempts made to obtain a solution NMR spectrum were unsuccessful. The ^{1}H NMR intensities of the solid-state CP-MAS NMR reveal that the methyl protons on the each cadmium atom resonate at δ 0.6 ppm while the methyl protons of *tert*-butyl groups attached to phosphorus appear at δ 1.7 ppm. However, the ^{31}P NMR spectrum of **13** in solid-state (Figure 11) displays at least four well-resolved signals in the range δ 30-50 ppm which can be assigned to phosphorus atoms having four different environments (*vide infra*; Section 2.3.7).

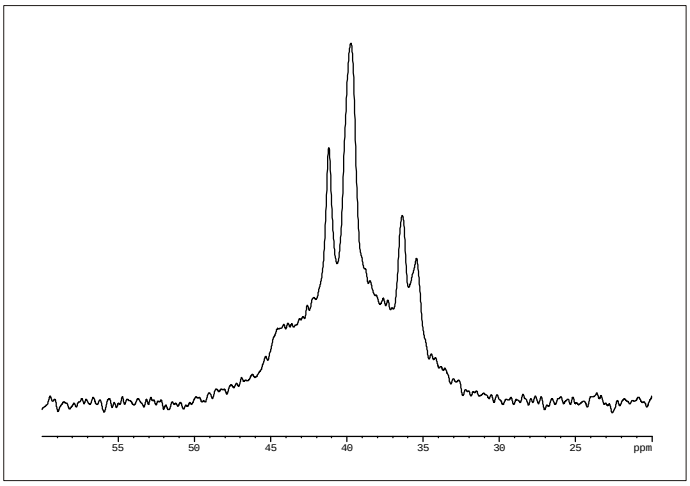

Figure 11. CP-MAS ^{31}P NMR Spectrum of Compound 13.

2.3.7. X-ray Crystal Structure of $[(CdMe)_{10}(Cd(THF))_4Cd_6(\mu_4\text{–}O)_2(\mu_3\text{–}OH)_2(t\text{BuPO}_3)_{12}]$ (13)

The single crystal X-ray diffraction study reveals that compound **13** consists of a core containing twenty cadmium atoms and twelve phosphorus atoms. Compound **13** has an apparent inversion center, however, this inversion center disappears due to small variations in the coordination geometry of the cadmium centers. While ten of the twenty cadmium atoms retain one methyl group on them, the remaining cadmium atoms lose both the attached methyl groups during the reaction. There are two cadmium centers which are hexa-coordinate and the remaining metal centers adopt tetra-, and penta-coordinate environments (Figure 12).

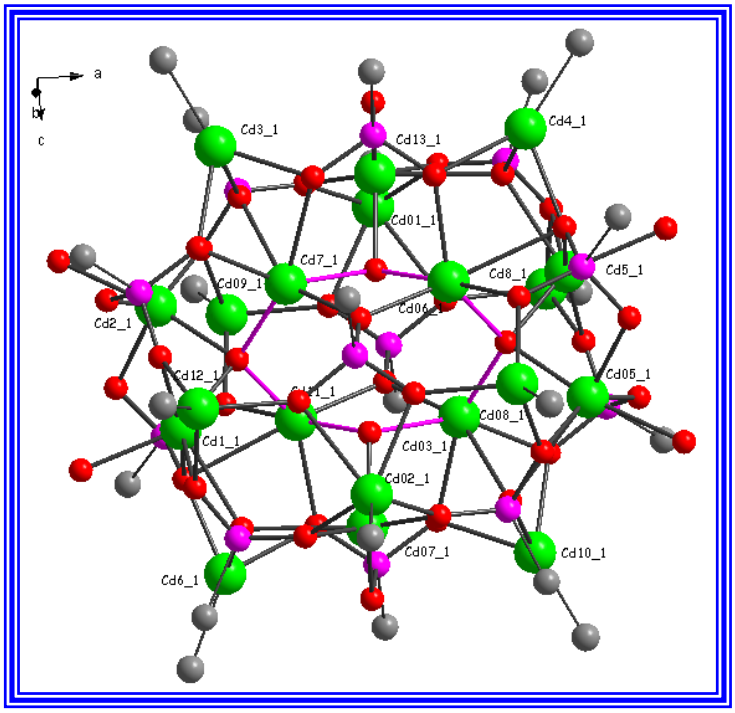

Figure 12. Molecular Structure of 13 Showing the $Cd_{20}P_{12}$ Unit (the solvent THF molecules, hydrogen atoms and the methyl groups of the *tert*-butylphosphonate are omitted)

Table 2. Coordination geometry and environment around cadmium atoms in **13**.

Coordination geometry	Types of cadmium atoms	Ligands coordinating to cadmium atoms	No. of cadmium atoms
tetrahedral	Cd(3), Cd(4), Cd(6), Cd(8), Cd(08), Cd(09), Cd(10), Cd(12)	three phosphonate oxygens and one methyl	8
Six coordinated octahedral	Cd(03), Cd(06), Cd(7), Cd(11)	one μ_4–O,one μ_3–O, four phosphonate oxygens	4
six coordinated octahedral	Cd(1), Cd(5), Cd(05)	one μ_4–O, four phosphonate oxygens, oneTHF	3
five coordinated square pyramidal	Cd(01), Cd(02)	four phosphonate oxygens, one methyl	2
five coordinated trigonal bipyramidal	Cd(07), Cd(13)	one μ_3–O, four phosphonate oxygens	2
five coordinated trigonal bipyramidal	Cd(2)	one μ_4–O, three phosphonate oxygens, one THF	1

The twenty cadmium atoms can be categorised in to six classes depending on the coordination geometry and the environment around them (Table 2).

Table 3. Various coordination modes of phosphonate moities

Atom	**P-O-M**	**P-O-M_2 (μ_2-O)**	**P-O-M_3 (μ_3-O)**	**Type**	**No. of P atoms**
P_13	O3_13	O1_13, O2_13	--	Type I	4
P_15	O3_15	O1_15, O2_15	--		
P_20	O1_20	O2_20, O3_20	--		
P_21	O1_21	O2_21, O3_21	--		
P_12	O3_12	O1_12	O2_12	Type II	2
P_14	O3_14	O1_14	O2_14		
P_11	--	O1_11, O2_11, O3_11	--	Type III	3
P_16	--	O1_16, O2_16, O3_16	--		
P_17	--	O1_17, O2_17, O3_17	--		
P_18	--	O1_18, O2_18	O3_18	Type IV	3
P_19	--	O1_19, O3_19	O2_19		
P_22	--	O1_22, O2_22	O3_22		

The phosphonate tetrahedra are linked to the cadmium polyhedra either by a corner sharing *via* an oxygen atom or by edge sharing *via* two oxygen atoms (Table 3). This coordination mode of phosphonates has resulted in nine CdO_2P four membered rings (Figure 13). Twenty cadmium atoms in molecule of **13** can be categorised in six types depending on the coordinating atoms and the coordination environment (Table 4)

Table 4. Details of the coordination environment of the cadmium centers

Cadmium atom	Coordinating atoms						Coordition geometry
Type I							
Cd3_1	CM6_1	O1_13	O2_21	O3_16			tetrahedral
Cd4_1	CM8_1	O2_14	O3_21	O3_22			tetrahedral
Cd6_1	CM7_1	O2_12	O2_19	O3_20			tetrahedral
Cd8_1	CM3_1	O1_22	O2_15	O3_17			tetrahedral
Cd08_1	CM9_1	O1_14	O2_11	O2_18			tetrahedral
Cd09_1	CM1_1	O1_12	O2_16	O2_17			tetrahedral
Cd10_1	CM2_1	O1_15	O2_20	O3_18			tetrahedral
Cd12_1	CM5_1	O2_13	O3_11	O3_19			tetrahedral
Type II							
Cd03_1	OT1_1	OQ2_1	O1_15	O1_17	O2_20	O3_18	octahedral
Cd06_1	OT2_1	OQ2_1	O1_11	O1_14	O2_14	O3_21	octahedral
Cd7_1	OT2_1	OQ11	O1_11	O1_13	O2_21	O3_16	octahedral
Cd11_1	OT1_1	OQ11	O1_12	O1_17	O2_12	O3_20	octahedral
Type III							
Cd1_1	OQ1_1	O2_12	O2_13	O2_19	O3_19	O1_32	octahedral
Cd5_1	OQ2_1	O1_12	O2_14	O2_15	O3_22	O1_33	octahedral
Cd05_1	OQ2_1	O2_18	O3_14	O3_15	O3_18	O1_34	octahedral
Type IV							
Cd01_1	CM10_1	O1_16	O2_17	O2_22	O3_17		square pyramidal
Cd02_1	CM4_1	O1_18	O1_19	O2_21	O3_11		square pyramidal
Type V							
Cd07_1	OT1_1	O1_18	O1_19	O1_20	O2_19		tbp
Cd13_1	OT2_1	O1_16	O1_21	O2_22	O3_22		tbp
Type VI							
Cd2_1	OQ1_1	O2_16	O3_12	O3_13	O1_31		tbp

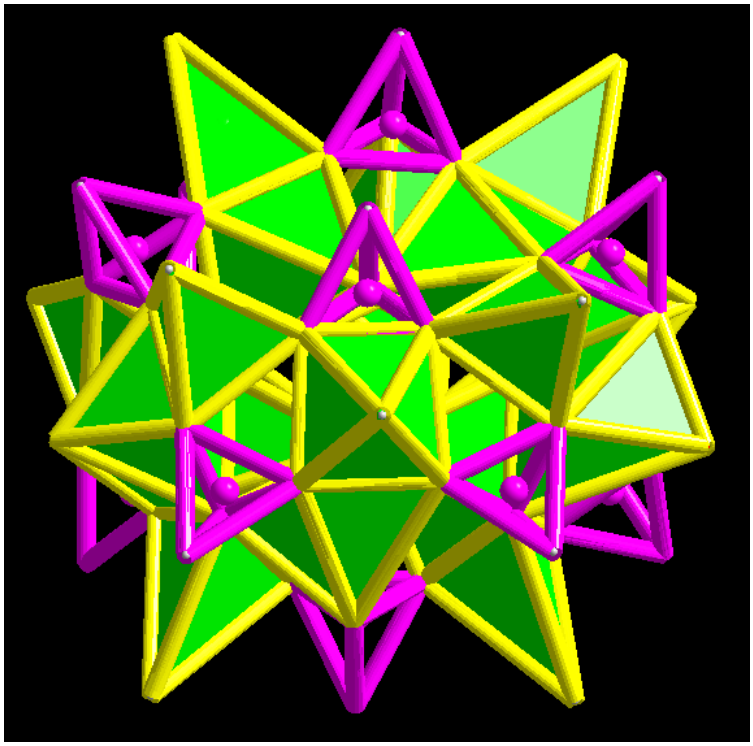

Figure 13. Polyhedral Arrangement Showing Cadmium (green) and Phosphorus (pink) atoms in 13.

Another way of understanding the structure of this molecule is by considering a eight membered Cd_4O_4 core (Figure 14) which is surrounded by remaining cadmium and phosphonate moieties resulting in compound **13**. The Cd_4O_4 core contains of two $Cd_3(\mu_3–OH)$ and $Cd_4(\mu_4–O)$ moieties, respectively, and adopts a crown conformation.

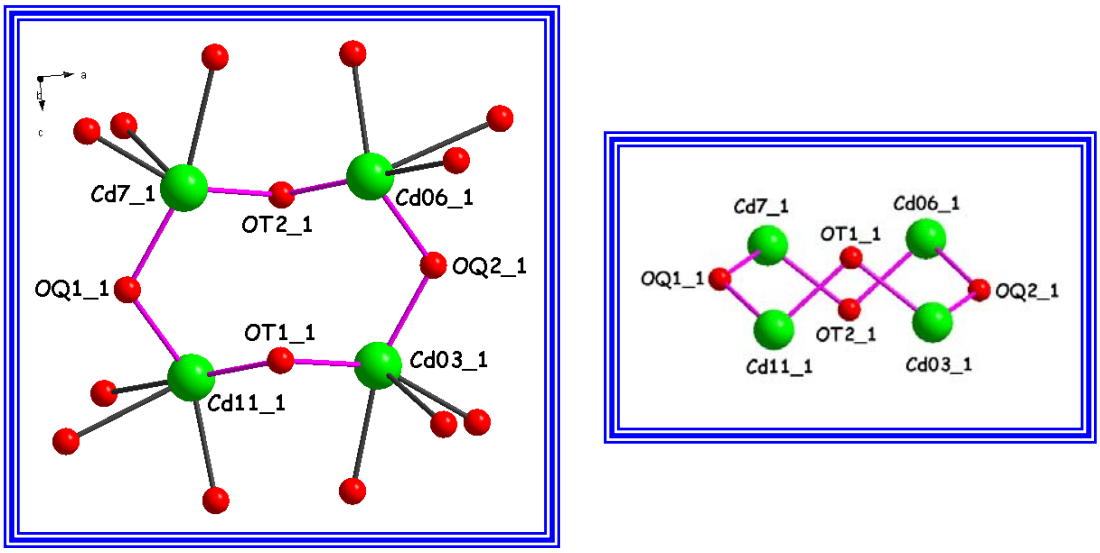

Figure 14. Central Cd_4O_4 Moiety in 13 and its Conformation

2.4. Synthesis of 2,4,6-tri-iso-propylphenylphosphonic Acid (16)

In recent times, the alkylphosphonic acids have been employed for the construction of several three-dimensional cage structures[96,97] It has been shown recently that by using *tert*-butyl- or phenylphosphonic acids it is possible to prepare larger aggregates. But as the aggregation of the compounds becomes larger, the solubility of the products decreases and it is very difficult to investigate their solution behavior by multinuclear NMR spectroscopy. Moreover in some cases, due to the poor solubility it is not possible to obtain crystals of the metallaphosphonates for X-ray investigations. Hence it is necessary to synthesise a new bulky phosphonic acid that can be used for further studies on metallaphosphonate compounds.

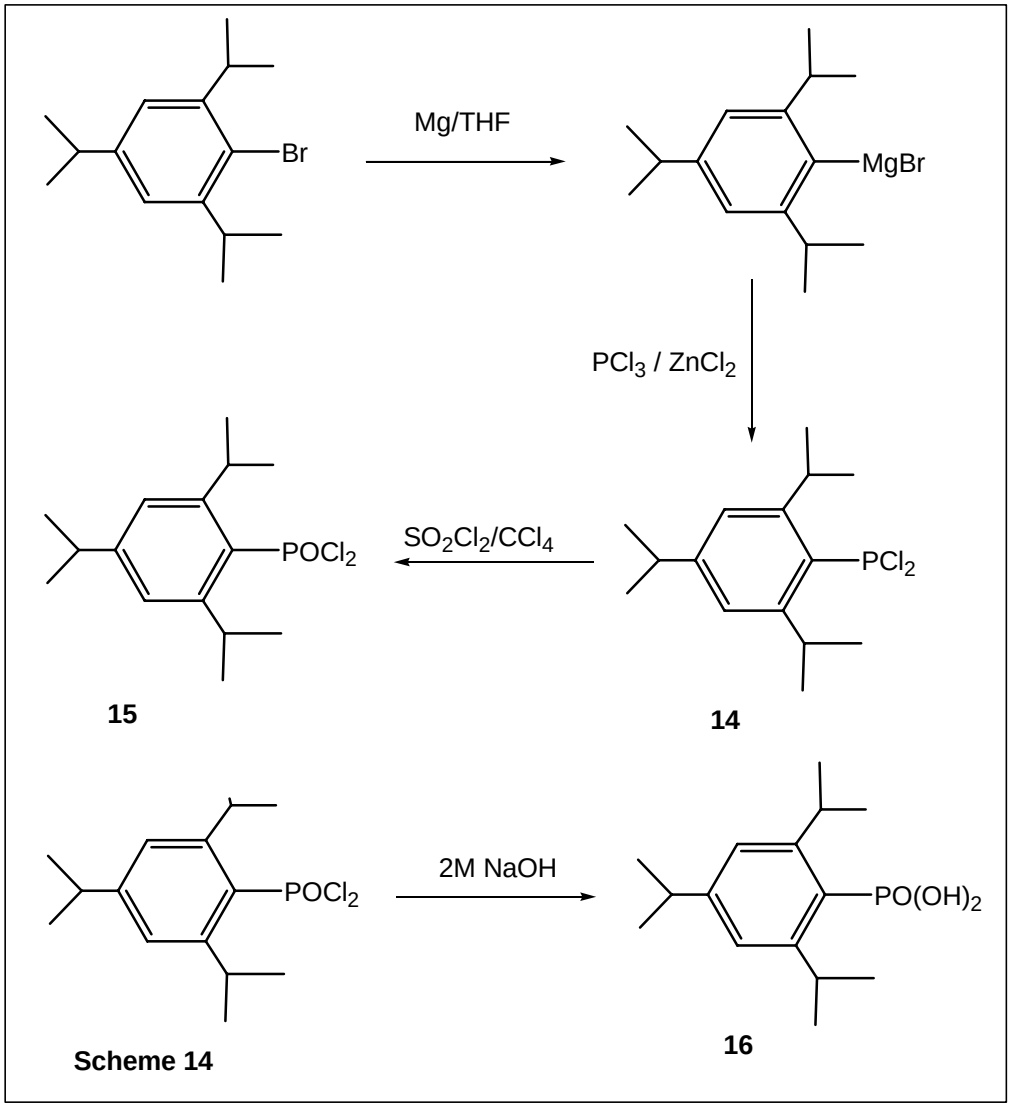

Scheme 14

Earlier, our research group has prepared soluble metallasiloxane compounds starting from bulky silanetriols. The resulting compounds are very highly soluble in common organic solvents and hence it was easy to study the behaviour of the metallasiloxane compounds in solution. In most cases only one product has dominated in the reactions and therefore the product yield was high.[71-74] Keeping these things in mind, it is necessary to develop a new synthetic method to obtain bulky phosphonic acids. We have decided to use the 2,4,6-tri-iso-propylphenyl moieties as a substituent in place of alkyl groups in the phosphonic acid system. The overall steps involved in this reaction are shown in Scheme 14.

2.4.1. Synthesis of 2,4,6-tri-iso-propylphenylphophonous dichloride (14)

The title compound can be prepared from the corresponding bromo compound. It has been reported that the reaction between lithiated 2,4,6-tri-iso-propylphenylbromide with the phosphorus trichloride in ether afforded **14** in moderate yield.[140] Product **14** crystallised from ether at –45 ^{o}C. However, we often found excess unreacted bromide, making separation of the product from the starting material difficult. In an another attempt, a THF solution of Li(2,4,6-*i*$Pr_3C_6H_2$) was reacted with phosphorus trichloride,[141] where they isolate a mixture of compounds containing **14** and bis(2,4,6-tri-iso-propylphenyl) chloride. The preparation of a Grignard solution of 2,4,6-tri-iso-propylphenylbromide may represent an alternative route to solve the above problem. But the addition of a Grignard solution in THF to the solution of phosphorus trichloride in a 1:1 ratio yielded a mixture of three compounds of composition 2,4,6-*i*$Pr_3C_6H_2PX_2$ (X_2 = Cl_2 (**14**), Br_2, ClBr), the presence of these compounds has been verified by ^{31}P NMR and mass spectroscopy.

In a similar procedure as for the preparation of mesitylphosphonous dichloride it was found that the use of $ZnCl_2$ could help in increasing the yield of the dichloro compound.[142] The addition of phosphorus trichloride to a suspension of the Grignard reagent with $ZnCl_2$ at

–78 ^{o}C afforded **14** in a yield of 80 %. The solubility of **14** is high even in pentane. Compound **14** is a hygroscopic solid and can be handled only for a short period of time in air. Product was **14** characterized by means of NMR, mass spectra, and elemental analysis. There are two different sets of doublets observed for *para*- and *ortho*-methyl protons of *i*Pr at 1.17 ppm (^{3}J (H,H) = 6.8 Hz) and 1.25 ppm, respectively. In the case of the methine protons of *ortho*-*i*Pr, which is splitted in to a doublet of a septet (^{3}J (H,H) + ^{4}J (P,H) = 4.69 Hz) by the phosphorus atom whereas the CH protons from *para*-*i*Pr resonates as a septet (2.85 ppm, ^{3}J = 6.8 Hz).

2.4.2. Synthesis of 2,4,6-tri-iso-propylphenylphophonic acid (16)

In order to obtain 2,4,6-tri-iso-propylphenylphophonic dichloride, compound **14** was then reacted with sulfuryl chloride at 0 ^{o}C to. The purity of the sample thus obtained for **15** was checked by ^{1}H NMR and ^{31}P NMR. The latter exhibits a singlet at δ 33.08 ppm.[141] Compound **16** was obtained in moderate yield (56 %) by hydrolysis of **15** using a 2 M solution of NaOH in an aqueous solution of acetone. The yield was affected by the contamination of **16** with bis-(2,4,6-tri-iso-propylphenylphosphonic) anhydride. The presence of the latter compound was identified through ^{31}P NMR (δ 13.91 ppm) and mass spectrometry. Compound **16** is soluble in common organic solvents such as hexane, toluene, diethyl ether, and THF. Unlike in the case of **14** the methyl protons of both the *ortho*- and *para*-*i*Pr groups in this case resonate together as inseparable doublets at δ 1.22 ppm (J (H,H) = 6.9 Hz). The resonances of the CH protons of the *ortho*-*i*Pr are shifted significantly upfield in comparison to that of **14**. The IR spectrum shows a broad band at 3445 cm^{-1} indicative of the presence of OH groups.

3. Summary and Outlook

3.1. Summary

The preparation of molecular precursors with controlled element composition has become a highly demanding subject due to its potential applications in the area of materials science. In earlier studies of siloxanes and phosphonates that contain group 4, 12, 13, and 14 metals, the feasibility of preparing such controlled products have been demonstrated. As mentioned in Section 1.7, the original aim of the present work was to synthesise group 12 metallasiloxane or -phosphonate aggregates and study their properties in solution. This study would also give insights in the effect of the substituents on the metal atoms and their role in the formation of the final products, *e*. *g*. the synthesis of iron (II) siloxane compounds.

In the first part of this work, we have synthesised five different zinc siloxane compounds **2** - **6** in moderate to good yields by alkane elimination reactions using either zinc dimethyl or diethyl with aminosilanetriol **1** (in the case of **2** MeLi was used). Compounds **2** - **6** have been completely structurally characterized by single crystal X-ray diffraction studies. The initially targeted anionic zinc siloxane **2** has a cubic structure containing six puckered eight-membered $Zn_2O_4Si_2$ rings (Figure 15). Four of these puckered eight-membered rings are further capped by lithium ions. The structure of **2** resembles the anionic group 13 anionic metallasiloxanes. Compound **2** is considered as a suitable precursor for mixed metal oxide systems.

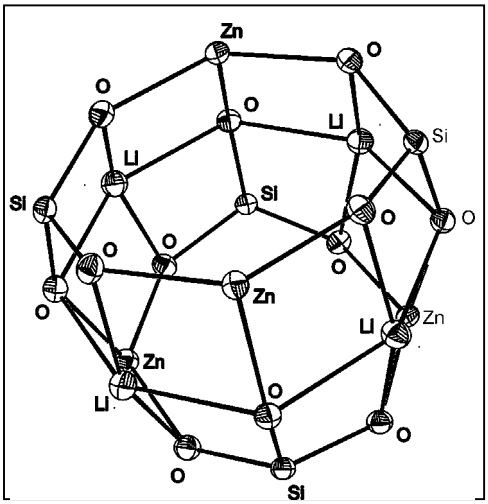

Figure 15. Core Structure of Lithium-zinc Siloxane 2

The reactions of **1** and zinc alkyls in different stoichiometric ratios have been carried out in order to understand the aggregation of the resulting zinc siloxanes. The reaction between zinc diethyl and **1** in 1:1 ratio yielded **3** as the major product that contains an unreacted hydroxyl group on each silicon atom. The solid-state structure of **3** reveals a dimeric product with two eight-membered $Zn_2O_4Si_2$ rings connected by the μ_3–oxygen atoms (Figure 16). The presence of hydroxyl groups can be exploited for further incorporation of metal atoms by reactions with suitable metal alkyls.

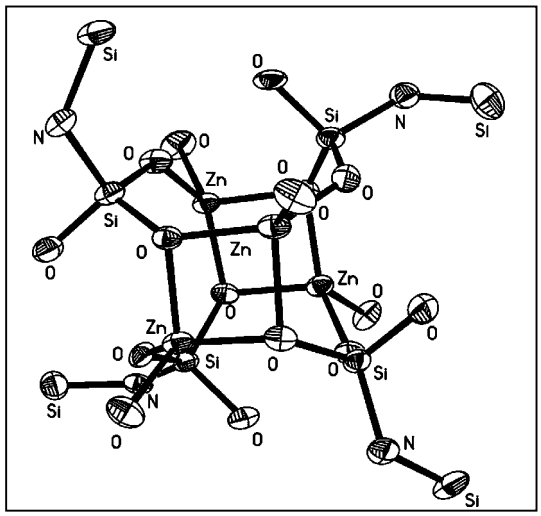

Figure 16. Core Structure of Zinc Siloxane 3 Containing Free Si–OH Groups

Moreover, changing the stoichiometric ratio of zinc dimethyl to **1** (2:1) forms the so far largest aggregate of a zinc siloxane compound, **4**. The solid-state structure of **4** exhibits an unprecedented arrangement of zinc and silicon atoms within the molecule (Figure 17). The composition of **4** indicates that it can be used as a potential precursor for the zinc orthosilicates which are widely utilised as a starting material to prepare manganese-doped zinc orthosilicate in the display industry. Further examination of the products **2 - 4** indicated that compound **3** could be an intermediate formed during the synthesis of **2** and **4**. The present reveals that the reaction of the hydroxyl groups in zinc siloxane **3** with MeLi or $ZnMe_2$ results in the products **2** and **4**, respectively.

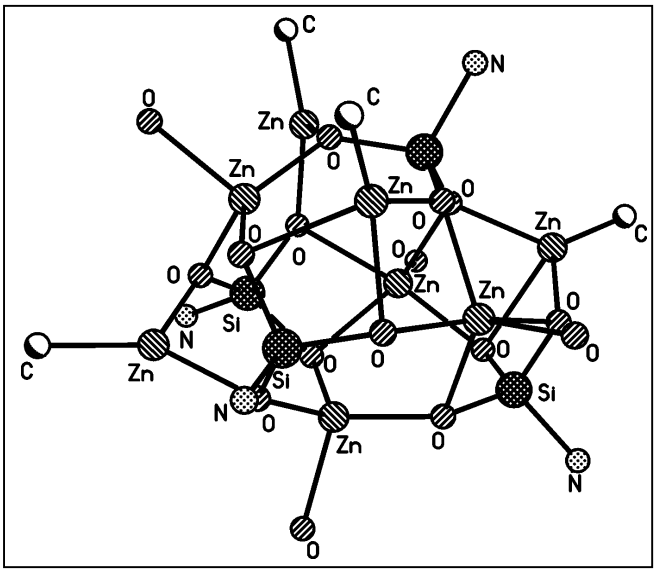

Figure 17. Core Structure of 4 Showing the Octanuclear Zinc Complex

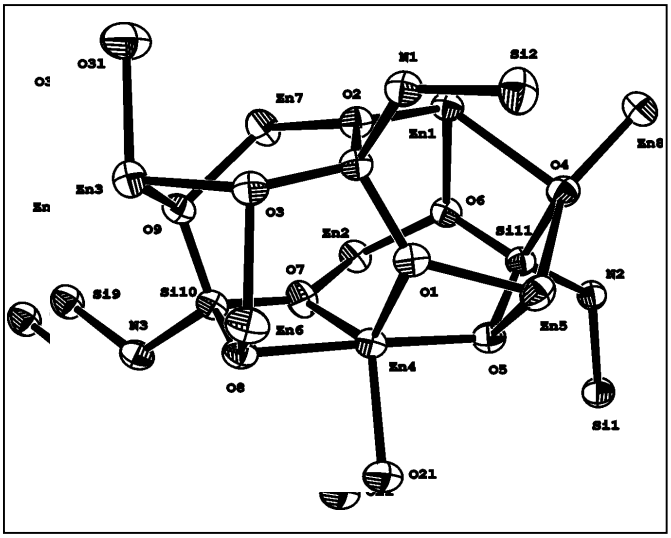

Figure 18. Core Structure of 5

In order to further understand the condensation process of aminosilanetriol **1**, the reaction between **1** and zinc dimethyl in a 1:3 stoichiometry has been carried out. Surprisingly, the reaction product **5** obtained from this reaction contains a Zn/Si ratio of 2.66 which is slightly less than in the starting material. This indicates the involvement of all three acidic –OH groups of **1** in the condensation with three equivalents of zinc dimethyl. The solid-state structure of **5** shows an improper merging of two different hexagonal zinc siloxane moieties that are connected with the silanolate moiety (Figure 18).

This study also examined the possibilities of isolating some of the key intermediate products formed during the formation of compounds **3** to **4**. Thus, the reaction between **1** and zinc dimethyl in a 1:1.75 stoichiometric ratio has been carried out. Interestingly three

different products **6** - **8** formed from this reaction. Among these compounds, **6** and **7** have been characterized by single crystal X-ray diffraction studies. The core of **6** contains a cubic polyhedron of $Zn_4Si_4O_{12}$ which is capped on the three faces by additional zinc atoms. The structure **7** is similar to that of **4**. Compound **8** has the proposed structure based on the comparison of the silicon NMR values.

Iron containing zeolites are widely used as catalysts for many organic reactions due to the redox property of iron. Iron containing silicates are ubiquitous in nature with both common oxidation states of iron. However, only few examples on the synthesis of ferrous siloxanes are known in the literature. The reaction between $Fe[N(SiMe_3)_2]_2$ and aminosilanetriol **1** in the presence of a heterocarbene in a 2:1 ratio afforded **9** in low yield (6 %). The solid-state structure of **9** indicates a drum-like structure containing a $Fe_4O_6Si_2$ core that is surrounded by the bulky amido substituents on half of the iron atoms. This reaction further demonstrates the effect of bulky substituents on the metal atom for the product formation and its stabilisation.

All above reactions and their products, **2** - **6** and **9**, clearly demonstrate that under suitable reaction conditions it is possible to control the condensation behaviour of aminosilanetriol **1**. Further the influence of the stoichiometry of the starting materials in the formation of molecular iron(II) and zinc siloxane aggregates has been demonstrated. Based on the above reactions of aminosilanetriol **1** with zinc dialkyls, the condensation behaviour of **1** can be summarised according to the following equations 1 - 3:

$$4\ RSi(OH)_3 + 4\ ZnEt_2 \longrightarrow \underset{\text{intermediate}}{4\ [(ZnEt)(O(HO)_2SiR)]} \longrightarrow \underset{\mathbf{3}}{[ZnO_2(HO)SiR]_4} \quad (1)$$

$$4\ RSi(OH)_3 + 8\ ZnMe_2 \longrightarrow \underset{\text{intermediate}}{[(ZnMe)_2(O_2(HO)SiR)]} \longrightarrow \underset{\mathbf{4}}{[(Zn_2Me)(O_3SiR)]_4} \quad (2)$$

$$3\ RSi(OH)_3 + 8\ ZnMe_2 \longrightarrow 8/3\ [(ZnMe)_3(O_3SiR)] \longrightarrow \underset{\mathbf{5}}{[Zn_8Me_7(O_3SiR)_3]} \quad (3)$$

Similar to zinc siloxane compounds, we have also examined the influence of the stoichiometric effect versus the product formation in the synthesis of zinc phosphonates. The reaction of *tert*-butylphosphonic acid with zinc diethyl in a 1:1 ratio affords zinc phosphonate **11** in a somewhat low isolated yield. The solid-state structure of this compound reveals the extended formation of cubic zinc phosphonate due to the presence of the tri-coordinated oxygen atom attached to zinc atoms. Due to the poor solubility, it was not possible to characterise **11** by NMR spectroscopy.

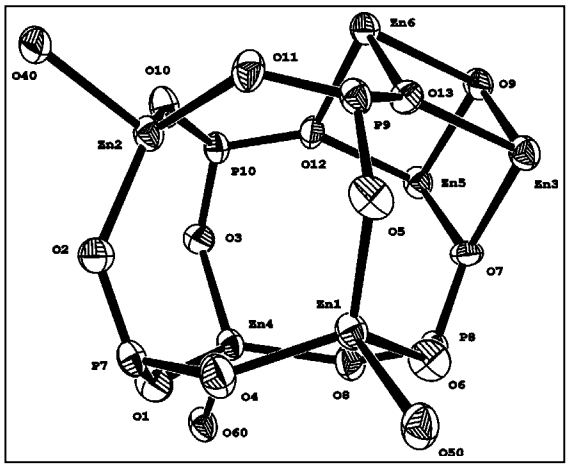

Figure 19. Core Structure of zinc phosphonate11 Showing $Zn_3\mu_3$–O Unit

In order to overcome the lack of solubility of the zinc phosphonates, a reaction of two equivalents of zinc dimethyl and one equivalent of *tert*-butylphosphonic acid was carried out. This reaction affords **12** in a very high yield (84 %). The X-ray crystal structure analysis of **12** reveals the presence of four zinc atoms, which are in plane; these zinc atoms are held together

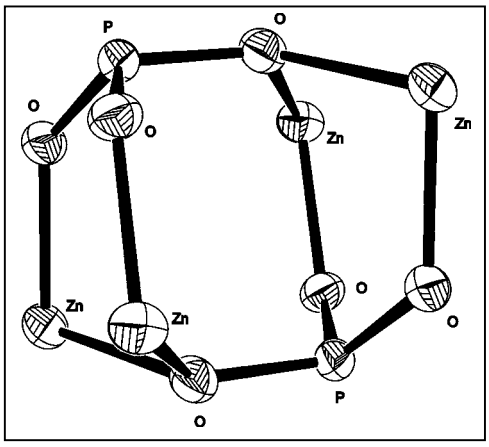

Figure 20. Core Structure of 12 Showing $Zn_4P_2O_6$Unit

by the phosphonate groups, which are above and below the zinc plane resembling the α-zirconium phosphate. It may be a starting material suitable for the further preparation of framework stuctures by exploiting the presence of methyl groups on planar zinc atoms.

Continuing the quest for the synthesis of larger aggregates of metallaphosphonates, the reaction of *tert*-butylphosphonic acid with cadmium dimethyl has been carried out. The solid-state structure of **13** reveals the largest aggregate of a cadmium phosphonate compound. This cluster contains an eight-membered Cd_4O_4 core. In spite of the surface methyl groups on cadmium, compound **13** is insoluble in common organic solvents. The solid-state ^{31}P MAS NMR shows the presence of four different phosphorus atoms present in the aggregate.

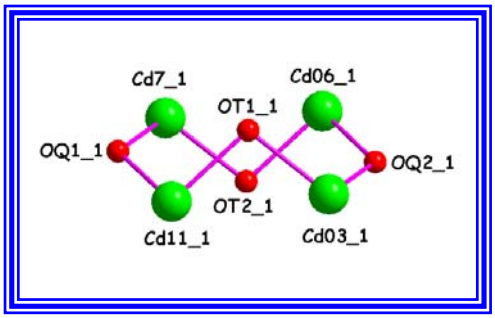

Figure 21. The Core Structure of 13 Showing Cd_4O_4 Unit

In order to overcome the poor solubility of the metallaphosphonate compounds, a bulky organic substituted phosphonic acid **16** was prepared by a multistep synthesis starting from 2,4,6-tri-iso-propylphenyl bromide. During this preparation, a convenient method for the synthesis of **14** has been established. Furthermore, compounds **14** and **16** were fully characterised by analytical and spectroscopic techniques. Compound **16** would prove to be an interesting and useful ligand in metal phosphonate chemistry.

3.2. Outlook

The focus of the work reported herein has been targeted on the synthesis and characterization of group 12 metallasiloxane and -phosphonate aggregates. A more general extension of this work would be using transition metal amides or rare earth amides as starting materials to synthesise new types of metallasiloxanes or -phosphonates.

By a simple change of stoichiometry of the reactants one can obtain a new variety of metallasiloxane and -phosphonate aggregates. These reactions also further indicate the molecular level controlled products are possible in the case of zinc siloxane and phosphonate compounds. This method could be applied to other systems containing metallasiloxane or -phosphonates. Moreover, the synthesis of bulky phosphonic acids offers advantage for the design of new highly soluble metallaphosphonate aggregates.

4. Experimental Section

4.1. General Procedures

All experimental manipulations, unless otherwise stated, were carried out in oxygen-free dry dinitrogen atmosphere using Schlenk glassware and techniques.[143] The handling of solids and the preparation of samples for spectral measurements were carried out inside a MBraun LABMASTER-130 dry-box where the O_2 and H_2O levels were normally kept below 1 ppm. The glassware used in all the manipulations were oven-dried at 150 °C for a minimum of 24 h, assembled hot, and cooled under high vacuum prior to use. Commercial grade solvents were purified and freshly distilled following conventional procedures prior to use.[144] For the use of highly air- and moisture-sensitive reactions, the solvents were freshly trap-to-trap distilled.

4.2. Physical Measurements

Melting points of all new compounds were measured on a Büchi melting point B-540 apparatus.

NMR spectra were recorded on Bruker Avance 200, AM 300, MSL 400 (CP-MAS), and Bruker Avance 500 NMR spectrometers. Chemical shifts are reported in ppm with reference to $SiMe_4$ (external) for ^{1}H, ^{13}C and ^{29}Si nuclei, and 85 % H_3PO_4 (external) for ^{31}P nuclei. Downfield shifts from the reference are quoted positive, upfield shifts are assigned negative values. All the NMR grade solvents were dried prior to use and the samples for measurements were freshly prepared in a dry-box. Heteroatom NMR spectra were recorded ^{1}H decoupled.

IR spectra were recorded on a Bio-Rad Digilab FTS7 spectrometer (only absorptions are reported, *vide infra*) and the samples were prepared normally as Nujol mulls between KBr plates.

Mass spectra were obtained on Finnigan MAT system 8230 or Varian MAT CH5 mass spectrometers by EI-MS methods.

Elemental analyses were performed at the Analytisches Labor des Instituts für Anorganische Chemie der Universität Göttingen.

Crystal structure determination: Intensity data for compounds **2**, **4**, **5**, **6**, **7**, **9**, and **11** were collected on a IPDS II Stoe image-plate diffractometer. The diffraction data for the compounds **3** and **12** were measured on a STOE-AED2 four circle diffractometer and compound **13** was measured on a Huber four-circle goniometer and a Siemens 1K-CCD area detector. The data for all the compounds were collected at low temperature (the temperatures for individual compounds are mentioned in the Tables in Section 6 using graphite monochromated MoK_α radiation (λ = 0.71073 Å). The data reduction and space group determination routines were carried out using Siemens SHELXTL family of programs.[145] The structures were solved using either SHELXS-96/97[146,147] programs. The refinement of the structures was carried out by full-matrix least-squares methods against F^2 using SHELXL-97. The various advanced features (*e.g.* restraints and constraints) of SHELXL programs were used to treat the disordered groups, lattice solvents such as THF, and the hydrogen atoms. In case of **13** the observed systematic absences did not correspond to any space group in the apparent orthorhombic crystal system, which suggested the presence of pseudo-merohedral twinning with a two-fold rotation about the ***c*** axis. Also non-hydrogen atoms in **13** were refined anisotropically except for atoms with very low (<0.1) occupancy; solvent molecules were refined isotropically. A riding model was used for the hydrogen atoms. The fractional contribution from the second twin domain was determined as 44 %. The

crystal data for all compounds along with the final residuals and other pertaining details are listed in Section 6 in tabular form.

4.3. Starting Materials

Tert-butylphosphonic acid (Acros or Aldrich) was dried under vacuum prior to use. The silanetriol (2,6-*i*$Pr_2C_6H_3$)N($SiMe_3$)Si$(OH)_3$,[62] Fe[N($SiMe_3$)$_2$]$_2$ · THF[148] 1,3-diisopropyl-4,5-dimethylimidazol-2-ylidene,[149] and cadmium dimethyl [150] were synthesized using reported procedures. Zinc dimethyl (2 M solution in toluene), zinc diethyl (1.1 M solution in toluene) and *N*,*N*,*N*',*N*'-tetramethyl-l,4-phenylenediamine (Aldrich), methyl lithium (1.6 M solution in diethyl ether, Acros) anhydrous $FeCl_2$, (Fluka), anhydrous $CdCl_2$ (Alfa) were purchased and used as received. 2,4,6-Tri-iso-propyl benzene was either purchased from Fluka or prepared by the reported procedure.[151] 2,4,6-Tri-iso-proplylphenyl bromide was prepared from the literature procedure.[140]

4.4. Synthesis of Zinc Siloxanes

4.4.1. Synthesis of [(L)ZnLi(O_3SiR)]$_4$ (L = 1,4-(NMe_2)$_2C_6H_4$, R = (2,6-*i*$Pr_2C_6H_3$)N($SiMe_3$)) (2)

A mixture of solutions of MeLi (2.4 mL of a 1.6 M solution in diethyl ether, 3.87 mmol) and $ZnMe_2$ (1.9 mL of a 2 M solution in toluene, 3.87 mmol) in THF (5 mL) was slowly added at room temperature to a suspension of RSi$(OH)_3$ (**1**) (1.27 g, 3.87 mmol) in hexane (40 mL). The reaction mixture was stirred for 10 min. and refluxed for 1.5 h. After cooling the solution to room temperature *N*,*N*,*N*',*N*'-tetramethyl-l,4-phenylenediamine (L) (0.64 g, 3.87 mmol) was added and stirred for another 1 h. The solution was filtered and concentrated to 1/3 of its volume. Colorless crystals were obtained at 0 ^oC from the concentrated solution.

2: Yield: 0.92 g, 42 %. Mp. 148 °C dec. IR (Nujol): $\tilde{\nu}$ = 1617, 1521, 1321, 1260, 1250, 1209, 1182, 1093, 1054, 1027, 967, 952, 913, 882, 836, 805, 736, 773, 682, 659, 599, 545, 466 cm^{-1}. ^1H NMR (500.13 MHz, C_6D_6, 25 °C, TMS): δ 0.36 (br, 36H, $Si(CH_3)_3$), 1.19 (br, 48H, $CH(CH_3)_2$), 2.81 (s, 48H, NCH_3), 3.80 (br, 8H, $CH(CH_3)_2$), 6.70 (s, 16H, LArH), 6.90 (br, 12H, aromat.): ^{29}Si NMR (99.36 MHz, C_6D_6, TMS): δ –64.8 (br, SiO_3), 2.1 (br, $Si(CH_3)_3$). MS (EI, 70 eV): *m*/*e* 162 (2,6-*i*$Pr_2C_6H_3$, 100 %), 177 (2,6-*i*$Pr_2C_6H_3NH_2$, 38 %). Anal. Calcd. for $C_{100}H_{168}Li_4N_{12}O_{12}Si_8Zn_4$ (2244.49) : C, 53.5; H, 7.5; N, 7.5. Found: C, 53.9; H 7.7; N, 7.7 %.

4.4.2. Synthesis of $[Zn(THF)(O_2(OH)SiR)]_4$ (R = (2,6-*i*$Pr_2C_6H_3$)N($SiMe_3$)) (3)

A solution of $RSi(OH)_3$ (**1**) (2.0 g, 6.1 mmol) in THF/hexane (5 mL, 40 mL) was added to a solution of $ZnEt_2$ (5.6 mL of a 1.1 M solution in toluene, 6.1 mmol) in hexane (10 mL) at room temperature. After the evolution of ethane gas ceased the resulting solution was stirred for further 16 h at room temperature. The volatile components were removed and the residue was dried for 6 h under vacuum. The remaining solid was washed with hexane (5 mL). Colourless crystals of **3** were obtained from toluene (5 mL) at room temperature.

3: Yield: 1.85 g, 62 %. Mp. 162 - 165 °C. ^1H NMR (500.13 MHz, $CDCl_3$, TMS): δ 0.03 (s, 36H, $Si(CH_3)_3$), 1.10 (d, 24H, *J* = 6.7 Hz, $CH(CH_3)(CH_3)$), 1.17 (d, 24H, *J* = 6.7 Hz, $CH(CH_3)(CH_3)$), 1.68 (br, 16H, OCH_2CH_2), 2.35 (s, 3H, $H_3CC_6H_5$), 3.62 (br, 16H, OCH_2), 3.70 (m, 8H, *J* = 6.7 Hz, $CH(CH_3)_2$), 6.94 (m, 12H, aromat.), 7.2 (m, 12H; $H_3CC_6H_5$). ^{13}C NMR (50.32 MHz, $CDCl_3$, TMS): δ 2.14 ($Si(CH_3)_3$), 21.45 ($C_6H_5CH_3$), 24.96 ($CH(CH_3)(CH_3)$), 25.06 ($CH(CH_3)(CH_3)$), 25.75 (OCH_2CH_2), 27.42 ($CH(CH_3)_2$), 69.95 (OCH_2), 123.03 (aromat. C-4), 123.36 (aromat. C-3, C-5), 125.29 (*p*-$C_6H_5CH_3$), 128.22 (*m*-$C_6H_5CH_3$), 129.03 (*o*-$C_6H_5CH_3$), 137.86 (H_3C-C_6H_5), 142.56 (aromat. C-2, C-6), 147.85 (aromat. C-1). ^{29}Si NMR (99.36 MHz, $CDCl_3$, TMS): δ –62.16 ($Si(OH)O_2$), 3.78 ($Si(CH_3)_3$).

IR (Nujol) $\tilde{\nu}$ = 3242, 1605, 1576, 1318, 1257, 1246, 1182, 1107, 1042, 1024, 967, 947, 908, 865, 823, 802, 753, 727, 693, 599, 549, 464 cm^{-1}. MS (EI, 70 eV): *m*/*e* (%) 162 (2,6-*i*$Pr_2C_6H_3$, 100 %), 177 (2,6-*i*$Pr_2C_6H_3NH_2$, 38 %). Anal. Calcd. for (**4**·C_7H_8) $C_{83}H_{148}N_4O_{16}Si_8Zn_4$ (1944.32): C, 51.2; H, 7.6; N, 2.8. Found: C, 50.75; H, 7.68; N, 2.87.

4.4.3. Synthesis of $[Zn_4(THF)_4(ZnMe)_4(O_3SiR)_4]$ (R = (2,6-*i*$Pr_2C_6H_3$)N($SiMe_3$)) (4)

A solution of $ZnMe_2$ (4 mL of a 2 M solution in toluene, 8.00 mmol) was slowly added to a suspension of $RSi(OH)_3$ (1.07 g, 3.87 mmol) in THF/hexane (5 mL, 40 mL) at room temperature. After the evolution of methane gas had ceased, the resulting solution was stirred for further 16 h at room temperature. The volatile components were removed and the residue was dried for 6 h under vacuum. The remaining solid was washed with THF/hexane (1:1) and finally recrystallised from toluene (5 mL) to yield colorless crystals of **4** at 0 °C.

4: Yield: 1.2 g, 64 %. Mp. > 200 °C. ^{1}H NMR (500.13 MHz, C_6D_6): δ –0.1, 0.018, 0.037, 0.060, 0.093 (s, 12H, ZnCH_3), 0.39 (m, 36H, Si(CH_3)$_3$), 1.37 (m, 48H, CH(CH_3)$_2$), 1.55 (m, 16H, OCH_2CH_2), 3.70 (m, 16H, OCH_2), 3.81 (br, 8H, $CH(CH_3)_2$), 7.01 (m, 12H, aromat.); ^{29}Si NMR (99.36 MHz, C_6D_6): δ –60.87, –61.34 (br; SiO_3), 3.58, 4.10 (s, $Si(CH_3)_3$). IR (nujol): $\tilde{\nu}$ = 1257, 1245, 1183, 1106, 1051, 1037, 966, 936, 917, 871, 833, 801, 754, 731, 694, 682, 600, 580, 546, 502 cm^{-1}. MS (EI, 70 eV): *m*/*e* (%) 162 (2,6-*i*$Pr_2C_6H_3$, 100 %), 177 (2,6-*i*$Pr_2C_6H_3NH_2$, 38 %). Anal. Calcd. for $C_{80}H_{148}N_4O_{16}Si_8Zn_8$ (2169.85): C, 44.3; H, 6.8; N, 2.6. Found: C, 44.4; H, 6.9; N, 2.2.

4.4.4. Conversion of 3 to 2

A solution of MeLi (5.2 mL of a 1.6 M solution in diethyl ether, 6.1 mmol) was added to a suspension of **3** (4.0 g, 2.1 mmol) in THF/hexane (10 mL, 40 mL) at room temperature. After the evolution of methane gas had ceased the resulting clear solution was stirred for

further 16 h at room temperature. To the resulting solution solid *N*,*N*,*N'*,*N*'-tetramethyl-l,4-phenylenediamine (L) (0.64 g, 3.9 mmol) was added and stirred for another 4 h. The solution was filtered and concentrated to 1/3 of its volume. Colorless crystals of **2** were obtained at room temperature (2.18 g, 45 %).

4.4.5. Conversion of 3 to 4

A solution of $ZnMe_2$ (1.6 mL of a 2 M solution in toluene, 6.1 mmol) was added to a suspension of **3** (1.5 g, 0.77 mmol) in THF/hexane (15 mL, 30 mL) at room temperature. After the evolution of methane gas had ceased the resulting clear solution was stirred for further 16 h at room temperature. The volatile components were removed and the residue was dried for 6 h under vacuum. The remaining solid was washed with hexane (5 mL). Colorless crystals of **4** were obtained in toluene (5 mL) at 0 ^{o}C (1.27 g, 67 %).

4.4.6. Synthesis of $[Zn_8Me_7(dioxane)_2(O_3SiR)_3]$ (R = (2,6-*i*$Pr_2C_6H_3$)N($SiMe_3$)) (5)

A solution of $ZnMe_2$ (4.5 mL of a 2 M solution in toluene, 9.17 mmol) was slowly added to a suspension of $RSi(OH)_3$ (1 g, 3.05 mmol) in dioxane/hexane (5 mL, 40 mL) at room temperature. After the evolution of methane gas had ceased the resulting solution was stirred for further 16 h at room temperature. The solution was concentrated to 10 mL and kept for crystallisation at room temperature to yield colorless crystals of **5**.

5: Yield: 1.53 g, 80 %. Mp. > 200 ^{o}C. ^{1}H NMR (200.13 MHz, $CDCl_3$, TMS): δ –0.73, (s, 21H, ZnCH_3), 0.07 (s, 27H, Si(CH_3)$_3$), 1.14 (d, 18H, CH(CH_3)$_2$), 1.23 (d, 18H, CH(CH_3)$_2$), 3.61 (br, 22H, dioxane + C*H*(CH_3)$_2$), 7.16 (m, 9H, aromat). ^{29}Si NMR (99.36 MHz, $CDCl_3$): δ –62.2 (SiO_3), 6.18 ($SiMe_3$). IR (nujol): $\tilde{\nu}$ = 1317, 1291, 1249, 1183, 1169, 1124, 1106, 1066, 1051, 1043, 1017, 945, 919, 869, 837, 807, 753, 729, 685, 647, 611, 582, 547, 519, 480, 464, 445 cm^{-1}. MS (EI, 70 eV): *m*/*e* (%) 162 (2,6-*i*$Pr_2C_6H_3$, 100 %), 177 (2,6-*i*$Pr_2C_6H_3NH_2$, 38 %).

Anal. Calcd. for $C_{71}H_{131}N_3O_{15}Si_6Zn_8$ (1958.44): C, 43.54; H, 6.74; N, 2.15. Found: C, 43.3; H, 6.8; N, 2.2.

4.4.7. Synthesis of zinc siloxanes (6-8)

A solution of $ZnMe_2$ (4.6 mL of a 2 M solution in toluene, 9.17 mmol) was slowly added to a suspension of $RSi(OH)_3$ (1.8 g, 3.87 mmol) in THF/hexane (10 mL, 40 mL) at room temperature. After the evolution of methane gas had ceased the resulting solution was further stirred overnight at room temperature. A white precipitate was obtained and filtered off. The filtrate was concentrated to 15 mL and kept at room temperature for crystallisation. Colorless crystals of **7** were obtained from the mother solution. Dissolving the precipitate in toluene gave colorless crystals of **6**.

6: Yield: 0.8 g, 25 %. Mp. > 300 °C. ^{1}H NMR (300.13 MHz, C_6D_6): δ 0.12, 0.02, (s, 6H, Zn(CH_3)), 0.06 (m, 36H, Si(CH_3)$_3$), 1.11 (m, 48H, CH(CH_3)$_2$), 1.75 (m, 16H, OCH$_2$CH_2), 3.64 (m, 24H. OCH_2 + CH(CH$_3$)$_2$), 6.93 (m, 12H, aromat.). ^{29}Si NMR (99.36 MHz, C_6D_6): δ –53.62, –61.10 (SiO_3), 5.17, 4.20 (Si(CH$_3$)$_3$). IR (nujol): $\tilde{\nu}$ = 1245, 1185, 1106, 1074, 1052, 1041, 1023, 967, 937, 916, 872, 837, 802, 755, 732, 680 cm^{-1}. MS (EI, 70 eV): *m*/*e* (%) 162 (2,6-*i*Pr$_2$C$_6$H$_3$, 100 %), 177 (2,6-*i*Pr$_2$C$_6$H$_3$NH$_2$, 38 %). Anal. Calcd. for $C_{82}H_{150}N_4O_{17}Si_8Zn_7$ (2146.5): C, 45.8; H, 7.0; N 2.6. Found: C, 47.1; H, 7.1; N, 2.5.

7: Mp. > 200 °C. ^{1}H NMR (300.13 MHz,$CDCl_3$): δ –0.15, –0.029, 0.059, 0.067, 0.088 (s, 12H, ZnCH_3), 0.15, (m, 36H, Si(CH_3)$_3$), 0.37 (m, 48H, CH(CH_3)$_2$), 1.81 (m, 16H, *O*CH_2CH$_2$), 3.73 (br, 24H, OCH_2 + CH(CH$_3$)$_2$), 6.95 (m, 12H, aromat). IR (nujol): $\tilde{\nu}$ = 1318, 1257, 1246, 1182, 1106, 1052, 1042, 1031, 966, 937, 917, 872, 835, 801, 753, 728, 693, 683, 600, 599, 546, 501 cm^{-1}. MS (EI, 70 eV): *m*/*e* (%) 162 (2,6-*i*Pr$_2$C$_6$H$_3$, 100 %), 177 (2,6-*i*Pr$_2$C$_6$H$_3$NH$_2$, 38 %). Anal. Calcd. for $C_{80}H_{148}N_4O_{16}Si_8Zn_8$ (2169.85): C, 44.28; H, 6.87; N, 2.58. Found: C, 45.26; H, 6.89; N 2.31.

4.5. Synthesis of [{FeL'}$_2${Fe(heterocarbene)}$_2${O_3SiR}$_2$] (R = (2,6-*i*Pr$_2$C$_6$H$_3$)N(SiMe$_3$)) (L' = (N(SiMe$_3$)$_2$) (heterocarbene = 1,3-diisopropyl-4,5-dimethylimidazol-2-ylidene) (9)

A solution of [Fe(N(SiMe$_3$)$_2$]$_2$ (3.5 g, 9.17 mmol) was slowly added to a suspension of RSi(OH)$_3$ (**1**) (1.5 g, 4.59 mmol) in THF/hexane (10 mL, 40 mL) at room temperature. The color of the solution turned from green to dark brown. The resulting solution was stirred for further 16 h at room temperature. A solution of heterocarbene (2 g, 11.47 mmol) in toluene (10 mL) was added and the stirring was continued for one more day. The volatile components were removed to obtain a brown as a solid. To this mixture toluene (10 mL) and THF (1 mL) was added. Colorless crystals of **9** were obtained after several days at 0 ^{o}C.

9: Yield: 0.19 g, 6.0 %. Mp. > 220 ^{o}C. IR (nujol): $\tilde{\nu}$ = 1260, 1245, 1221, 1186, 1100, 1043, 1019, 983, 964, 945, 927, 885, 836, 820, 801, 752, 723, 680, 607, 567, 544, 491 cm^{-1}. Anal. Calcd. for $C_{64}H_{128}Fe_4N_8O_6Si_8$ (1407.44): C, 49.47; H, 8.30; N, 7.21. Found: C, 47.7; H, 8.0; N, 6.2.

4.6. Synthesis of Group 12 Metal Phosphonates

4.6.1. Synthesis of [{(ZnEt)$_3$(Zn(THF))$_3$}{*t*BuPO$_3$}$_2${μ_3–OEt}] (11)

A solution of ZnEt$_2$ (3.2 mL of a 1.1 M solution in toluene, 3.62 mmol) was added to a solution of *tert*-butylphosphonic acid (**10**) (0.5 g, 3.62 mmol) in THF/hexane (30 mL, 5 mL) at room temperature. After the evolution of methane gas had ceased the resulting solution was stirred for further 2 h at room temperature. A gel was formed and it was was filtered over celite. The solution was concentrated to 10 mL and kept at 0 ^{o}C for crystallisation. Colorless crystals of **11** were obtained after a week.

11: Yield: 0.085 g, 8.9 %. Mp. > 250 °C. IR (nujol): $\tilde{\nu}$ = 1299, 1262, 1232, 1202, 1155, 1107, 1092, 1056, 1038, 1019, 998, 981, 920, 881, 834, 803, 722, 661 cm^{-1}. Anal. Calcd. for $C_{24}H_{56}O_{13}P_4Zn_6$ – 3 THF (1068.93): C, 26.97; H, 5.28. Found: C, 24.5; H, 5.2.

4.6.2. Synthesis of [{$Zn_4Me_4(THF)_2$}{*t*$BuPO_3$}$_2$] (12)

A solution of $ZnMe_2$ (3.6 mL of a 2 M solution in toluene, 7.24 mmol) was added to a solution of *tert*-butylphosphonic acid (**10**) (0.5 g, 3.62 mmol) in THF/hexane (10 mL, 20 mL) at room temperature. After the evolution of methane gas had ceased the resulting clear solution was stirred for further 2 h at room temperature and then heated to reflux for 1 h. The volatile components were removed until a slight turbid solution was noticed and the solution was warmed up further till the turbidity disappeared. Colorless crystals of (**12**) were obtained after a day.

12: Yield: 1.12 g, 84 %). M.p. > 250 °C. ^{1}H NMR (200.13 MHz, THF-d^8): δ –0.88 (s, ZnCH_3), 1.17 (d, ^3J = 15.43 Hz, 18H, C(CH_3)$_3$). ^{31}P NMR (81.02 MHz, THF-d^8): δ 39.58. IR (nujol): $\tilde{\nu}$ = 1262, 1170, 1145, 1105, 1059, 1033, 965, 919, 862, 833, 805, 722, 658, 578, 548, 514, 432 cm^{-1}. Anal. Calcd. for $C_{20}H_{46}O_8P_2Zn_4$ (738.08): C, 32.61; H, 6.25. Found: C, 32.1; H 6.3.

4.6.3. Synthesis of [$(CdMe)_{10}(Cd(THF))_4Cd_6(\mu_4$–$O)_2(\mu_3$–$OH)_2$(*t*$BuPO_3)_{12}$] (13)

(i) $CdMe_2$ (0.65 g, 4.6 mmol) was added dropwise to a THF solution (50 mL) of *tert*-butyl phosphonic acid (**10**) (0.32 g, 2.3 mmol) at room temperature. After the evolution of methane gas had ceased the resulting solution was stirred for further 6 h. The solution was then concentrated to 5 mL and toluene (5 mL) was added and kept for crystallisation. Colorless crystals of **13** were obtained after a month at room temperature (Yield: 0.12 g, 14 %).

(ii) $CdMe_2$ (0.51 g, 3.6 mmol) was added dropwise to a THF solution (50 mL) of *tert*-butyl phosphonic acid (0.3 g, 2.2 mmol) and water (8 mg, 0.72 mmol) at room temperature. After the evolution of methane gas had ceased the resulting solution was stirred for further 6 h. The solution was then concentrated to 5 mL and toluene (5 mL) was added and kept for crystallisation. Colorless crystals of **13** were obtained after a month at room temperature.

13: M.p. > 300 ^oC. Solid State MAS NMR: ^1H NMR (399.92 MHz, TMS): δ 0.6 (s, Cd (CH_3), 1.7 (br, $C(CH_3)_3$). ^{31}P NMR (161.90 MHz, 85 % H_3PO_4): δ 35.4, 36.3, 39.7, 41.2. IR (nujol): $\tilde{\nu}$ = 3181, 2232, 1615, 1478, 1461, 1393, 1365, 1261, 1231, 1202, 1127, 1051, 1027, 969, 884, 832, 804, 727, 680, 660, 557, 520, 508, 487, 435 cm^{-1}. Anal. Calcd. for $C_{58}H_{140}Cd_{20}O_{40}P_{12}$ – 4 THF (4097.61): C, 17.00; H, 3.44. Found: C, 16.25; H, 3.48.

4.7. Synthesis of Bulky Phosphonic Acid

4.7.1. Synthesis of 2,4,6-tri-iso-propylphenylphosphonous dichloride (14)

(i) A Grignard solution of 2,4,6-tri-iso-propylphenylmagnesium bromide (prepared from 2,4,6-tri-iso-propylphenyl bromide (20 g, 70.6 mmol) with Mg (1.69 g, 70.6 mmol) in 200 mL of THF with a few drops of methyl iodide to initiate the reaction)* was cooled to –78 ^oC and a solution of anhydrous $ZnCl_2$ (19.2 g, 141 mmol) was added. The suspension was stirred over night and the solution was cooled to –78 ^oC. Phosphorus trichloride (9.7 g, 70.6 mmol) was added slowly over a period of half an hour and the reaction mixture was stirred for 6 h at room temperature. The volatile components were removed under vacuum and a pale yellow colored product was obtained. The solid was then dissolved in diethylether (200 mL) and filtered. Diethyl ether was removed under vacuum and the residue was washed twice with 20 mL of pentane. (crude product 26.5 g, 81 %). The crude product contained mainly 2,4,6-tri-iso-propylphenylphosphonous dichloride (**14**) as seen from the ^{31}P NMR, the minor product was 2,4,6-iPr$_3$C$_6$H$_2$P(Cl)Br.

* 2,4,6-tri-iso-propylphenylmagnesium bromide was prepared under gentle reflux. This has to be done very carefully. If the reaction is vigorous then remove the heating (if it is violent cool it with an ice bath or dry ice-acetone mixture).

14: Mp: 95 - 97 ^{o}C. ^{1}H NMR (200.13 MHz, $CDCl_3$, TMS): δ 1.25 (d, 12H, ^{3}J = 6.9 Hz, *o*-CH(CH_3)$_2$), 1.17 (d, 12H, ^{3}J = 6.8 Hz, *p*-CH(CH_3)$_2$), 2.89 (sept, 1H, ^{3}J = 6.8 Hz, *p*-CH(CH$_3$)$_2$), (d(sept.), 2H, ^{3}J (H,H) + ^{4}J (P,H) = 4.69 Hz, *o*-CH(CH$_3$)$_2$), 7.09 (d, 2H, aromat.), ^{31}P NMR (81.02 MHz, $CDCl_3$, TMS): δ 165.20. IR (nujol) $\tilde{\nu}$ = 1601, 1558, 1546, 1260, 1241, 1191, 1166, 1133, 1104, 1083, 1059, 1038, 959, 940, 922, 898, 879, 843, 806, 756,722, 651, 644, 610, 577, 548, 523, 485, 406 cm^{-1}. MS (EI, 70 eV): *m*/*e* (%) 304 ($C_{15}H_{22}PCl_2$, 70 %), 289 ($C_{14}H_{19}PCl_2$, 38 %). Anal. Calcd for $C_{15}H_{23}PCl_2$ (305.22): C, 59.03; H, 7.60; Cl, 23.23. Found: C, 60.0; H, 7.9; Cl, 20.5.

(ii) Phosphorus trichloride (1.2 g, 8.83 mmol) was dissolved in THF and cooled to –78 ^{o}C. To this solution was added a Grignard solution of 2,4,6-tri-iso-propylphenylmagnesium bromide (prepared from 2,4,6-tri-iso-propylphenyl bromide (2.5 g, 8.83 mmol) with Mg (0.21 g, 8.83 mmol) in 200 mL of THF)* slowly *via* cannula over a period of 1 h. After complete addition the reaction mixture was stirred for 16 h. The volatile components were removed under vacuum and the product was washed with two portions of 50 mL of hexane. (crude product 0.95 g, 73.4 %). The crude product contained a mixture of compounds, 2,4,6-*i*Pr$_3$C$_6$H$_2$PX$_2$ (X$_2$ = Cl$_2$ (a), Br$_2$ (b) and ClBr (c)). This mixture gave an identical mass spectrum as that for method (a) and also the phosphorous NMR with three different peaks. ^{31}P NMR (81.02 MHz, $CDCl_3$, TMS): δ 165.20 (a), 160.2 (c), 153.0 (b).

4.7.2. Synthesis of 2,4,6-tri-iso-propylphenylphosphonic dichloride (15)

The procedure for the preparation was similar to the reported one [141] except that the addition of sulfuryl chloride was done very slowly to a solution of **14** (10 g, 32.79 mmol) in

carbon tetrachloride at 0 °C. After the removal of all volatiles in vacuum **15** was washed twice with hexane (5 mL). (crude product 7.2 g, 68 %). Further purification was achieved by dissolving the compound in an ether / pentane mixture and cooled to 0 °C. ^{31}P NMR (200.13 MHz, $CDCl_3$, TMS): δ 33.08.

4.7.3. Conversion of 2,4,6-tri-iso-propylphenylphosphonic dichloride (15) to 2,4,6-tri-iso-propylphenylphosphonic acid (16)

The procedure was followed similar to the reported method for the preparation of 2,4,6-tri-tert-butyl phenylphosphonic acid.[152] NaOH (~2 M) was used for the hydrolysis of **15** (5 g, 15.57 mmol). However, in this case we obtained a mixture of **16** and bis(2,4,6-tri-iso-propylphenylphosphonic) anhydride was obtained. 2,4,6-Tri-iso-propylphenylphosphonic acid was separated by repeated washings with a mixture of ether / pentane (1:10) followed by drying in vacuum for 24 h.

16: Yield (2.5 g, 56 %). Mp: 214 - 217 °C. ^{1}H NMR (300.13 MHz, $CDCl_3$, TMS): δ 1.22 (d, 18H, *J*(H,H) = 6.9 Hz, *o,p*-CH(C*H*$_3$)$_2$), 2.87 (sept. 1H, *J*(H,H) = 6.9 Hz, *p*-CH(C*H*$_3$)$_2$), 3.99 (sept. 2H, *J*(H,H) = 6.7, *o*-CH(C*H*$_3$)$_2$), 7.11 (d, 2H, aromat.), 10.53 (br, 2H, O*H*). ^{31}P NMR (121.49 MHz, $CDCl_3$, TMS): δ 28.25. IR (KBr) $\tilde{\nu}$ = 3445, 2958, 2929, 2869, 2324, 1606, 1560, 1543, 1459, 1425, 1383, 1364, 1254, 1181, 1144, 1106, 1083, 1070, 1050, 994, 944, 908, 881, 797, 652, 579, 527 cm^{-1}. MS (EI, 70 eV): *m*/*e* (%) 284 ($C_{15}H_{25}PO_3$, 86 %), 269 ($C_{14}H_{22}O_3P$ 100 %). Anal. Calcd for $C_{15}H_{23}O_3P$ (284.33): C, 63.36; H, 8.86; Found: C, 62.94; H, 7.90.

5. Handling and Disposal of Solvents and Residual Waste

1. The recovered solvents were distilled or condensed into cold-traps under vacuum and collected in halogen-free or halogen-containing solvent containers, and stored for disposal.
2. Used NMR solvents were classified into halogen-free and halogen-containing solvents and were disposed as heavy metal wastes and halogen-containing wastes, respectively.
3. The heavy metal residues were dissolved in nitric acid and after neutralisation stored in the containers for heavy metal wastes.
4. Drying agents such as KOH, $CaCl_2$, and P_4O_{10} were hydrolyzed and disposed as acid or base wastes.
5. Whenever possible, sodium metal used for drying solvents was collected for recycling.[153] The non-reusable sodium metal was carefully hydrolysed in cold ethanol and poured into the base-bath used for cleaning glassware.
6. Ethanol and acetone used for solid CO_2 cold-baths were subsequently used for cleaning glassware.
7. The acid-bath used for cleaning glassware was neutralized with Na_2CO_3 and the resulting NaCl solution was washed-off in the communal water drainage.
8. The residue of the base-bath used for glassware cleaning was poured into the container for base wastes.

Amounts of various types of disposable wastes generated during the work:

Metal containing wastes	10 L
Halogen-containing solvent wastes	7 L
Halogen-free solvent wastes	35 L
Acid wastes	10 L
Base wastes	20 L

6. Crystal Data and Refinement Details

Table CD1. Crystal data and structure refinement for ($2\cdot C_6H_{14}$).

Identification code	ra125
Empirical formula	$C_{106}H_{182}Li_4N_{12}O_{12}Si_8Zn_4$
Formula weight	2330.60
Temperature	133(2) K
Wavelength	0.71073 Å
Crystal system	monoclinic
Space group	*P*2(1)/*n*
Unit cell dimensions	a = 24.7513(5) Å, $\alpha = \gamma = 90^o$.
	b = 19.9986(4) Å, β = 99.75 (10)^o.
	c = 25.2954(5) Å.
Volume	12339.8(4) Å^3
Z	4
Calculated density	1.254 Mg/m^3
Absorption coefficient	0.904 mm^{-1}
F(000)	4968
θ range for data collection	1.31 to 24.84 deg.
Index ranges	$-29 \le h \le 29$, $-23 \le k \le 23$, $-29 \le l \le 29$
Reflections collected	202689
R (int)	0.0837
Refinement method	Full-matrix least-squares on F^2
Data / restraints / parameters	21207 / 0 / 1380
Goodness-of-fit on F^2	1.029
Final R indices [$I > 2\sigma(I)$]	$R1$ = 0.0299, $wR2$ = 0.0813
R indices (all data)	$R1$ = 0.0375, $wR2$ = 0.0838
Largest difference peak and hole	0.650 and –0.453 e·Å^3

Table CD2. Crystal Data and Structure Refinement Details for 3·C_7H_8.

Identification code	R1008
Empirical formula	$C_{83}H_{148}N_4O_{16}Si_8Zn_4$
Formula weight	1944.25
Temperature	200(2) K
Wavelength	0.71073 Å
Crystal system	monoclinic
Space group	$P2_1$
Unit cell dimensions	a = 17.117(3) Å, $\alpha = \gamma = 90^o$.
	b =16.692(5) Å, β = 91.45 (7)^o.
	c =17.399(4) Å.
Volume	4970(2) Å^3
Z	2
Calculated density	1.299 Mg/m^3
Absorption coefficient	1.109 mm^{-1}
F(000)	2068
θ range of collection	3.51 to 22.49 deg
Index range	$-7 \le h \le 18$, $-17 \le k \le 17$, $-18 \le l \le 18$
Reflections collected	6978
R (int)	0.2388
Refinement method	Full-matrix least-squares on F^2
Data/ restraints/ parameters	6928/1498/1014
Goodness-of-fit on F^2	1.050
Final R indices [$I > 2\sigma(I)$]	$R1$ = 0.0569, $wR2$ = 0.1386
R indices (all data)	$R1$ = 0.0775, $wR2$ = 0.1536
Largest difference peak and hole	0.687 and –0.536 e·Å^{-3}

Table CD3. Crystal data and structure refinement for 4·3 C_7H_8.

Identification code	ra186
Empirical formula	$C_{101}H_{172}N_4O_{16}Si_8Zn_8$
Formula weight	2446.11
Temperature	133(2) K
Wavelength	0.71073 Å
Crystal system	triclinic
Space group	*P*-1
Unit cell dimensions	a = 14.5274(7) Å, α = 99.197(4)°.
	b = 16.0523(10) Å, β = 91.338(4)°.
	c = 27.4893(14) Å, γ = 112.005(4)°.
Volume	5842.7(5) Å^3
Z	2
Calculated density	1.390 Mg/m^3
Absorption coefficient	1.754 mm^{-1}
F(000)	2572
θ for data collection	1.52 to 24.82 deg.
Index ranges	$-17 \le h \le 17$, $-18 \le k \le 18$, $-32 \le l \le 32$
Reflections collected	39805
R(int)	0.0629
Refinement method	Full-matrix least-squares on F^2
Data / restraints / parameters	17747 / 2 / 1164
Goodness-of-fit on F^2	1.014
Final R indices [$I > 2\sigma$(I)]	$R1$ = 0.0393, $wR2$ = 0.0961
R indices (all data)	$R1$ = 0.0514, $wR2$ = 0.0997
Largest difference peak and hole	0.877 and –0.653 e·A^{-3}

Table CD4. Crystal data and structure refinement for 5·C_7H_8·$C_4H_8O_2$.

Identification code	r363b
Empirical formula	$C_{71}H_{131}N_3O_{15}Si_6Zn_8$
Formula weight	1958.29
Temperature	133(2) K
Wavelength	0.71073 Å
Crystal system	triclinic
Space group	*P*1
Unit cell dimensions	a = 12.893(3) Å, α = 68.66(3)°.
	b = 13.297(3) Å, β = 69.74(3)°.
	c = 15.071(3) Å, γ = 79.88(3)°.
Volume	2254.4(8) Å^3
Z	1
Calculated density	1.442 Mg/m^3
Absorption coefficient	2.226 mm^{-1}
F(000)	1022
θ range for data collection	1.52 to 24.83 deg.
Index ranges	$-15 \le h \le 15$, $-15 \le k \le 15$, $-17 \le l \le 17$
Reflections collected	34851
R(int)	0.0584
Refinement method	Full-matrix least-squares on F^2
Data / restraints / parameters	13876 / 3 / 958
Goodness-of-fit on F^2	0.992
Final R indices [$I > 2\sigma(I)$]	$R1$ = 0.0395, $wR2$ = 0.0947
R indices (all data)	$R1$ = 0.0431, $wR2$ = 0.0959
Largest difference peak and hole	0.743 and –0.414 e·A^{-3}

Table CD5. Crystal data and structure refinement for 6·2 C_7H_8.

Identification code	r1021
Empirical formula	$C_{96}H_{166}N_4O_{17}Si_8Zn_7$
Formula weight	2330.64
Temperature	133(2) K
Wavelength	0.71073 Å
Crystal system	triclinic
Space group	*P*-1
Unit cell dimensions	a = 14.512(3) Å, α = 96.43(3)°
	b = 15.663(3) Å, β = 100.64(3)°
	c = 28.867(6) Å, γ = 114.54(3)°
Volume	5734(2) Å^3
Z	2
Calculated density	1.350 Mg/m^3
Absorption coefficient	1.581 mm^{-1}
F(000)	2456
θ range for data collection	1.46 to 24.85°.
Index ranges	$-17 \le h \le 17$, $-18 \le k \le 18$, $-34 \le l \le 33$
Reflections collected	120336
R (int)	0.0937
Refinement method	Full-matrix least-squares on F^2
Data / restraints / parameters	19778 / 1 / 1123
Goodness-of-fit on F^2	1.018
Final R indices [$I > 2\sigma(I)$]	$R1$ = 0.0326, $wR2$ = 0.0664
R indices (all data)	$R1$ = 0.0505, $wR2$ = 0.0679
Largest diffifference peak and hole	0.993 and –0.457 e·Å^{-3}

Table CD6. Crystal data and structure refinement for 9·1.5 C_7H_8.

Identification code	r200
Empirical formula	$C_{74.50}H_{140}Fe_4N_8O_6Si_8$
Formula weight	1692.06
Temperature	133(2) K
Wavelength	0.71073 Å
Crystal system	triclinic
Space group	*P*-1
Unit cell dimensions	a = 12.620(5) Å, α = 93.94(4)°.
	b = 14.783(6) Å, β = 97.85(3)°.
	c = 27.220(12) Å, γ = 109.69(3)°.
Volume	4700.8(3) Å^3
Z	2
Calculated density	1.195 Mg/m^3
Absorption coefficient	0.755 mm^{-1}
F(000)	1814
θ range for data collection	1.47 to 24.84 deg.
Index ranges	$-14 \le h \le 14$, $-17 \le k \le 17$, $-32 \le l \le 27$
Reflections collected	45117
R (int)	0.0695
Refinement method	Full-matrix least-squares on F^2
Data / restraints / parameters	16133 / 1 / 917
Goodness-of-fit on F^2	0.998
Final R indices [$I > 2\sigma(I)$]	$R1$ = 0.0497, $wR2$ = 0.1354
R indices (all data)	$R1$ = 0.0731, $wR2$ = 0.1452
Largest difference peak and hole	1.031 and -1.016 e·A^{-3}

Table CD7. Crystal data and structure refinement for 11.

Identification code	test
Empirical formula	$C_{36}H_{80}O_{16}P_4Zn_6$
Formula weight	1285.10
Temperature	133(2) K
Wavelength	0.71073 Å
Crystal system	triclinic
Space group	*P*-1
Unit cell dimensions	a = 12.512(3) Å, α = 89.39(3)°.
	b = 13.218(3) Å, β = 85.99(3)°.
	c = 16.542(3) Å, γ = 78.10(3)°.
Volume	2670.7(9) $Å^3$
Z	2
Calculated density	1.598 Mg/m^3
Absorption coefficient	2.830 mm^{-1}
$F(000)$	1328
θ range for data collection	1.57 to 24.84 deg.
Index ranges	$-14 \leq h \leq 12$, $-15 \leq k \leq 15$, $-19 \leq l \leq 19$
Reflections collected	22491
R (int)	0.0981
Refinement method	Full-matrix least-squares on F^2
Data / restraints / parameters	031 / 0 / 575
Goodness-of-fit on F^2	0.783
Final R indices [$I > 2\sigma(I)$]	$R1$ = 0.0376, $wR2$ = 0.0796
R indices (all data)	$R1$ = 0.0621, $wR2$ = 0.0833
Largest difference peak and hole	0.741 and –0.654 $e \cdot A^{-3}$

Table CD8. Crystal data and structure refinement for 12.

Identification code	r1009a
Empirical formula	$C_{20}H_{46}O_8P_2Zn_4$
Formula weight	737.99
Temperature	150(2) K
Wavelength	0.71073 Å
Crystal system	Monoclinic
Space group	*P*2(1)/*n*
Unit cell dimensions	a = 9.933(2) Å, $\alpha = \gamma = 90^o$.
	b = 11.311(2) Å, β = 95.59(3)^o.
	c = 13.865(3) Å
Volume	1550.3(5) Å^3
Z	2
Calculated density	1.581 Mg/m^3
Absorption coefficient	3.197 mm^{-1}
F(000)	760
θ range for data collection	3.60 to 25.03°.
Index ranges	$-11 \le h \le 11$, $-12 \le k \le 13$, $-15 \le l \le 16$
Reflections collected	3640
R (int)	0.1860
Refinement method	Full-matrix least-squares on F^2
Data / restraints / parameters	2728 / 0 / 159
Goodness-of-fit on F^2	1.113
Final R indices [$I > 2\sigma(I)$]	$R1$ = 0.0513, $wR2$ = 0.1256
R indices (all data)	$R1$ = 0.0586, $wR2$ = 0.1318
Largest difference peak and hole	1.198 and –0.649 e·Å^{-3}

Table CD9. Crystal data and structure refinement for 13.

Identification code	raq
Empirical formula	$C_{80.55}H_{185.10}Cd_{20}O_{45.64}P_{12}$
Formula weight	4503.83
Temperature	133(2) K
Wavelength	0.71073 Å
Crystal system	monoclinic
Space group	*P*2(1)/*c*
Unit cell dimensions	a = 24.303(5) Å, α = 90°.
	b = 25.294(5) Å, β = 90.14(3)°.
	c = 25.107(5) Å, γ = 90°.
Volume	15434(5) $Å^3$
Z	4
Calculated density	1.938 Mg/m^3
Absorption coefficient	2.878 mm^{-1}
F(000)	8694
θ range for data collection	3.32 to 25.19°.
Index ranges	$-28 \le h \le 28$, $0 \le k \le 30$, $0 \le l \le 29$
Reflections collected	158685
R (int)	0.1052
Refinement method	Full-matrix least-squares on F^2
Data / restraints / parameters	27363 / 713 / 1550
Goodness-of-fit on F^2	1.056
Final *R* indices [$I > 2\sigma(I)$]	$R1$ = 0.0587, $wR2$ = 0.1270
R indices (all data)	$R1$ = 0.0980, $wR2$ = 0.1482
Largest difference peak and hole	2.429 and –1.956 $e \cdot Å^{-3}$

7. References

[1] N. N. Greenwood, A. Earnshaw, *Chemistry of the Elements*, 1st ed., Pergamon Press, Oxford, **1984**.

[2] F. A. Cotton, G. Wilkinson, C. A. Murillo, M. Bochmann, *Advanced Inorganic Chemistry*; 6th ed., John Wiley and Sons, New York, **1999**.

[3] A. F. Wells, *Structural Inorganic Chemistry*, 5th ed., Clarendon Press, Oxford, **1984**, 329.

[4] B. Mason, *Principles of Geochemistry*, 3rd ed., Wiley, New York, **1966**, 372.

[5] P. Henderson, *Inorganic Geochemistry*, Pergamon Press, Oxford, **1982**.

[6] *The Evolution of Crystalline Rocks*, D. K. Bailey, R. MacDonald, (Eds.), Academic Press, London, **1976**, 484.

[7] A. F. Cronstedt, *Kongl. Svenska Vetensk. Acad. Handl*. **1756**, *17*, 120.

[8] O. Weigel, E. Steinhoff, *Z. Kristallogr.* **1925**, *61*, 125-154.

[9] J. W. McBain, in *A Survey of the Main Principles of Colloid Science, 4th Colloid Symp. Monogr*. **1926**, *4*, 7-18.

[10] *Zeolite Microporous Solids*: *Synthesis, Structure and Reactivity*, E. G. Derouane, F. Lemos, C. Naccache, F. R. Ribeiro, (Eds.), Kluwer Academic Press, Dordrecht, **1992**.

[11] *Catalytic Science and Technology*, *Vol.1*, S. Yoshida, N. Takezawa, T. Ono, (Eds.), Kodansha, Tokyo and VCH, Weinheim, **1991**.

[12] H. Kessler, in *Stud. Surf. Sci. Catal.*: *Recent Advances in Zeolite Science*, J. Klinowski, P. J. Barrie, (Eds.), Elsevier, Amsterdam, **1989**, *52*, 17.

[13] W. Johnson, A. J. Jacobson, W. M. Butler, S. E. Rosenthal, J. F. Brody, J. T. Lewandowski, *J. Am. Chem. Soc*. **1989**, *111*, 381-383.

[14] L. Smart, E. Moore, *Solid State Chemistry*, Chapman and Hall, London, **1992**, p181.

[15] F. Schüth, *Chem. uns. Zeit* **1995**, *29*, 42-52.

[16] A. Dyer, *An Introduction to Zeolite Molecular Sieves*, John Wiley: New York, **1988**.

[17] C. Baerlocher, W. M. Meier, D. H. Olson, *Atlas of Zeolite Structure Types*, 5th ed., Elsevier, London, **2001**.

[18] R. M. Milton, in *Molecular Sieves*, Soc. of Chem. Ind., London, **1968**, 199.

[19] For a Survey of Preparation of Zeolites through Hydrothermal Synthesis see: C. S. Cundy, P. A. Cox, *Chem. Rev.*, **2003**, *103*, 663-701.

[20] D. W. Breck, *Zeolite Molecular Sieves*: *Structure*, *Chemistry and Use*, Wiley, New York, **1974**.

[21] R. M. Barrer, *Zeolites and Clay Minerals as Sorbents and Molecular Sieves*, Academic Press, London, **1978**.

[22] R. J. Argauer, G. R. Landolt, U. S. Patent, 3,702,886, **1972**.

[23] E. M. Flanigen, J. M. Bennett, R. W. Grose, J. P. Cohen, R. L. Patton, R. L. Kirchner, J. V. Smith, *Nature*, **1978**, *271*, 512-516.

[24] R. W. Grose, E. M. Flanigen, *U. S. Patent*, 4,061,724, **1977**; *Chem. Abs. 88*: 142183.

[25] D. Freude, H. Ernst, T. Mildner, H. Pfeifer, I. Wolf, in *Stud. Surf. Sci. Catal.*: *Acid Base Catalysis II*, H. Hattori, M. Misono, Y. Ono, (Eds.), Elsevier: Amsterdam and Kodansha, Tokyo, **1989**, *90*, 105.

[26] T. Inui, H. Matsuda, Y. Takegami, in *Proc. 6th Int. Zeolite Conf.*, D. Olson, A. Bisio, (Eds.), Butterworths, Guildford, **1984**, 316.

[27] W. Hölderich, M. Hesse, F. Näumann, *Angew. Chem.* **1988**, *100*, 232-251; *Angew. Chem. Int. Ed. Engl.* **1988**, *27*, 226-246.

[28] J. A. Biscardi, G. D. Meitzner, E. Iglesia, *J. Catal.* **1998**, *179*, 192-202.

[29] Y. Ono, *Catal. Rev. Sci. Eng.* **1992**, *34*, 179-226.

[30] M. V. Frash, R. A. van Santen, *Phys. Chem. Chem. Phys.* **2000**, *2*,1085-1089.

[31] N. Kumar, L.–E. Lindfors, *Catal. Lett.* **1996**, *38*, 239-244.

[32] (a) J. M. Thomas, R. Raja, G. Sankar, R. G. Bell, *Acc*. *Chem*. *Res*. **2001**, *34*, 191-200. (b) D. E. De Vos, M. Dams, B. F. Sels, P. A. Jacobs, *Chem*. *Rev*. **2002**, *102*, 3615-3640.

[33] For Recent Developments of Metallosilicate and Metallophosphate molecular sieves Chemistry see: K. J. Balkus, *Prog*. *Inorg*. *Chem*. **2001**, *50*, 217-268.

[34] P. Behrens, G. D. Stucky, *Angew. Chem*. **1993**, *105*, 729; *Angew. Chem. Int. Ed. Engl.* **1993**, *32*, 696-699.

[35] C. T. Kresge, M. E. Leonowicz, W. J. Roth, J. C. Vartuli, J. S. Beck, *Nature* **1992**, *359*, 710-712.

[36] L. A. M. M. Barbosa, R. A. van Santen, J. Hafner, *J*. *Am*. *Chem*. *Soc*. **2001**, *123*, 4530-4540.

[37] M. F. Ciraolo, P. Norby, J. C. Hanson, D. R. Corbin, C. P. Grey, *J*. *Phys*. *Chem*. *B* **1999**, *103*, 346-356.

[38] (a) K. A. Franz, W. G. Kehr, A. Siggel, J. Wieczoreck, W. Adam, in *Ullman's Encyclopedia of Industrial Chemistry*, 5th ed., B. Eivers, S. Hawkins, G. Schulz, (Eds.) VCH, Weinheim, **1990**, Vol. *A15*, 519. (b) H. W. Leverenz, *An Introduction to Luminescent Solids*, John Wiley and Sons, New York, **1949**.

[39] (a) A. Morell, N. J. El Khiati, *J*. *Electrochem*. *Soc*. **1993**, *140*, 2019-2022. (b) C. Barthou, J. Benoit, P. Benalloul, A. Morell, *J*. *Electrochem*. *Soc*. **1994**, *141*, 524-528. (c) K. C. Mishra, K. H. Johnson, B. G. Deboer, J. K. Berkowitz, J. Olsen, E. A. Dale, *J*. *Lumin*. **1991**, *47*, 197-206.

[40] (a) T. Minami, T. Miyata, K. Kitamura, S. Takata, I. Fukuda, *Japanese J*. *Appl*. *Phys*. *Part 2-Letters*, **1990**, *30*, L315-L318. (b) T. Miyata, T. Minami, K. Saikai, *J*. *Lumin*. **1994**, *60-61*, 926-929.

[41] R. K. Iler, *The Chemistry of Silica*: *Solubility*, *Polymerization*, *Colloid and Surface Properties and Biochemistry*, John Wiley and Sons, Chichester, UK, **1979**, p 892.

[42] *Ultrastructure Processing of Advanced Materials*, D. R. Uhlmann, D. R. Ulrich (Eds.), Wiley-Interscience, New York, **1992**.

[43] *Better Ceramics Through Chemistry V*, *Materials Research Proceedings*, *Vol. 271*, M. J. Hampden–Smith, W. G. Klemperer, C. J. Brinker, (Eds.), Mat. Res. Soc., Pittsburgh, **1992**.

[44] *Inorganic Materials*, D. W. Bruce, D. O'Hare, (Eds.), Wiley, New York, **1992**.

[45] C. L. Bowes, G. A. Ozin, *Adv*. *Mater*. **1996**, *8*, 13-28.

[46] D. B. Amabilino, J. F. Stoddart, *Chem*. *Rev*. **1995**, *95*, 2725-2828.

[47] A. Stein, S. W. Keller, T. E. Mallouk, *Science*, **1993**, *259*, 1558-1564.

[48] *Sol–Gel Science*; C. J. Brinker, G. W. Scherer, Academic Press, Boston, **1990**.

[49] L. G. Hubert–Pfalzgraf, *Coord*. *Chem*. *Rev*. **1998**, *178*, 967-997.

[50] R. C. Mehrotra, *J*. *Non–Cryst*. *Solids*, **1988**, *100*, 1-15.

[51] C. Sanchez, J. Livage, M. Henry, F. J. Babonneau, *J*. *Non–Cryst*. *Solids*, **1988**, *100*, 65-76.

[52] C. D. Chandler, C. Roger, M. J. Hampden–Smith, *Chem*. *Rev*. **1993**, *93*, 1205-1241.

[53] *Sol–Gel Technology for Thin Films, Fibers, Preforms, Electronics, and Specialty Shape*, L. C. Klein (Eds.), Noyes, Park Ridge, **1988**.

[54] A. H. Cowley, R. A. Jones, *Angew*. *Chem*. **1989**, 1*01*, 1235-1243; *Angew*. *Chem*. *Int*. *Ed*. *Engl*. **1989**, *28*, 1208-1215.

[55] A. G. Williams, L. V. Interrante, In *Better Ceramics Through Chemistry*; Materials Research Society, Symposia Proceedings, *Vol*. *32*, C. J. Brinker, D. E Clark, D. R. Ulrich, (Eds.), North Holland, New York, **1984**, p 152.

[56] A. W. Apblett, A. C. Warren, A. R. Barron, *Chem*. *Mater*. **1992**, *4*, 167-182.

[57] F. Chaput, A. Lecomte, A. Dauger, J. P. Boilot, *Chem*. *Mater*. **1989**, *1*, 199-201.

[58] D. M. Hoffman, *Polyhedron*, **1994**, *13*, 1169-1179.

[59] For the Preparation of Organosilanols: P. D. Lickiss, *Adv*. *Inorg*. *Chem*. **1995**, *42*, 147-262.

[60] V. Chandrasekhar, S. Nagendran, R. Boomishankar, R. J. Butcher, *Inorg*. *Chem*. **2001**, *40*, 940-945.

[61] V. Chandrasekhar, S. Nagendran, S. Kingsley, V. Krishnan, R. Boomishankar, R. J. Butcher, *Proc. Indian Acad. Sci. (Chem. Sci.)* **2000**, *112*, 171-178.

[62] V. Chandrasekhar, S. Nagendran, R. J. Butcher, *Organometalics* **1999**, *18*, 4488-4492.

[63] M. G. Voronkov, E. A. Maletina, V. K. Roman, *Heterosiloxanes*, (*Soviet Scientific Review Supplement, Series Chemistry, Vol. 1*), Academic Press, London **1988**.

[64] *Tailor–Made Silicon–Oxygen Compounds*: *From Molecules to Materials*, R. Corriu, P. Jutzi, (Eds.), Vieweg: Braunschweig, **1996**.

[65] (a) L. King, A. C. Sullivan, *Coord*. *Chem*. *Rev*. **1999**, *189*, 19-57. (b) J. Beckmann, K. Jurkschat, *Coord*. *Chem*. *Rev*. **2001**, *215*, 267-300.

[66] V. Lorenz, A. Fischer, S. Giessmann, J. W. Gilje, Y. Gun'ko, K. Jacob, F. T. Edelmann, *Coord*. *Chem*. *Rev*. **2000**, *206-207*, 321-368.

[67] (a) R. Duchateau, *Chem*. *Rev*. **2002**, *102*, 3525. (b) F. J. Feher, T. A. Budzichowski, *Polyhedron* **1995**, *14*, 3239. (c) H. C. L. Abbenhuis, *Chem*. *Eur*. *J*. **2000**, *6*, 25.

[68] (a) K. W. Terry, T. D. Tilley, *Chem*. *Mater*. **1991**, *3*, 1001-1003. (b) K. W. Terry, P. K. Ganzel, T. D. Tilley, *Chem*. *Mater*. **1992**, *4*, 1290-1295.

[69] K. W. Terry, C. G. Lugmair, P. K. Gantzel, T. D. Tilley, *Chem*. *Mater*. **1996**, *8*, 274-280.

[70] N. Maxim, A. Overweg, P. J. Kooyman, J. H. M. C. van Wolput, R. W. J. M. Hanssen, R. A. van Santen, H. C. L. Abbenhuis, *J. Phys*. *Chem*. **2002**, *106*, 2203-2209. (b) R.

W. J. M. Hanssen, A. Meetsma, R. A. van Santen, H. C. L. Abbenhuis, *Inorg. Chem.* **2001**, *40*, 4049-4052. (c) Z. Fei, S. Busse, F. T. Edelmann, *J. Chem. Soc.*, *Dalton Trans*. **2002**, 2587-2589.

[71] R. Murugavel, A. Voigt, M. G. Walawalkar, H. W. Roesky, *Chem. Rev.* **1996**, *96*, 2205-2236.

[72] R. Murugavel, V. Chandrasekhar, H. W. Roesky, *Acc. Chem. Res.* **1996**, *29*, 183-189.

[73] R. Murugavel, A. Voigt, M. G. Walawalkar, H. W. Roesky, *Organosilicon Chemistry III*: *From Molecules to Materials*, N. Auner, J. Weis, (Eds.), Wiley-VCH Verlag GmbH, Weinheim, **1998**, 376-394.

[74] R. Murugavel, M. Bhattacharjee, H. W. Roesky, *Appl. Organomet. Chem.* **1999**, *13*, 227-243.

[75] H. N. Stokes, *Chem. Ber.* **1891**, *24*, 933-942.

[76] (a) H. Schmidbaur, *Angew. Chem.* **1965**, *77*, 206-216; *Angew. Chem. Int. Ed. Engl.* **1965**, *4*, 201. (b) F. Schindler, H. Schmidbaur, *Angew. Chem.* **1967**, *79*, 697-732; *Angew. Chem. Int. Ed. Engl.* **1967**, *6*, 683-694.

[77] (a) M. Veith, O. Schütt, J. Blin, S. Becker, J. Freres, V. Huch, *Z. Anorg. Allg. Chem.* **2002**, *628*, 138-146. (b) M. Veith, M. Jarczyk, V. Huch, *Angew. Chem.* **1997**, *109*, 140-142; *Angew. Chem. Int. Ed. Engl.* **1997**, *36*, 117-119.

[78] (a) C. A. Zechmann, T. J. Boyle, M. A. Rodriguez, R. A. Kemp, *Inorg. Chim. Acta.* **2001**, *319*, 137-146. (b) R. Fandos, A. Otero, A. Rodríguez, M. J. Ruiz, P. Terreros, *Angew. Chem.* **2001**, *113*, 2968-2971; *Angew. Chem. Int. Ed.* **2001**, *40*, 2884-2887.

[79] R. Murugavel, M. G. Walawalkar, G. Prabusankar, P. Davis, *Organometallics* **2001**, *20*, 2639-2642.

[80] M. Veith, M. Jarczyk, H. Vogelgesang, *Organometallics* **2002**, *21*, 380-388.

[81] N. Winkhofer, H. W. Roesky, M. Noltemeyer, W. T. Robinson, *Angew. Chem*. **1992**, *104*, 670-671; *Angew. Chem. Int. Ed. Engl*. **1992**, *31*, 599-601.

[82] (a) M. L. Montero, A. Voigt, M. Teichert, I. Usón, H. W. Roesky, *Angew*. *Chem*. **1995**, *107*, 2761-2763; *Angew*. *Chem*. *Int*. *Ed*. *Engl*. **1995**, *34*, 2504-2506. (b) A. Voigt, R. Murugavel, E. Parisini, H. W. Roesky, *Angew*. *Chem*. **1996**, *108*, 823-825; *Angew*. *Chem*., *Int*. *Ed*. *Engl*. **1996**, *35*, 748-750. (c) A. Voigt, M. G. Walawalkar, R. Murugavel, H. W. Roesky, E. Parisini, P. Lubini, *Angew*. *Chem*. **1997**, *109*, 2313-2315; *Angew*. *Chem*., *Int*. *Ed*. *Engl*. **1997**, *36*, 2203-2205.

[83] U. Ritter, N. Winkhofer, R. Murugavel, A. Voigt, D. Stalke, H. W. Roesky, *J. Am*. *Chem*. *Soc*. **1996**, *118*, 8580-8587.

[84] N. Winkhofer, A. Voigt, H. Dorn, H. W. Roesky, A. Steiner, D. Stalke, A. Reller, *Angew*. *Chem*. **1994**, *106*, 1414-; *Angew*. *Chem*. *Int*. *Ed*. *Engl*. **1994**, *33*, 1352-1354.

[85] A. I. Gouzyr, H. Wessel, C. E. Barnes, H. W. Roesky, M. Teichert, I. Usón, *Inorg*. *Chem*. **1997**, *36*, 3392-3393.

[86] A. Voigt, R. Murugavel, H. W. Roesky, *Organometallics* **1996**, *15*, 5097-5101.

[87] (a) M. Fujiwara, H. Wessel, H.–S. Park, H. W. Roesky, *Tetrahedron*, **2002**, *58*, 239-243. (b) M. Fujiwara, H. Wessel, H.–S. Park, H. W. Roesky, *Chem. Mater.* **2002**, *14*, 49-75.

[88] D. E. C. Corbridge, *Phosphorus*: *An Outline of its Chemistry*, *Biochemistry and Technology*, 5th ed., Elsevier, Amsterdam, **1995**.

[89] *Inorganic Phosphate Materials*, T. Kanazawa, (Eds.), Kodansha, Tokyo, **1988**.

[90] S. T. Wilson, B. M. Lok, C. A. Messina, T. R. Cannan, E. M. Flanigen, *J. Am. Chem. Soc.* **1982**, *104*, 1146-1147.

[91] E. M. Flanigen, B. M. Lok, R. L. Patton, S. T. Wilson, *Proc*. *7th Int*. *Zeolite Conf*. *Tokyo*, Y. Murakami, A. Ijima, J. W. Ward (Eds.), Kodansha, Tokyo, **1986**, 103.

[92] T. E. Gier, G. D. Stucky, *Nature* **1991**, *309*, 508-510.

[93] P. Feng, X. Bu, G. D. Stucky, *Nature* **1997**, *388*, 735-741.

[94] X. Bu, P. Feng, G. D. Stucky, *Science* **1997**, *278*, 2080-2085.

[95] T. E. Gier, X. Bu, P. Feng, G. D. Stucky, *Nature* **1998**, *395*, 154-157.

[96] (a) M. R. Mason, *J. Cluster Sci*. **1998**, *9*, 1-23. (b) M. R. Mason, A. M. Perkins, R. M. Matthews, J. D. Fisher, M. S. Mashuta, A. Vij, *Inorg. Chem*. **1998**, *37*, 3734-3746. (c) M. R. Mason, A. M. Perkins, V. V. Ponomarova, A. Vij, *Organometallics* **2001**, *20*, 4833-4839.

[97] M. G. Walawalkar, H. W. Roesky, R. Murugavel, *Acc. Chem. Res*. **1999**, *32*, 117-126.

[98] M. G. Walawalkar, *Dissertation*, Cuvillier, Göttingen **1997**.

[99] Y. Yang, *Dissertation*, Cuvillier, Göttingen **1999**.

[100] D. Chakraborthy, *Dissertation*, Cuvillier, Göttingen **1999**.

[101] C. G. Lugmair, T. D. Tilley, A. L. Rheingold, *Chem. Mater*. **1997**, *9*, 339-348.

[102] M. Sathiyendiran, R. Murugavel, *Inorg. Chem*. **2002**, *41*, 6404-6411.

[103] R. Murugavel, M. Sathiyendiran, M. G. Walawalkar, *Inorg. Chem*. **2001**, *40*, 427-434.

[104] M. Sathiyendiran, R. Murugavel, *Chem. Lett*. **2001**, *1*, 84-85.

[105] A. Clearfield, *Prog. Inorg. Chem*. **1998**, *47*, 371-510.

[106] G. Cao, H.–G. Hong, T. E. Mallouk, *Acc. Chem. Res*. **1992**, *25*, 420-427.

[107] R. C. Finn, J. Zubieta, R. C. Haushalter, *Prog. Inorg. Chem*. **2003**, *51*, 421-601.

[108] Y. Yang, J. Pinkas, M. Noltemeyer, H.–G. Schmidt, H. W. Roesky, *Angew. Chem*. **1999**, *111*, 706-708; *Angew. Chem. Int. Ed*. **1999**, *38*, 664-666.

[109] V. Chandrasekhar, S. Kingsley, *Angew. Chem*. **2000**, *112*, 2410-2412; *Angew. Chem. Int. Ed*. **2000**, *39*, 2320-2322.

[110] V. Chandrasekhar, S. Kingsley, B. Rhatigan, M. K. Lam, A. L. Rheingold, *Inorg. Chem*. **2002**, *41*, 1030-1032.

[111] (a) M. Mehring, M. Schürmann, *Chem*. *Commun*. **2001**, 2354-2355. (b) M. Mehring, G. Guerrero, F. Dahan, P. H. Mutin, A. Vioux, *Inorg*. *Chem*. **2000**, *39*, 3325-3332.

[112] H. W. Roesky, *Solid State Sci*. **2001**, *3*, 777-782.

[113] A. Choudhury, C. N. R. Rao, *Chem*. *Commun*. **2003**, 366-367.

[114] K. Su, T. D. Tilley, M. J. Sailor, *J*. *Am*. *Chem*. *Soc*. **1996**, *118*, 3459-3468.

[115] D. K. Murray, T. Howard, P. W. Goguen, T. R. Krawietz, J. F. Haw, *J*. *Am*. *Chem*. *Soc*. **1994**, *116*, 6354-6360.

[116] G. Anantharaman, N. D. Reddy, H. W. Roesky, J. Magull, *Organometallics* **2001**, *20*, 5777-5779.

[117] M. A. Malik, P. O'Brien, M. Motevalli, A. C. Jones, *Inorg*. *Chem*. **1997**, *36*, 5076-5081.

[118] (a) M. Driess, K. Merz, S. Rell, *Eur*. *J*. *Inorg*. *Chem*. **2000**, 2517-2522. (b) K. Merz, H. M. Hu, S. Rell, M. Driess, *Eur*. *J*. *Inorg*. *Chem*. **2003**, 51-53.

[119] G. Anantharaman, H. W. Roesky, H.–G. Schmidt, M. Noltemeyer, J. Pinkas, *Inorg*. *Chem*. **2003**, *42*, 970-973.

[120] R. Murugavel, V. Chandrasekhar, A. Voigt, M. Noltemeyer, H.–G. Schmidt, H. W. Roesky, *Organometallics* **1995**, *14*, 5298-5301.

[121] A. Klemp, H. Hatop, H. W. Roesky, M. Noltemeyer, H. G. Schmidt, *Inorg*. *Chem*. **1999**, *38*, 5832-5836.

[122] (a) A. J. Elias, H.–G. Schmidt, M. Noltemeyer, H. W. Roesky, *Organometallics*, **1992**, *11*, 462-464. (b) H. Li, M. Eddaoudi, T. L. Groy, O. M. Yaghi, *J*. *Am*. *Chem*. *Soc*. **1998**, *120*, 8571-8572. (c) A. Bondi, *J*. *Phys*. *Chem*. **1964**, *68*, 441-451. (d) J. E. Huheey, In *Inorganic Chemistry*: *Principles of Structure and Reactivity*, Harper and Row, New York, **1983**.

[123] G. Anantharaman, H. W. Roesky, J. Magull, *Angew*. *Chem*. **2002**, *114*, 1274-1277; *Angew*. *Chem*. *Int*. *Ed*. **2002**, *41*, 1226-1229.

[124] J. Arnold, T. D. Tilley, A. L. Rheingold, S. J. Geib, *Inorg*. *Chem*. **1987**, *26*, 2106-2109.

[125] (a) M. A. Camblor, M. E. Davis, *J. Phys*. *Chem*. **1994**, *98*, 13151-13156. (b) M. Yoshikawa, S. I. Zones, M. E. Davis, *Microporous Mater*. **1997**, *11*, 137-148.

[126] (a) V. R. Choudhary, S. K. Jana, *Appl*. *Catal*. *A*: *General*, **2002**, *224*, 51-62. (b) D. P. Ivanov, M. A. Rodkin, K. A. Dubkov, A. S. Kharitonov, G. I. Panov, *Kinetics and Catalysis*, **2000**, *41*, 771-775. (c) A. S. Kharitonov, G. A. Sheveleva, G. I. Panov, V. I. Sobolev, Y. A. Paukhus, V. N. Romannikov, *Appl*. *Catal*. *A*: *General*, **1993**, *98*, 33-43. (d) G. I. Panov, G. A. Sheveleva, A. S. Kharitonov, Y. A. Paukhus, V. N. Romannikov, L. A. Vostrikova, *Appl*. *Catal*. *A*: *General* **1992**, *82*, 31-36.

[127] (a) K. L. Fujdala, T. D. Tilley, *J. Catal.* **2003,** *216*, 265-275. (b) T. A. Chesnokova, E. V. Zhezlova, A. N. Kornev, Y. V. Fedotova, L. N. Zakharov, G. K. Fukin, Y. A. Kursky, T. G. Mushtina, G. A. Domrachev, *J. Organomet. Chem.* **2002**, *642,* 20-31. (c) A. N. Kornev, T. A. Chesnokova, V. V. Semenov, E. V. Zhezlova, L. N. Zakharov, L. G. Klapshina, G. A. Domrachev, V. S. Rusakov, *J. Organomet. Chem.* **1997**, *547,* 113-119. (d) F. Liu, K. D. John, B. L. Scott, R. T. Baker, K. C. Ott, W. Tumas, *Angew. Chem.* **2000**,*112*, 3257-3260; *Angew. Chem. Int*. *Ed*. **2000**, *39*, 3127-3130.

[128] A. G. Davis, B. P. Roberts, *J. Chem*. *Soc*. *B*, **1968**, 1074-1078.

[129] V. I. Sobolev, G. I. Panov, A. S. Kharitonov, V. N. Romannikov, A. M. Volodin, K. G. Ione, *J. Catal*. **1993**, *139*, 435-443.

[130] A. K. Cheetham, G. Férey, T. Loiseau, *Angew*. *Chem*. **1999**, *111*, 3466-3492; *Angew*. *Chem*. *Int*. *Ed*. **1999**, *38*, 3268-3292.

[131] C. N. R. Rao, S. Natarajan, A. Choudhury, S. Neeraj. A. A. Ayi, *Acc. Chem. Res.* **2001**, *34*, 80-87.

[132] X. Bu, P. Feng, T. E. Gier, G. D. Stucky, *J. Solid State Chem.* **1998**, *136*, 210-215.

[133] For Recent Work on Zinc Phosphate: (a) A. Katovic, G. Giordano, S. Kowalak, *Stud. Surf. Sci. Catal.* **2002**, *142A*, 39-44. (b) B. C. Tischendorf, T. M. Alam, R. T. Cygan, J. U. Otaigbe *J. Non−Cryst. Solids* **2003**, *316*, 261-272. (c) A. Simon−Masseron, J. L. Paillaud, J. Patarin, *Chem. Mater.* **2003**, *15*, 1000-1005. (d) Z. E. Lin, Y. W. Yao, J. Zhang, G. Y. Yang, *J. Chem. Soc., Dalton Trans.* **2002**, 4527-4528. (e) X. M. Chen, Y. N. Zhao, R. J. Wang, L. A. Ming, Z. H. Mai, *J. Chem. Soc., Dalton Trans.* **2002**, 3092-3095. (f) Y. L. Liu, W. Liu, Y. Xing, Z. Shi, Y.L. Fu, W. Q. Pang, *J. Solid State Chem.* **2002**, *166*, 265-270. (g) T. R. Jensen, R. G. Hazell, A. N. Christensen, J. C. Hanson, *J. Solid State Chem.* **2002**, *166*, 341-351. (h) Y. N. Zhao, J. Ju, X. M. Chen, X. H. Li, Y. Wang, R. J. Wang, M. Li, Z. H. Mai, *J. Solid State Chem.* **2002**, *166*, 369-374. (i) Y. N. Zhao, Y. W. Yao, X. H. Li, X. M. Chen, M. Li, Z. H. Mai, *Chem. Lett.* **2002**, 542-543. (j) S. Natarajan, *J. Chem. Soc., Dalton Trans.* **2002**, 2088-2091.

[134] (a) J.–G. Mao, A. Clearfield, *Inorg. Chem.* **2002**, *41*, 2319-2324. (b) J.–G. Mao, Z. Wang, A. Clearfield, *Inorg. Chem.* **2002**, *41*, 2334-2340. (c) G. B. Hix, B. M. Kariuki, S. Kitchin, M. Tremayne, *Inorg. Chem.* **2001**, *40*, 1477-1481. (d) F. Fredoueil, M. Evain, M. Bujoli−Doeuff, B. Bujoli, *Eur. J. Inorg. Chem.* **1999**, 1077-1079. (e) F. Fredoueil, V. Penicaud, M. Bujoli−Doeuff, B. Bujoli, *Inorg. Chem.* **1997**, *36*, 4702-4706.

[135] J. Zhu, X. Bu, P. Feng, G. D. Stucky, *J. Am. Chem. Soc.* **2000**, *122*, 11563-11564.

[136] A. Clearfield, G. D. Smith, *Inorg. Chem.* **1969**, *8*, 431-436.

[137] (a) C. V. K. Sharma, A. Clearfield, *J. Am. Chem. Soc.* **2000**, *122*, 1558-1559. (b) F. Fredoueil, M. Evain, D. Massiot, M. Bujoli−Doeuff, P. Janvier, A. Clearfield, B.

Bujoli, *J. Chem. Soc., Dalton Trans*. **2002**, 1508-1512. (c) P. Ayyappan, O. R. Evans, Y. Cui, K.A. Wheeler, W. Lin, *Inorg. Chem*. **2002**, *41*, 4978-4980. (d) P. Ayyappan, O. R. Evans, B. M. Foxman, K. A. Wheeler, T. H. Warren, W. Lin, *Inorg. Chem*. **2001**, *40*, 5954-5961. (e) C. V. K. Sharma, A. Clearfield, A. Cabeza, M. A. G. Aranda, S. Burque, *J. Am. Chem. Soc*. **2001**, *123*, 2885-2886. (f) N. Choi, I. Khan, R. W. Matthews, M. McPartlin, B. P. Murphy, *Polyhedron* **1994**, *13*, 847-850. (g) N. El Messbahi, J.–P. Silvestre, N. Q. Dao, M.–R. Lee, Y. Leroux, A. Neuman, H. Gillier−Pandraud, *Phosphorus*, *Sulfur*, *Silicon*, *Relat. Elem*. **2000**, *164*, 45-59.

[138] (a) E. K. Brechin, R. A. Coxall, A. Parkin, S. Parsons, P. A. Tasker, R. E. Winpenny, *Angew. Chem*. **2001**, *113*, 2772-2775; *Angew. Chem. Int. Ed*. **2001**, *40*, 2700-2703. (b) M. I. Khan, J. Zubieta, *Prog. Inorg. Chem*. **1995**, *43*, 1-149.

[139] (a) A. K. Duhme, H. Strasdeit, *Eur. J. Inorg. Chem*. **1998**, 657-662. (b) J. Fornies, J. Gomez, E. Lalinde, M. T. Moreno, *Inorg. Chem*. **2001**, *40*, 5415-5419. (c) M. Weidenbruch, M. Herrndorf, A. Schäfer, S. Pohl, W. Saak, *J. Organomet. Chem*. **1989**, *361*, 139-145.

[140] G. M. Whitesides, M. Eisenhut, W. M. Bunting, *J. Am. Chem. Soc*. **1974**, *96*, 5398-5407.

[141] S. Freeman, M. J. P. Harger, *J. Chem. Soc., Perkin Trans*. **1987**, 1399-1406.

[142] *Synthetic Methods of Organometallic and Inorganic Chemistry*, *Vol. 4*, W. A. Hermann, A. Salzer (Eds.), G. Thieme, Stuttgart, **1996**.

[143] D. F. Shriver, M. A. Drezdzon, *The Manipulation of Air−Sensitive Compounds*, 2nd ed., McGraw−Hill, New York, **1969**.

[144] D. D. Perrin, W. L. F. Armarego, *Purification of Laboratory Chemicals*, 3rd ed., Pergamon, London, **1988**.

[145] G. M. Sheldrick, SHELXTL−PLUS, Siemens X−ray Instruments, Madison, **1990**.

[146] G. M. Sheldrick, SHELXS−97, *Program for Structure Solution, Acta Crystallogr. Sect*. *A* **1990**, *46*, 467-473.

[147] G. M. Sheldrick, SHELXL−97, *Program for Structure Refinement*, Universität Göttingen, **1997**.

[148] M. M. Olmstead, P. P. Power, S. C. Shoner, *Inorg*. *Chem*. **1991**, *30*, 2547-2551.

[149] N. Kuhn, T. Kratz, *Synthesis* **1993**, 561-562.

[150] *Synthetic Methods of Organometallic and Inorganic Chemistry*, *Vol*. *5*, W. A. Hermann, A. Salzer (Eds.), G. Thieme, Stuttgart, **1996**.

[151] M. Ghiaci, J. Asghari, *Synth*. *Commun*. **1998**, *28*, 2213-2220.

[152] M. Yoshifuji, K. Ando, K. Toyota, I. Shima, N. Inamoto, *J. Chem*. *Soc*., *Chem*. *Commun*. **1983**, 419-420.

[153] B. Hübler−Blank, M. Witt, H. W. Roesky, *J. Chem. Educ.* **1993**, *70*, 408-409.

Lebenslauf

Ganapathi Anantharaman, geboren am 02. Mai 1976 in Madras, Indien

Staatsangehörigkeit	indisch
Familienstand	ledig
Eltern	Subramanian Ganapathi, *rtd. Clerk* Ganapathi Rajalakshmi

Schulausbildung

Juni 1981 - Mai 1986	Sri Venkatanivasam Middle School, Chennai, Indien (Grundschule, Classes I - IV)
Juni 1986 - Mai 1988	Anjuham Higher Secondary School, Chennai, Indien (Classes VI- VII)
Juni 1988 - Mai 1991	Madras Seva Sadan Higher Secondary School, Chennai, Indien (Gymnasium, Classes VIII - X)
Juni 1991 - Mai 1993	Anjuham Higher Secondary School, Chennai, Indien (Classes XI - XII)

Hochschulausbildung

1993 - 1996	Studium der Chemie, Physik und Mathematik an der *University of Madras*, Chennai, Indien
21. Januar 1997	*Bachelor of Science* (Zwischenprüfung, Hauptfach: Chemie)
1997 - 1999	*Studium der Chemie, Indian Institute of Technology, Bombay*
06. August 1999	*Master of Science* (*Abschußprüfung, Fach: Chemie*)
1999 - 2000	*Research Assistant (sechs monate), Indian Institute of Technology, Bombay*
05. Feb. 2002	Äquivalenzprüfung zum Diplomexamen - Fach Chemie, Universität Göttingen
April 2000 - Juni 2003	Anfertigung der Dissertation unter Anleitung von Prof. Dr. Dr. h.c. mult. H.W. Roesky am Institut für Anorganische Chemie der Universität Göttingen